Index

Sommario

1. Cardiopatch in un modello di lesione necrotizzante acuta

In questo progetto di ricerca si è voluto testare la possibilità di utilizzare *in vivo* a livello cardiaco un nuovo tipo di materiale biodegradabile a base di collagene. Si è scelto come modello animale il ratto e come tipo di danno la lesione necrotizzante acuta del miocardio (*LNA*) viste le precedenti esperienze nel nostro laboratorio. Sono stati utilizzati ratti Wistar del peso compreso tra 200 e 250 grammi. Dopo anestesia, gli animali sono intubati e collegati ad un apparecchio per la ventilazione artificiale. Si procede quindi con una toracotomia per esporre il cuore. La lesione è una lesione da freddo (*cryoinjury*), provocata accostando alla superficie cardiaca una bacchetta metallica raffreddata in azoto liquido: vengono eseguite tre applicazioni da 1 minuto ciascuna. Si crea così un danno transmurale con zona di necrosi-apoptosi.

La potenzialità della spugna di collagene (*cardiopatch*) nello sviluppare angiogenesi/arteriogenesi è quindi stata valutata attraverso l'impianto sul ventricolo sinistro sano (gruppo 2) o con cryoinjury (gruppo3) di ratti fino a 60 giorni dalla lesione. Il contenuto di vasi sanguini e l'infiltrato cellulare extra-vascolare è stato analizzato nel *cardiopatch*, la zona di cryoinjury e nella zona "border" del miocardio vicino alla zona di lesione.

In vitro questo biomateriale mantiene la differenziazione di cardiomiociti, cellule muscolari lisce e cellule endoteliali. Quando impiantato nel peritoneo, lo scaffold induce una notevole neoangiogenesi, ma anche una risposta immunitaria innata con abbondante infiltrato macrofagico e cellule giganti da corpo estraneo.

Nel cuore , il cardiopatch è quasi completamente riassorbito in 60 giorni e viene popolato da nuove arteriole e capillari sia nel cuore intatto che con cryoinjury (le arteriole nella cryoinjury rispetto la zona intatta sono 2,3 volte di più, i capillari nella cryoinjury rispetto la zona intatta sono 1,7 volte di più). A sua volta il cardiopatch esercita un effetto "trofico" sul tessuto di granulazione in via di organizzazione, aumentando la densità vascolare di questa zona di 2,7 volte per quanto riguarda le arteriole e di 4 volte per i capillari.

Le cellule interstiziali nel cardiopatch esprimono raramente (<1%) marcatori per cellule staminali cardiogeniche come Sca-1 o MDR1, mentre cellule positive per marcatori di cellule delle creste neurali come GFAP e nestina vanno dal 3/30% al 30/70% nei cardiopatches posti su cuori intatti o con cryoinjury rispettivamente. Miofibroblasti e cardiomiociti sono assenti, mentre molti macrofagi si trovano nel cardiopatch anche a 60 giorni dall'impianto. Il Western Blotting di cardiopatches staccati da cuori intatti o con cryoinjury ha confermato la presenza di cellule muscolari lisce e endoteliali, ma non di cardiomiociti.

Riassumendo questa spugna di collagene è stata capace di evocare una forte risposta angiogenetica e arteriogenetica in cuori sia intatti che con cryoinjury, rappresentando così un ideale mezzo per angio-arteriogenesi terapeutica e come potenziale utile substrato per la semina di cellule staminali.

2. Cardiopatch in un modello di lesione necrotizzante cronica

Dopo aver utilizzato la spugna di collagene in un modello di lesione necrotizzante acuta, si è quindi deciso di utilizzare questo biomateriale in un modello di lesione necrotizzante cronica (LNC) sempre nel miocardio di ratto. In vista anche di una possibile applicazione clinica di questo materiale, questo modello sembra infatti avvicinarsi di più al quadro di ischemia cronica nell'uomo.

Gli animali sono stati divisi in 4 gruppi sperimentali:

1. animali sottoposti a LNC a livello cardiaco.
2. animali nei quali si è applicato il *cardiopatch* al cuore intatto.

3. animali sottoposti a LNC a livello cardiaco, e successiva collocazione (dopo 30 giorni) del *cardiopatch* nella zona della lesione.
4. animali sham-operated.

I vari animali sono stati sacrificati ai time points di 15, 30 e 60 giorni. Dopo prelievo e congelamento degli organi sono state ottenute criosezioni cardiache su cui fare le analisi istologiche e citochimiche: ematossilina-eosina, tricromica di Masson, immunoperossidasi e immunofluorescenza.

In particolare, nella regione sottoposta alla *cryoinujury* e nel cuore intatto sono state studiate quattro zone :

Zona 1: tessuto danneggiato presente nel cuore con LNC.

Zona 2: *cardiopatch* applicato al cuore intatto.

Zona 3: tessuto danneggiato presente nel cuore con LNC e sul quale si è applicato il *cardiopatch*.

Zona 4: *cardiopatch* applicato al cuore con LNC.

Il biomateriale, quando applicato in un cuore di ratto intatto o danneggiato, è in grado di attrarre una considerevole neovascolarizzazione, caratterizzata dalla formazione di capillari e arteriole. Il *cardiopacth* stimola la neovascolarizzazione nella adiacente zona cardiaca danneggiata, mentre da questa non vengono emanati significativi stimoli induttivi di neovascolarizzazione nel *cardiopatch* (probabilmente a causa di una riduzione di fattori di crescita angiogenetici/arteriogenetici rilasciati dal tessuto di granulazione in via di maturazione). A 15 giorni dall'applicazione del cardiopatch nei cuori con LNC, l'aumento di vasi sanguigni è significativo nella zona 3, ma diminuisce leggermente a 30 giorni. L'efficacia del biomateriale è così discutibile in prospettiva di un uso a lungo termine. In questo contesto si renderebbe necessario l'uso fattori di crescita angiogenetici (come VEGF) in modo da aumentare la neovascolarizzazione.

Il biomateriale impiegato in questo studio inoltre non si è rivelato in grado di influire sulla mobilizzazione locale di cellule staminali cardiogene residenti in quanto nel *cardiopatch* non si sono trovate cellule con profilo fenotipico riconducibile a questa tipologia.

3. Cardiopatch e cellule mesenchimali del midollo osseo in un modello di lesione necrotizzante cronica.

Visti i precedenti risultati incoraggianti, ma non sufficienti nella prospettiva di un uso terapeutico più complesso di questo biomateriale, è diventata indispensabile un'ulteriore ingegnerizzazione del *cardiopatch*. Si è quindi pensato di iniettare nel patch delle cellule staminali mesenchimali del midollo osseo (BM-MSCs), cellule ben caratterizzate dal punto di vista fenotipico e largamente utilizzate nella terapia dell'infarto al miocardio sia in modelli animali che in alcuni recenti trials sull'uomo. Le cellule inoltre esprimono costituivamente la GFP, rendendole perciò facilmente rintracciabili dopo trapianto.

I ratti Wistar sottoposti a LNC, dopo 30 giorni sono stati divisi nei seguenti gruppi:
1. animali sottoposti a sola LNC;
2. animali con LNC che ricevono un'iniezione inta-miocardica di BM-MSC vicino la zona di danno;
3. animali in cui il patch è attaccato al miocardio infartuato e quindi iniettato con semplice medium;
4. animali in cui il patch è attaccato al miocardio sano e le cellule iniettate all'interno dello scaffold;
5. animali in cui lo scaffold è attaccato al miocardio danneggiato e successivamente iniettato con circa $4x10^6$.

Dal giorno precedente la seconda operazione gli animali sono stati trattati con ciclosporina per evitare reazioni di rigetto.
Dopo trapianto le BM-MSCs hanno attivato programmi di differenziamento che hanno portato all'origine di capillari, arteriole e cardiomiociti.
Alcune delle BM-MSCs GFP^+ trapiantate sono positive per marcatori di cellule endoteliali (CD31) e muscolari (SM α-actina) in capillari e arteriole, rispettivamente. In particolare, nel gruppo 5, molte delle BM-MSCs sono state ritrovate disperse nell'interstizio, ma varie hanno partecipato alla formazione di vasi sia nel cardiopatch che nella zona di cryoinjury. Tuttavia il contributo all'angiogenesi delle cellule GFP^+ nella zona di cryoinjury è molto limitato.
Due settimane dopo il trapianto alcune delle BM-MSCs sono anche marcate con Troponina T cardiaca. Nessuna presenza di cellule positive per cTnT è stata però rinvenuta nel miocardio danneggiato di animali del gruppo 5.
Nel patch e nella zona di LNC sono presenti anche molti macrofagi e un coinvolgimento di queste cellule nel processo di angiogenesi/arteriogenesi non è da escludere.
Si è detto che l'utilizzo del solo biomateriale nella riparazione del danno cardiaco non era sufficiente per influire sulla mobilizzazione locale di cellule staminali cardiogene residenti. Il ricorso a cellule staminali del midollo osseo sembra poter sopperire alla mancanza di cellule con profilo fenotipico cardiomiocitario, anche se probabilmente la percentuale di conversione in cardiomiociti non è così elevata da garantire un recupero funzionale adeguato.

Summary

1. Cardiopatch in a model of Acute Myocardial Injury (AMI)

In this research project we tested the possibility of using a new biodegradable collagen-based material *in vivo* at cardiac level. We chose the rat as animal model and the acute necrotizing injury (ANI) as type of lesion. Wistar rats of 200-250 grams were used. After anaesthesia, animals were intubated and ventilated mechanically with room air. The heart was exposed through a left thoracotomy and a left ventricular acute necrotizing injury (ANI, freeze-thaw procedure) was created by three sequential exposures (60 s each, 20 s of non-freezing interval) of a liquid nitrogen-cooled cryoprobe (a stainless-steel cylinder, 8mm of diameter). The potential of collagen scaffold (Cardiopatch) for attracting angiogenesis/arteriogenesis was studied *in vivo* by implantation on a healthy (group 2) or cryoinjured left ventricle (group 3) of rats up to 60 days postinjury times. Blood vessel content and extra-vascular cell infiltration were evaluated within the Cardiopatches, the cryoinjury zones, and the "border zones" of the myocardium facing the cryoinjury zones.

In vitro, this biomaterial supported differentiation of cardiomyocytes, smooth muscle and endothelial cells. When implanted in the peritoneum, the scaffold induced a striking neoangiogenesis but also an innate immune response with an abundant macrophage infiltrate and some foreign body giant cells.

In the heart, cardiopatches were almost completely absorbed in 60 days and became populated by new arterioles and capillaries in both intact and cryoinjured heart (arterioles in cryoinjury vs. intact zone were about 2,3-fold higher; capillaries in cryoinjury vs. intact zone were 1.7-fold higher). In turn, cardiopatches exerted a "trophic" effect on the organizing granulation tissue that emerged from the wound healing process increasing vessel density of this tissue of 2.7-fold for arterioles and 4-fold for capillaries.

Interstitial cells in cardiopatches rarely (<1%) expressed markers of cardiogenic stem cells such as Sca-1- or MDR1, whereas markers of neural crest cells GFAP+/nestin+ cells ranged from 3/30% to 30/70% in cardiopatches placed on intact vs cryoinjured heart, respectively. Myofibroblasts and cardiomyocyte were absent but macrophages largely accommodated in the cardiopatches even after 60 days from implantation. Western blotting of cardiopatches detached from intact/cryoinjured hearts confirmed that endothelial and smooth muscle cells but not cardiomyocyte markers were expressed in the patches.

The porous collagen scaffold was able to evoke a powerful angiogenetic and arteriogenetic response in the intact and cryoinjured hearts, representing an ideal tool for therapeutic angio-arteriogenesis and a potentially useful substrate for stem cell seeding.

2. Cardiopatch in a model of Chronic Myocardial Injury (CMI)

After using the collagen scaffold in a model of AMI, this biomaterial was also applied in a model of Chronic Myocardial Injury (CMI) again in a rat myocardium. In view of a possible clinical application, this model seems closer to the clinical picture of chronic ischemia in human.

The animals were divided in 4 experimental groups:

1. animals that received a chronic necrotizing injury (CNI) at cardiac level
2. animals in which the scaffold was applied to the intact heart;
3. animals in which the scaffold was sutured to a cryoinjured heart;
4. Sham-operated animals.

The animals were sacrificed at time points of 15, 30 and 60 days. After collecting and freezing the organs, cardiac cryosections were obtained for the histological analysis: haematoxylin-eosin, Masson's thrichrome, immunoperoxidase and immunofluorescence.

In detail, four zones were studied in the region of cryoinjury or in the intact heart:
Zone 1: damaged tissue in hearts with CNI;
Zone 2: cardiopatch in intact hearts;
Zone 3: damaged tissue in hearts with CNI and cardiopatch;
Zone 4: cardiopatch in hearts with CNI.
When applied in intact or damaged rat heart, the biomaterial was able to attract a remarkable neovascularization, with the formation of capillaries and arterioles. The scaffold promoted neovascularization in the damaged zone, while this zone was not able to induce a important neovascularization in the cardiopatch any longer, as occurred in the ANI model. The mutual influence between the cardiopatch and the zone with CNI was lacking, probably due to a reduction of angiogenic/arteriogenic growth factors released from the granulation tissue. After 15 days from the application of cardiopatch in hearts with CNI, the rise of blood vessel was significant in zone 3, but it slightly decreased at 30 days. The efficacy of the biomaterial is so debatable in prospective of a long run use. In this contest it would be necessary to use angiogenetic growth factors (such as VEGF) in order to improve the neovascularisation.
The biomaterial was also unable to mobilize resident cardiogenic stem cells: in the cardiopatch no cells with this phenotypic pattern were found.

3. Cardiopatch and Bone Marrow derived Mesenchymal Stem Cells (MSCs) in a model of Chronic Myocardial Injury (CMI)

As these results were encouraging, but not sufficient with regard to a more complex therapeutic use of this the biomaterial, it became essential to test an additional manipulation of the cardiopatch.
The patch applied in a model of CMI was therefore injected with BM-MSCs, a phenotypically well-characterized cell population that is extensively used as a therapy in the myocardial infraction both in animal models and in human trials. In addition, these cells constitutively expressed the GFP (Green Fluorescent Protein), a green fluorescent marker that can be easily tracked after transplantation.
The Wistar rats underwent ~~to~~ CNI and after 30 days were divided into the following groups:
1. animals that received cryoinjury alone;
2. animals with CMI that received via an intra-myocardial route the BM-MSCs alone near the damaged zone;
3. animals in which the patch was attached to the injured myocardium and than injected with medium alone;
4. animals in which the patch was attached to the normal myocardium and the cells injected within it;
5. animals in which the scaffold was implanted in the damaged hearts and subsequently injected with about $4x10^6$ GFP^+ BM-MSCs.

The day before the second operation the rats started the treatment with 10mg/Kg/day of Cyclosporine (CsA) until the sacrifice to avoid the risk of rejection.
After 15 days post-injection numerous GFP^+ cells were found in the myocardium of animals of group 2 (rats with CMI received GFP^+ BM-MSCs alone near the damaged zone), or in the cardiac patch and fibrotic myocardium of animals in groups 4 (patch attached to normal myocardium and the cells injected within it) and 5 (scaffold implanted in damaged hearts and subsequently injected with GFP^+ BM-MSCs). This suggests that the cells injected in the patch were able to move from the patch to the myocardium.
Also in this case the material was able to induce neovascularization.
After transplant the BM-MSCs were able to activate differentiation programs and form capillaries, arterioles and cardiomyocytes.

Some of the transplanted GFP^+ BM-MSCs were positive for endothelial (CD31) and smooth muscle (SM α-actin) cell marker and were found in capillaries and arterioles, respectively. In particular, in group 5, most of the BM-MSCs were dispersed into the interstice and several participated in vessel formation both in cardiopatch and in the cryoinjured zone. However, the contribute of GFP^+ cells to neoangiogenesis in the cryoinjured zone was very limited.
Two weeks after transplantation some of the engrafted MSCs were stained positive for cardiac troponin T. No presence of cTnT positive cells was detected in the injured myocardium of animals in group 5.
In previous models, the use of the collagen scaffold only in cardiac repair was not sufficient to mobilize resident cardiogenic stem cells locally. The use of BM-MSCs was able to avoid the lack of cells with the phenotypic profile of cardiomyocytes, even if the percentage of conversion to this kind of cell was not big enough to ensure an adequate functional recovery.

Introduction

1.1. Myocardial Infarction

Acute myocardial infarction (AMI or MI), more commonly known as a "heart attack", is a medical condition that occurs when the blood supply to a part of the heart is interrupted. The resulting ischemia or oxygen shortage causes damage and potential death of heart tissue *(Robbins et Cotran, 2007)*.

MI is the most common cause of mortality in the developed world. About 1.5 million individuals in the United States suffer an acute MI annually and approximately one third of them die; in survivors the damage becomes chronic and is responsible of cardiac failure (CHF), a condition in which the heart is not able to pump a sufficient amount of blood through the body.

MI may occur at virtually any age, but the frequency rises progressively with increasing age (especially men over 40 and women over 50) and with presence of important risk factors that predispose to atherosclerosis, such as hypertension, cigarette smoking, diabetes mellitus, obesity, genetic hypercholesterolemia, and other causes of hyperlipoproteinemia.

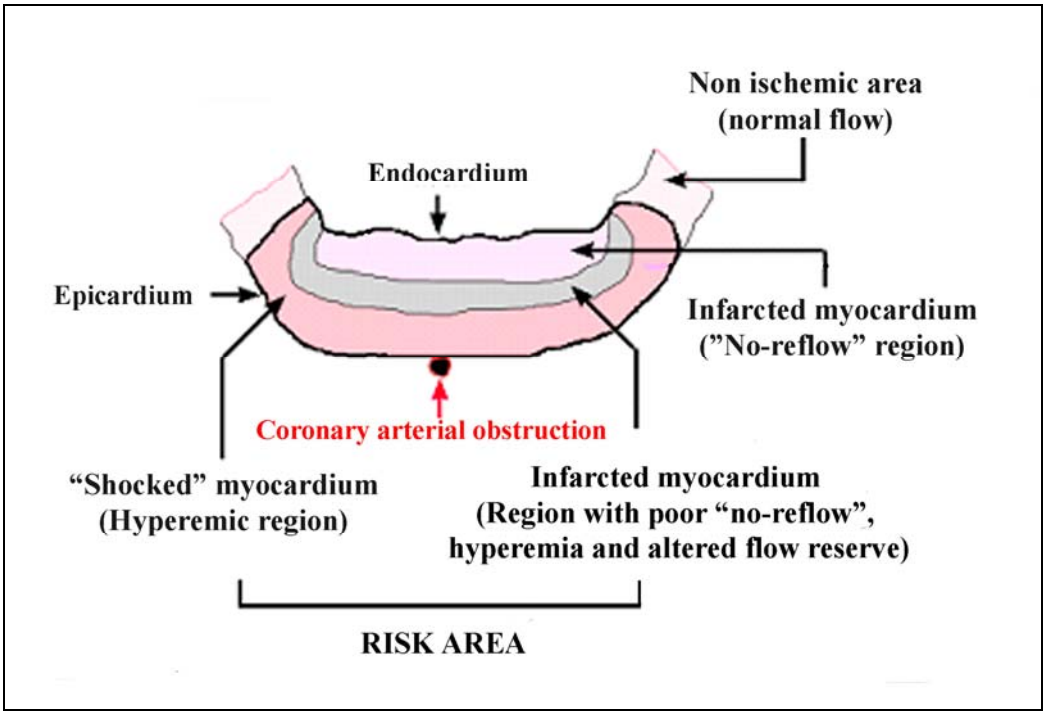

Figure 1. Different regions of damage in the infarcted myocardium. After coronary artery occlusion, necrosis begins in a small zone of the myocardium beneath the endocardial surface in the center of the ischemic zone and then proceeds progressively externally through the cardiac wall.

1.1.1 Myocardial response

As consequence of coronary arterial obstruction, the local blood supply is blocked and the myocardium undergoes profound functional, biochemical, and morphological changes.

The progression of ischemic necrosis in the myocardium begins with an irreversible injury of ischemic myocytes in the subendocardial zone. With more extended ischemia, a wave front of cell death moves through the myocardium to involve progressively more of the transmural thickness of the ischemic zone. The precise location, size, and specific morphologic features of an acute myocardial infarct depend on:

- location, severity, and rate of development of coronary atherosclerotic obstructions

- size of the vascular bed perfused by the obstructed vessels
- duration of the occlusion
- metabolic/oxygen needs of the myocardium at risk
- extent of collateral blood vessels
- presence, site, and severity of coronary arterial spasm
- other factors, such as alterations in blood pressure, heart rate, and cardiac rhythm.

Beside this irreversible cardiomyocyte damage, ischemia includes the formation of a "shocked" or "hibernating" myocardium, a normally perfused but hypocontractile border zone myocardium (BZM) important for the remodelling process and the development of congestive heart failure (Figure 1). The BZM initially involves a narrow perimeter around the infarct, but as remodelling occurs the BZM extends to involve more normally perfused myocardium, until congestive heart failure develops.

1.1.2 The wound healing process

In general, four phases of cardiac wound healing can be distinguished *(Cleutiens et al., 1999)*. Phase 1 is characterized by death of cardiomyocytes, via necrosis or apoptosis. Apoptosis is a major source of myocyte loss after infarction and the peak has been reported 6–8 h after infarction in humans and rats. Fatty acid binding protein (FABP), troponin T, and creatine kinase, skeletal–brain hybrid type (CK-MB) and serum glutamic-oxaloacetic transaminase (SGOT) are released into the blood and they can be used as markers of myocyte death.

The majority of the apoptotic cells after infarction cannot be phagocytosed by neighbouring cells and secondary necrosis occurs from 12 h until 4 days after infarction. This type of cardiomyocyte death evokes an early inflammatory response (phase 2 of cardiac wound healing). One of the first features of this inflammatory response is activation of the complement system, and release of several cytokines, such as IL-6 and IL-8, which occurs 12–16 h after the onset of ischemia in humans.

Within 6–8 h after the onset of infarction neutrophilic granulocytes (PMN) migrate into the infarcted area. Peak numbers of granulocytes are observed 24–48 h after infarction. Granulocytes help to remove the dead myocytes. Granulocyte infiltration is followed by an influx of other inflammatory cells, including lymphocytes, plasma cells and macrophages.

Two to three days after infarction new extracellular matrix proteins are deposited, first in the border zone between infarcted and non-infarcted tissue, and later in the central area of the infarct. This marks the onset of phase 3 of the process of cardiac wound healing, the formation of granulation tissue, which increases the tensile strength of the infarct and prevents cardiac rupture.

The process starts with deposition of fibrin, followed by the deposition of other extracellular matrix proteins, such as fibronectin and tenascin. Within a few days after infarction, myofibroblasts have surrounded the infarcted area and produce interstitial collagens. Complete collagen cross-linking may take a few weeks to occur.

Concomitant with activation of collagen synthesis, collagen degradation is activated by specific matrix metalloproteinases that cleave interstitial collagens. Increased collagenolytic activity can result in loss of structural support, distortion of tissue architecture, reduction of cardiac stiffness, wall thinning and even rupture of the myocardium.

Granulation tissue is also characterized by the presence of many blood vessels. Within a few days after infarction new blood vessels start to appear in the wound. These new blood vessels are derived from pre-existing blood vessels or from endothelial cells that migrate from the border zone into the wound (neoangiogenesis).

2–3 week old granulation tissue in an infarcted heart is characterized as a cell rich tissue, containing (partly) cross-linked interstitial collagens, macrophages, blood vessels, and (myo)fibroblasts. The fourth phase of cardiac wound healing is the period of scar tissue formation.

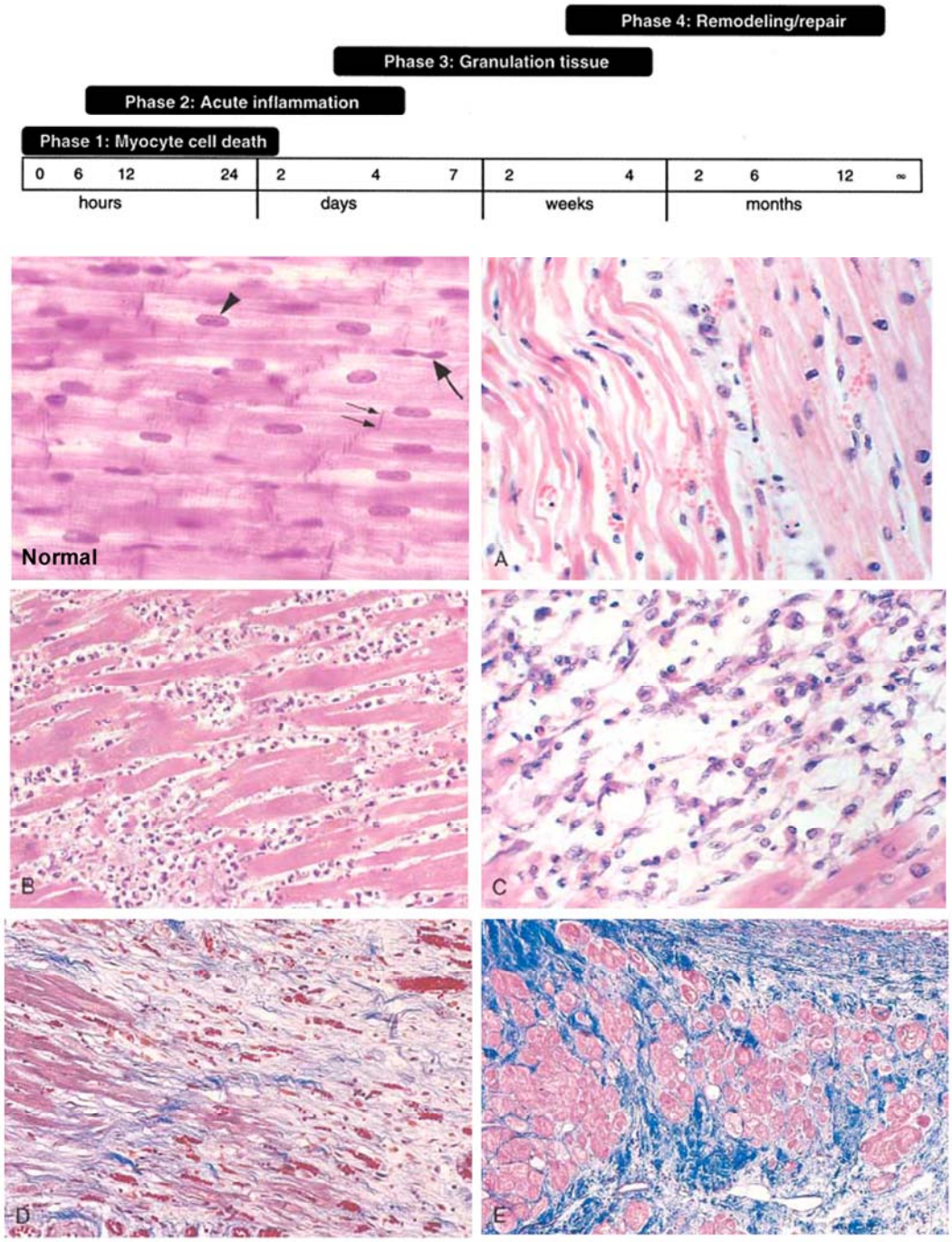

Figure 2. Temporal and histological stages of myocardial infraction. The histology of myocardium is shown, emphasizing the centrally-placed nuclei of the cardiac myocytes (arrowhead), intercalated discs (representing specialized end-to-end junctions of adjoining cells; highlighted by a double arrow) and the sarcomeric structure visible as cross-striations within myocytes. A capillary endothelial cell is indicated by an arrow (Normal). One-day-old infarct showing coagulative necrosis along with wavy fibers (elongated and narrow), compared with adjacent normal fibers (at right). Widened spaces between the dead fibers contain edema fluid and scattered neutrophils (A). Dense polymorphonuclear leukocytic infiltrate in area of acute myocardial infarction of 3 to 4 days' duration (B). Nearly complete removal of necrotic myocytes by phagocytosis (approximately 7 to 10 days) (C). Granulation tissue characterized by loose collagen and abundant capillaries (D). Well-healed myocardial infarct with replacement of the necrotic fibers by dense collagenous scar. A few residual cardiac muscle cells are present (E). *(modified from Robbins et Cotran, 2007 and from Cleutiens et al., 1999)*

Except the majority of myofibroblasts, cells start to disappear from the wound, probably by apoptosis, and the collagen become almost completely cross-linked. This so formed scar tissue has a permanent nature and can not be reabsorbed because of the lack of cardiomyocyte regeneration. It is however a dynamic tissue: cellular, vascularized, metabolically active and contractile *(Sun et Weber, 2000).* The repair process described above requires usually two months to complete in most human infarcts (summary in Table 1). The time course of gross and microscopic changes can vary: in general, a larger infarct will evolve through these changes more slowly than a small infarct. Moreover, cardiac wound healing is accelerated in smaller animals such as mice and rats, compared to humans.

Table 1. Evolution of Morphologic Changes in Myocardial Infarction

Time	**Gross Features**	**Light Microscope**	**Electron Microscope**
Reversible Injury			
0–½ hr	None	None	Relaxation of myofibrils; glycogen loss; mitochondrial swelling
Irreversible Injury			
½–4 hr	None	Usually none; variable waviness of fibers at border	Sarcolemmal disruption; mitochondrial amorphous densities
4–12 hr	Occasional dark mottling	Beginning coagulation necrosis; edema; hemorrhage	
12–24 hr	Dark mottling	Ongoing coagulation necrosis; pyknosis of nuclei; myocyte hypereosinophilia; marginal contraction band necrosis; beginning neutrophilic infiltrate	
1–3 days	Mottling with yellow-tan infarct center	Coagulation necrosis, with loss of nuclei and striations; interstitial infiltrate of neutrophils	
3–7 days	Hyperemic border; central yellow-tan softening	Beginning disintegration of dead myofibers, with dying neutrophils; early phagocytosis of dead cells by macrophages at infarct border	
7–10 days	Maximally yellow-tan and soft, with depressed red-tan margins	Well-developed phagocytosis of dead cells; early formation of fibrovascular granulation tissue at margins	
10–14 days	Red-gray depressed infarct borders	Well-established granulation tissue with new blood vessels and collagen deposition toward core of infarct	
2–8 wk	Gray-white scar, progressive from border toward core of infarct	Increased collagen deposition, with decreased cellularity	
>2 mo	Scarring complete	Dense collagenous scar	

1.1.3 Changes in the non-infarcted myocardium

Several studies have shown that the non-infarcted myocardium also plays an important role in the repair/remodelling process.

Changes in the non-infarcted myocardium, even if not as dramatic as the changes in the infarct, affect both the non-infarcted left ventricle and the right ventricle and many of the constituents of the myocardium, including the cardiomyocytes, the endothelial cells and the extracellular matrix.

The remodeling process known to occur in the border zone is characterized by myocyte slippage, elongation, hypertrophy, and a significant net loss of cardiac myocytes *(Beltrami et al., 1994)*. Cardiomyocytes are also the major cells undergoing apoptosis, while the synthesis of DNA is very low. Apoptosis is related to increased expression of pro-apoptotic genes *(Zhao et al., 2004)* and may contribute to the remodeling process after infarction *(Kajstura et al., 1996)* and to the induction or progression of cardiac failure after infarction *(Sabbah et al., 2000)*. The molecular mechanisms responsible remain largely unknown. Nevertheless it seems that the myocyte apoptosis is causally related to increased oxidative stress *(Li et al., 1998; Nogiri et al., 2006)*.

DNA synthesis is more prominent in the endothelial cells lining the capillaries, but it is still not high enough to fully compensate for the amount of cardiomyocyte hypertrophy. The result is a decrease of the capillary to myocyte fiber ratio and, hence, an increase of the oxygen diffusion distance *(Kuizinga et al., 1998)*. The relative oxygen deficit is associated with a shift of the myocyte phenotype to a fetal phenotype in the rat, and enables the myocyte to function at a lower energy consumption level *(Boheler et Schwartz, 1992)*.

Within 1 week after infarction, besides changes in the cardiomyocyte and endothelial cell components, the amount of interstitial collagens changes and at least doubles in the human and the rat heart *(Volders et al., 1993; Cleutjens et al., 1995)*. As in the infarct, type I collagen deposition is preceded by type III collagen. An increase in interstitial collagens may be beneficial to the heart in that it may help to prevent dilatation. Increased amounts of interstitial collagens will, on the other hand, it also increases the stiffness of the heart and result in a reduced cardiac function.

1.1.4 Complications

Clinical complications of myocardial infarction occur in a time-dependent manner and depend upon the size and location of the infarction, as well as pre-existing myocardial damage. Complications can include:

- Arrhythmias and conduction defects, with possible "sudden death"
- Extension of infarction, or re-infarction
- Congestive heart failure (pulmonary edema)
- Cardiogenic shock
- Pericarditis
- Mural thrombosis, with possible embolization
- Myocardial wall rupture, with possible tamponade
- Papillary muscle rupture, with possible valvular insufficiency
- Ventricular aneurysm formation

Sudden death is defined as death occurring within an hour of onset of symptoms. Such an occurrence often complicates ischemic heart disease. Such patients tend to have severe coronary atherosclerosis (>75% lumenal narrowing). Often, a complication such as coronary thrombosis or plaque haemorrhage or rupture has occurred. The mechanism of death is usually an arrhythmia.

1.2 Tissue engineering

The purpose of tissue engineering is to generate new tissues combining cells and biomaterials to replace or re-establish physiological function lost in unhealthy or damaged organs. These constructs have to mimic the tissue microarchitecture and the microenvironment surrounding the cells in the body.

There are three major components in a tissue engineering system:

- Cells: they must be able to proliferate and differentiate in a controlled and reproducible manner.
- Scaffold: furnishes a 3D support for attachment of the cells and growth of the tissues.
- Bioreactors: not always necessary, they furnish the *in vitro* environment for developing functional tissue.

The scaffold plays a central role in a tissue engineering system. It can allow the regeneration in vivo of remaining healthy tissues or guide the formation of a tissue from dissociated implanted cells, *ex vivo* and *in vivo*. In another application, the scaffold may temporarily replace the extracellular matrix (ECM) for the cells, until they produce their own.

The ideal scaffold must meet several criteria. It should be biocompatible, sterilizable and avoid the foreign body response. It should also have a complex, three-dimensional and porous structure. These features have to enable a uniform spatial distribution of the seeded cells and their organization in a functional tissue. One solution for a good cell distribution is the adding of cell to the scaffold during the manufacturing process; unfortunately several of these processes involve heat or toxic chemicals that can damage or kill cells. The seeded cells need to be supplied with nutrients, so the scaffold should allow vascularisation near the most far and internal cells. At the same time, the polymer scaffold should have good mechanical properties and enable handling in culture and during transplantation. If necessary, it should be possible insert microstructures or portions of different materials in order to optimize cellular growth or mechanical properties. Finally, a key factor could be the ability to release growth factors, or other signals in a time-dependent fashion for cellular chemotaxis.

In general, biomaterials for tissue engineering and regeneration can be divided into three categories:

- Synthetic polymers
- Natural polymers
- Polymers resulting from a mix of the previous two.

Synthetic polymers have defined chemical and physical properties, such as molecular weight, degradation time and hydrophobicity, that can be controlled. However, they usually do not interact with the cells in a useful way, but they operate as mechanical support only. The most popular synthetic scaffold are the degradable polyesters composed of lactide (PLA) and glycolide (PGA) and their copolymers (PLGA). These polymers are biocompatible and FDA approved and are easy to manufacture. However, degradation of these polyester scaffolds is accompanied by accumulation of acidic products that affects cell viability and causes intense inflammatory reactions.

Natural polymers include ECM proteins and derivatives and materials derived from plants and seaweed. The most utilized polymers derived from ECM are type I collagen and fibronectin. They have the advantage of containing particular adhesive sequences, such as RGD, on their surfaces that can facilitate cell adhesion and maintain cell differentiation. Another natural polysaccharide widely used is alginate, a negatively charged polysaccharide from seaweed that forms hydrogels in the presence of calcium ions and can be developed as a 3D porous scaffold using a simple process based on freeze-dry technique. These materials allow prolonged culture of various primary mammalians cells and intense neovascularisation, but usually they do not posses sufficient mechanical strength and their composition strongly depends on the isolation procedure.

Table 2. Comparison between synthetic and natural polymers used in tissue engineering.

	Advantages	Disadvantages	Examples
Synthetic polymers	- Defined chemical and physical properties - Precise geometric form and mechanical properties - Safe - Easy to build	- Function as mechanical support only - Biodegradation can induce an inflammatory response	- PLA - PGLA
Natural polymers	- Facilitate cellulare adhesion - Induce only a mild inflammatory response	- Composition strictly correlated to the procedures	- Collagen I - Fibronectin

1.3 Cardiac regenerative medicine

Cardiac tissue engineering is an approach able to help the restoration of altered cardiac function. Three different approaches can be utilized:
- Induction or stimulation of endogenous repair mechanisms (such as cytokine mobilization);
- Transplantation of isolated cells;
- Use of engineered tissue construct.

1.3.1 Cytokine mobilization

Mobilization of Bone Marrow Stem Cells (BMSCs) with cytokines might offer a noninvasive therapeutic approach treating MI and other forms of cardiac pathology. The bone marrow is, in effect, a large reservoir of adult stem cells distal from the heart that can be enrolled for cell-mediated cardiac repair via regeneration of healthy myocardial tissue and recovery of cardiac function. These could be accomplished by neo-angiogenesis, cardiogenesis, and/or paracrine effects.
The best-studied cytokine in this regard is Granulocyte-colony stimulating factor (G-CSF). Several studies have showed that i.v. injection of G-CSF improve ventricular function in mice *(Orlic et al., 2001; Deindl et al., 2006; Kanellakis et al., 2006)*, rat *(Sugano et al., 2005)*, rabbit *(Minatogouchi et al., 2004)* and pig *(Kasegawa et al., 2006; Iwanaga et al., 2004)*. On the other hand, other groups have found no evidence of beneficial effects in mice *(Deten et al., 2005)* or baboons *(Norol et al., 2003)*.
The mechanism of action of this cytokine is not yet clearly understood and it could be acting in different ways. Misao et al *(2006)* demonstrated that bone marrow-derived progenitor cells recruited into the infarcted myocardium are the primary mediators of the beneficial effects of G-CSF. But this seems not be the only mechanism involved in the process of amelioration. G-CSF is in effect able to mobilize 1% of progenitor cells, while the remaining 99% is constituted by committed granulocytes and monocytes. Thus, these leukocytes could play an important role in repairing the damaged myocardium. Recently Minatoguchi et al. *(2004)* showed in a rabbit model that G-CSF increases the area of surviving myocardial tissue,

accelerating absorption of necrotic tissue via an increased number of macrophages and reducing granulation and scar tissues via expression of matrix metalloproteinases (MMPs).
Another possibility is that G-CSF treatment acts directly on cardiomyocytes protecting against oxidation-induced cell death *(Harada et al., 2005)*: cardiomyocytes would express G-CSF receptor and G-CSF activates the Jak/Stat pathway . G-CSF also would be able to reduce apoptosis of endothelial cells and increase vascularization in the infarcted hearts, further protecting against ischemic injury.
Moreover, the combination of G-CSF and myelo-suppressives *(Misao Y. et al., 2007)* may be a useful new therapy that overcomes the insufficiency seen in some cases with G-CSF alone. This therapy may reflect repair-related paracrine effects such the augmented expression of MMP-1, which is involved in the decrease of collagen during the scar-formation process, or, similarly, increased levels of the angiogenic growth factor VEGF, which may be related to the increase in microvessels. In addition, the regeneration of myocardial tissue may occur by recruitment of $CD34^{+}CXCR4^{+}$ cells into the infarcted myocardium.
Based on these results, several human trials were recently carried out. Conflicting findings arrived from different recent studies, but in summary, we can say that therapy with G-CSF could in the future be a powerful and promising tool in the restoration of injured myocardium.

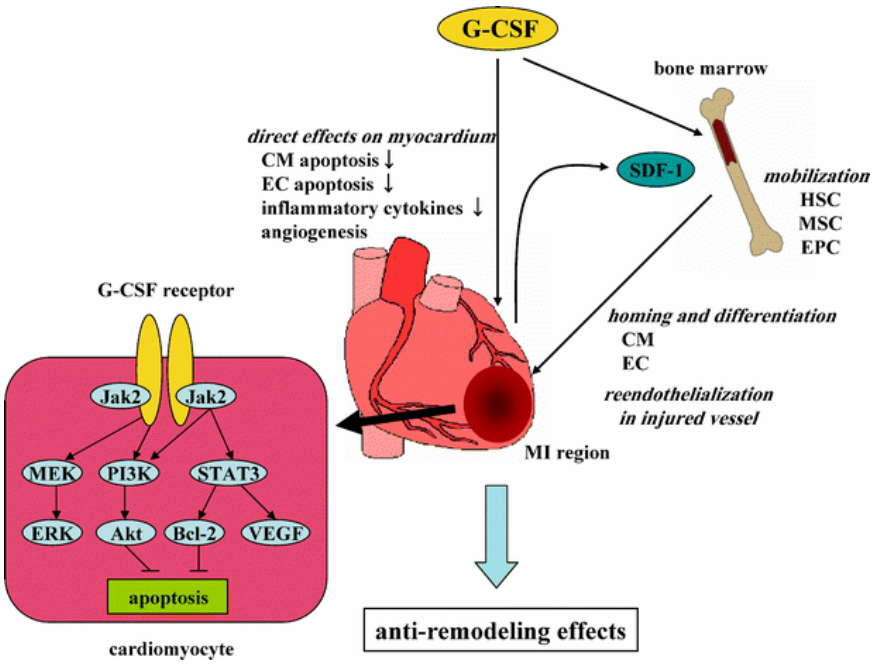

Figure 3. Hypothetical scheme demonstrating the possible mechanisms of cardioprotection induced by G-CSF. *CM* Cardiomyocyte, *EC* endothelial cell, *EPC* endothelial progenitor cell, *ERK* extracellular signal-regulated kinase, *HSC* hematopoietic stem cell, *Jak2* Janus kinase 2, *MEK* ERK kinase, *MI* myocardial infarction, *MSC* mesenchymal stem cell, *PI3K* phosphatidylinositol 3-kinase, *SDF-1* stromal cell-derived factor-1, *STAT3* signal transducer and activator of transcription 3, *VEGF* vascular endothelial growth factor. *(from Takano et al., 2006)*

1.3.2 Cell therapy

Various types of cells have been considered for the repair of myocardial tissue damage. It is possible to divide the sources of cellular recruitment into allogeneic and autologous. Allogeneic derivation uses cells derived from embryos (ESCs), fetal or neonatal cardiomyocytes (from cadaver donors) or haematopoietic stem cells, meanwhile the autologous derivation uses cells harvested from the same person who will receive the therapy: skeletal and smooth muscle cells (or skeletal muscle progenitor cells), cardiomyocytes (CM), multipotent adult stem cells such as bone marrow derived cells (haematopoietic and mesenchymal), endothelial progenitors (EPCs), mesenchymal stem cells (MSCs), resident myocardial progenitors, or fetal stem cells (from amniotic liquid and umbilical cord blood).

Embryonic stem cells. Due to their high plasticity this type of cell is one of the most promising sources for therapy of the infarcted myocardium. ESCs are derived from the inner cell mass of blastocyst stage embryos. They are totipotent as able to differentiate into derivatives of all three primary germ layers that arise during development (ectoderm, endoderm and mesoderm *(Bradley et al., 1984)* and thus into all somatic cells of the adult individual. In particular when cultivated in suspension (embryos body formation) the ESCs are able to differentiate into cardiomyocytes. ESC-derived cardiomyocytes express the major cardiac proteins, show contractile characteristics and may also have the capacity to couple electromechanically with the host myocardium successfully *(Mummery et al., 2003; Xu et al., 2002; Westfall et al., 1997; Maltsev et al., 1993)*.
Rodents have mainly been used to study the behavior of transplanted ESCs either in uninjured or infarcted hearts *(Singla et al., 2007; Kofidis et al., 2004; Behfar et al., 2002; Min et al., 2002; Yang et al., 2002)*, resulting in engraftment, improved left ventricular (LV) function and reduced LV remodelling.
Despite that, the propagation, CM differentiation and selection of ESCs have to be improved in order to obtain a sufficient number of cells available for patients. In addition, ESCs have obvious limitations due to ethical issues, immunogenicity and propensity to teratoma formation.

Skeletal myoblasts. These cells are progenitor cells that normally mediate regeneration of skeletal muscle. They have characteristics similar to cardiomyocytes, including the organisation of their contractile units. In addition, skeletal myoblasts have high proliferative capacity, are resistant to the ischemia and eliminate the need for immunosuppression *(Menasche, 2005; Pagani et al., 2003; Murry et al., 1996)*.
Preclinical and clinical studies of post MI administration of skeletal myoblasts demonstrate engraftment and functional improvement *(reviewed by Menasche, 2007)*. Despite their beneficial effects, the engrafted myoblasts do not differentiate into cardiac myocytes and remain committed to a skeletal muscle fate *(Reinecke et al., 2004)*. They also do not express the adhesion or gap junction proteins required to electromechanically couple with host myocardium *(Reinecke et al., 2000)* and, in rats, the grafts do not beat in synchrony with host rat myocardium *(Leobon et al., 2003)* . These cells may secrete a variety of angiogeneic and antiapoptotic factors that contribute to protect the damaged myocardium.

Bone marrow mesenchymal stem cells. Besides supporting haematopoietic stem cells (HSCs), BM-MSCs allow the stromal regeneration and are involved in the process of bone regeneration after fracture *(Stocum, 2001)*. In humans, BM-MSCs are usually isolated from marrow aspirates of the superior iliac crest of the pelvis *(Digirolamo et al., 1999)*. In most animals, bone marrow is obtained from the same sites, while in rodents it is commonly harvested from diaphysis of tibia and splint bone. These cells represent only a small fraction (0,001-0,01%) of the total population of nucleated bone marrow cells, but they can be plated

and enriched using normal cell culture techniques. In culture, by the second passage the BM-MSCs retain a spindle shape and express a large number of surface molecules, but not haematopoietic markers. Some markers are given in table 3. Some variations in surface markers has been seen from laboratory to laboratory, but generally they have remarkably reproducible attributes.

Table 3. Surface molecules present on hMSC.

hMSC Surface Markers	
Positive	**Negative**
CD13, CD29, CD44, CD49a, b, c, d, e, f, CD51, CD54, CD58, Cd71, CD73, CD90, CD102, CD105, CD106, CDw119, CD120a, CD120b, CD123, CD124, CD126, CD127, CD140a, CD166, P75, TGFb1R, TGFbIIR, HLA- A, B, C, SSEA-3, SSEA-4, D7	CD3, CD4, CD6, CD9, CD10, CD11a, CD14, CD15, CD18, CD21, CD25, CD31, CD34, CD36, CD38, CD45, CD49d, CD50, CD62E,L,S, CD80, CD86, CD95, Cd117, CD133, SSEA-1

Experimental studies have demonstrated that BM-MSCs can maintain their properties for several passages and are able to differentiate into cells of mesodermic origin such as osteoblasts, chondroblasts, adipocytes, fibroblasts and skeletal myoblasts *(Fridenshtein, 1982; Haynesworth et al., 1992; Gronthos, 1996; Prockop, 1997; Pittinger et al.,1999).* Moreover, these cells have the capacity to develop into non-mesodermic cell types: endothelial cells *(Reyes et al., 2002; Jiang et al., 2002)*, neuroectodermic cells *(Jiang ed al., 2002; Kopen et al., 1999; Woodbury et al., 2000)* and endodermic cells *(Jiang et al., 2002; Schwartz et al., 2002).*

It seems possible that BM-MSCs injected directly in an adult heart may differentiate in cardiomyocytes, endothelial cells , pericytes and smooth muscle cells *(Gojo et al., 2003)*.

Summarizing, as recently reviewed *(Pittenger and Martin, 2004)*, hMSCs posses:

- ease of isolation
- high expansion potential
- genetic stability
- reproducible attributes from isolate to isolate
- reproducible characteristics in widely dispersed laboratories
- compatibility with tissue engineering principles
- potential to enhance repair in many vital tissues

Thus, these cells may provide an excellent model for cellular therapeutic development. In particular, MSCs appear to have low immunogenicity and the ability to home to the site of myocardial injury when administrated after acute infarction *(Saito et al., 2002; Bittira et al., 2003).*

In the following table are recorded the latest studies where BM-MSCs were used for cardiac repair.

Table 4. Example of transplantation of BM-MSC in rodent or canine model.

Cell Type	Species Donor/ Recipient	N° of injected cells	Model	Histology	Results	Angio-genesis	Refs.
BM-MSC	R/R (isogenic)	$1x10^6$ cells diluted in DMEM	No AMI	Cells are incorporated and aligned with host cardiomyocytes. They are positive for sarcomeric myosin heavy chain. There is positivity for connexin43 between transplanted cells and the surrounding non-labeled cells.	ND	ND	*Wang et al., 2000*
BM-MSC	R/R (isogenic)	$2x10^6$ cell diluted in 50µl of DMEM	Proximal occlusion in the left coronary artery	Single cell or cluster of cells*:* in the scar the cells express a fibroblast phenotype, out of the infarcted region they show characteristics of cardiomyocytes (anti connexin43 show integration of the stained cells with the native cardiac myofibers).	ND	ND	*Wang et al., 2001*
BM-MSC	M/M (isogenic)	c-kit$^+$, $3x10^4$-$2x10^5$ in 5µl of PBS; c-kit$^-$, $5x10^4$-$5x10^5$ in 5µl of PBS: heterologous transplant	Coronary occlusion	The new myocytes Lin- c-kit+ express connexin43 and nuclear and cytoplasmic proteins typical of cardiac tissue: myocyte enhancer factor 2, MEF2; the cardiac specific transcription factor GATA-4; early marker of myocitic development Csx/Nkx2,5; light and heavy chains of myosin; TnI and TnT; desmin; atrial natriuretic factor, ANF; α actin.	Reduction of the infarcted area and improvement of cardiac hemodyna-mic.	The new myocardium is 68% of the infarcted region in the left ventricle; this tissue includes proliferating myocytes and vascular structures (arterioles and capillaries)	*Orlic et al., 2001*
BM-MSC	D/D	$2x10^7$ cell of bone marrow in PBS: autologous transplant	Chronic occlusion of left anterior descendent coronary artery	HE and IHC with canine anti-CD34	Improvment of ventricular function in the border zone in the animals with cells and worsening in those with PBS only. Worsening over time of ventricular function in the infarcted zone in both groups. No meaningful difference in the healthy region in both groups.	The density of microvessels at 30 days in the border zone is statistically bigger in the group treated with cells. The density in the healthy and infarcted zone is not different between groups.	*Hamano et al., 2002*
		No cells	Chronic occlusion of left anterior descendant coronary artery				
		$2x10^7$ BM cells in PBS: autologous transplant	No AMI	Controls for testing local and systemic toxicity of the injected BMSCs: no remarkable differences in white blood cells, alanin aminotransferase, aspartate aminotransferase, creatinin, LDH, CK; no		ND	

				remarkable differences also for ECG, cardiac function or in the movement of the cardiac wall. No histological differences in the migration of inflammatory cells. A little fibrosis was located in the injection area.			
BM-MSC and SKEL. MYOB.	R/R (isogenic)	$1x10^6$ cells in DMEM: autologous transplant	/	After 6 weeks, the cells in the cardiac myofibers express connexin43 in junction with other transplanted cells and the native cardiomyocytes. After 4 weeks the myoblasts form parallel myofibers.	ND	ND	*Chedraw y et a., 2002*
BM-MSC	H/M (CB17 SCID)	No AMI	Cells injected into the chamber of left ventricu-lum	In 12 animals single cells are diffused in the myocardium between 4 and 60 days. The cells differentiate and express TnT, desmin, α-actinin, fosfolamban.	ND	ND	*Toma et al., 2002*
BM-MSC	M/R	$6x10^6$ cells diluted in 300µl of DMEM (heterologous transplant)	Occlusion of descendent coronary artery 1 week after the second injection of cells	Labeled cells in the infarcted zone express sarcomeric myosin heavy chain, TnI and TnC	ND	Neovasculari-zation: labeled cells that express SM α–actin	*Saito et al., 2002*
			Left toracotomy only after 1 week from the injection (control)	No labeled cells in the myocardium	ND	ND	
BM-MSC	R/R (Lewis isogenic)	$5x10^6$ cells diluted in 500µl of DMEM. Same amount also injected 24h later.	No AMI	At 1 week labeled cells had homed in the bone marrow, but not in the myocardium	ND	ND	*Bittira et al., 2003*
			Coronary artery ligation	Labeled cells are near the infarct area. Evidence of myogenic differentiation. At 4 weeks he labeled cells are positive for cardiomyocytes specific TnI and connexin 43 staining.	ND	The labeled cells appear in the vascular walls and express SM α-actin	
BM-MSC	D/D	$0,5x10^6$ cells/kg	AMI following the cell injection	Deposition of collagen fibers and evidence of macrophages near the labelled cells. TnI detected in the plasma.	ND	ND	*Vulliet et al., 2004*
BM-MSC	R/R	$5x10^6$ cells in 2.5 ml of PBS.	Coronary artery ligation	Transplanted cells express vWf VIII and PCNA	Increase of SDF-1 expression. Improvement of cardiac function	Vessel and angiogenesis density is higher in the rats that received the MSC	*Ma et al., 2005*

Legend: BM-MSC = Bone Marrow Derived Mesenchymal Stem Cells; SKEL. MYOB. = Skeletal Myoblasts; R = Rat; M = Mouse; D = Dog; H = Human; DMEM = Dulbecco's Modified Eagle's Medium; PBS = Phosfate Buffer Solution; AMI = Acute Myocardial Infarction; HE = Heamatoxilin-Eosin; IHC = Immunohistochemistry; ECG = Electrocardiogram.

Endothelial Progenitor cells. The presence of circulating endothelial progenitor cells (EPCs) in humans was reported for the first time in 1997 *(Ashara et al., 1997)*. Using magnetic beads with antibodies to CD34, it is possible to separate a population from human peripheral blood that attach to fibronectin and grow well using medium for endothelium. The majority of circulating EPC reside in the bone marrow in close association with haematopoietic stem cells (HSC) and the bone marrow stroma that provides an optimal microenvironment. EPCs in the peripheral blood may derive from the bone marrow and be not yet incorporated into the vessel wall. These cells are functional precursors of endothelial cells, expressing AC133 and other endothelial cell surface markers *(Yin et al., 1997)*. They can also be mobilized with growth factors and cytokines and can home to injured areas *(Aicher et al., 2005)*.
When injected in a rat MI model *(Kocher et al., 2001)*, hEPC administered intravenously were able to migrate to the ischemic region and resulted in neovascularization and reduction of apoptosis in the treated animals.
This kind of cell probably facilitates angiogenesis, increasing perfusion and protecting the hypertrophied cardiomyocytes in the border zone from apoptosis. The possibility of production of proangiogenic factors directly from these cells also can not be excluded.

Cardiac stem cells. The heart may also contain a resident population of progenitor cells with cardiomyogenic potential. These cells express c-kit, sca-1, and MDR1 *(Quaini et al., 2002)*. c-kit$^+$ cells have been isolated from the adult rat heart: they are self-renewing, clonogenic and multipotent and when injected acutely into an ischemic heart, these cells give rise to myocytes, smooth muscle and endothelial cells, reconstituting the majority of infarcted myocardium *(Beltrami et al., 2003)*. Moreover, in another experiment after intracoronary administration of c-kit$^+$ cells, ventricular function was improved in a rat infarct model *(Dawn et al., 2005)*.
A subset of cells has also been isolated based on Sca-1 expression. These cells were able to differentiate into cardiomyocytes both *in vitro* and *in vivo (Oh et al., 2003)*.
In addition a Hoeschst dye-effluxing side population has been isolated from the adult mouse heart. The information on this kind of cell remains limited, but when cocoltured with unfractionated cardiac cells, some of the cardiac side population cells began to express the sarcomeric protein α-actinin *(Martin et al., 2003)*.
Recently, another progenitor population was reported that expresses isl1. Purified isl1$^+$ cells could be expanded in culture and they differentiated into cardiomyocytes only when mixed with cardiomyocytes. These cells are multipotent and can also give rise to endothelial, cardiac and smooth muscle cells *(Cai et al., 2003; Laugwitz et al., 2005; Moretti et al., 2006).*
Clearly these cells are not physiologically sufficient for repairing a damaged heart, but their properties could be very useful for cardiac cellular therapy.

1.3.3 Use of biomaterials

The choice of a scaffold must take into account the parameters previously described in the paragraph 1.2. Several tissue engineering approaches are being explored for cardiac repair. The most common is seeding cardiomyocytes, especially fetal and neonatal, onto a porous scaffold, typically constructed from a biodegradable polymer, such as Polyglycolic-Lactic Acid (PGLA), or natural polymers, such as collagen or alginate. Other cells like SMCs or embryonic stem cells have also been used with good results. Seeded myocardial constructs have been able to beat synchronously with the host myocardium, conduct action potentials, induce intense vascularization and in some cases improve ventricular function.
Some examples of cardiac tissue engineered constructs utilized *in vivo* are reported in Table 5.

Table 5. Some engineered cardiac muscle scaffold utilized *in vivo*. PGA = polyglycolic acid; KN-PCLA e WV-PCLA = ε-caprolatton and lattic acid copolymers; PTFE = polytetrafluoroetiline; EHT = engineered heart tissue, PIPAm = poly(N-isopropilacrilamide); UBM = urinary bladder matrix; AMI = acute myocardial infarction; RVOT = right ventricular outflow tract; LAD = left anterior descending coronary artery; SMC =smooth muscle cells; PEUU = polyester urethane urea.

Scaffold	Cells	Experimental Model	Results	References
Gelfoam (gelatin mix)	Rat fetal cardiomyocytes	Implant into the subcutaneous tissue or into cryoinjured heart of rat	The cells contract uniformly and spontaneously. Blood vessels grow in the surrounding tissue. The cells in the implant create junctions with resident cells.	Li et al., 1999
Alginate	Rat fetal cardiomyocytes	AMI in SD rats	Intense neovascularization of the endogenous coronary net. Presence of myofibers in collagen rich tissue. Decrease of LV dilatation and no changes in the LV contractility.	Leor et al., 2000
Gelatin	Rat adult or fetal cardiomyocytes	RVOT in Lewis rats	The seeded cells survive and the scaffold dissolves after 12 weeks. The patch surface is covered by endothelial cells.	Sakai et al., 2001
5 patches in comparison: gelatin PGA KN-PCLA WV-PCLA PTFE (non-biodegradable)	No cells seeded	RVOT in Lewis rats	The resident cells migrate in all the biodegradable materials. They are mostly fibroblasts. The cells secrete matrix and form tissue which is endothelized on the endocardic surface. The PCLA promotes more cellular colonization.	Ozawa et al., 2002
3 patches in comparison: gelatina PGA PCLA	Rat aorta SMC	RVOT in Lewis rats	The cells survive after the implant. The PCLA scaffold is replaced by several cells, mostly SM α-actin^{+}, and by ECM with several elastin positive regions. The PCLA allow a better cellular penetration and do not became thinner or dilate *in vivo*; no inflammatory response.	Ozawa et al., 2002
EHT (type I liquid collagen and matrigel)	Rat neonatal cardiomyocytes	Healthy Fischer rats	The echocardiographic analysis does not show LV function change. Intense vascularization after 14 days. Formation of organized structural cardiac muscle with cells positive for actinin, connexin 43 and cadherin.	Zimmermann et al., 2002 Eschenhagen et al., 2002 Zimmermann et al., 2004

PIPAAm (utilized for seeding cell layers)	Layers of rat neonatal cardiomyocytes	Subcutaneous transplant in Nude rats	Spontaneous contraction. Cardiac tissue structure and enhanced neovascularisation.	Shimizu et al., 2002
PCLA	Rat aorta SMC, labeled with BrdU	LAD ligation in Lewis rats	Formation of elastic tissue. Improvement of LV systolic function. Decrease of abnormal chamber distensibility. The cells migrate into the heart.	Matsubayashi et al., 2003
PCLA	SMC from Lewis rats	RVOT in Lewis rats	Formation of elastic tissue. Presence of fibroblasts and collagen after 22 weeks. Increase of the capillairy number. The SMC develop a cardiac phenotype. Endothelization of endocardic patch surface.	Ozawa et al., 2004
Collagen I	Mouse ESC $EGFP^+$	LAD ligation in rats	Stable intramyocardial implant incorporated into the surrounding area. It prevented thinning of the ventricular wall. The inoculated cells expressed connexin-43 and alpha-sarcomeric actin in vivo.	Kofids et al., 2005a
UBM and ePTFE	No cells seeded	LV infarct in swine	Appearance of fibrocellular tissue that included contractile cells. UBM better than synthetic.	Robinson et al., 2005
Liquid matrigel	Mouse ESC $EGFP^+$	LAD ligation in mice	The injectible liquid tissue solidifies at body temperature. The ESC express connexin 43. Cardiac functionality is improved.	Kofids et al., 2005b
PGA	Mouse ESC tranfected with GFP	LAD ligation in mice	After 8 weeks blood pressure and LV function are improved. GFP positive tissue was detected in infarcted area.	Ke et al., 2005
EHT (type I liquid collagen and matrigel)	Layers of rat neonatal cardiomyocytes	LAD ligation in Wistar rats	Integration and electric doubling of EHT with the host myocardium (no arrhythmias). Positive effect on LV systolic and diastolic function.	Zimmermann et al., 2006
Porous acellular Bovine pericardium	Rat MSC	Surgically created myocardial defect in the right ventricle in syngeneic rats	No aneurismal dilatation. Intimal thickening on the endocardial surface, but not thrombus formation. Intact layers of endothelial and mesothelial cells identified on the inner and outer surface of the patch. Some MSC differentiate into cardiomyocytes (staining for α-sarcomeric actin)	Wei et al., 2006

Collagen Hydrogels	Lamb fetal skeletal myoblast	Autologous implantation in healty myocardium of lambs	Fetal skeletal myoblasts engraft in native myocardium. At 24 and 30 weeks postimplantation, donor cells double-stained for green fluorescent protein and Troponin I, while losing skeletal (type II) myosin expression.	Fuchs et al., 2006
UBM	No cells seeded	Defect on right ventricular wall in swine	The extracellular matrix scaffolds were repopulated by α-smooth muscle actin–positive cells 60 days after implantation into the porcine heart. The presence of the cells corresponded to areas of the remodeling scaffold that showed early signs of electrical conductivity.	Ota et al., 2007
Collagen I	hMSC	LAD ligation in Fisher rats	At 1 week about 23% of cells engraft into the infarct area. Reduction of interior diameter at systole, increased anterior wall thickness and 30% increase in fractional shortening. hMSC were not detectable at 4 weeks after patch application.	Simpson et al., 2007
Basic fibroblast growth factor-loaded porous acellular bovine pericardium	Rat MSC	Surgically created myocardial defect in the right ventricle in syngeneic rats	None of the patches were thinned or dilated. Endothelialization and remesothelialization were observed on the endocardial and epicardial surfaces. Newly regenerated muscle fibers, glycosaminoglycans, smooth muscle cells, and microvessels. The MSC differentiate into cardiomyocytes, smooth muscle cells, and endothelial cells.	Chang et al., 2007
PEUU	No cells	Proximal left coronary ligation in Lewis rat	Formation of a tissue rich in SMC with mature contractile phenotype and improvement of cardiac remodeling and contractile function at the chronic stage.	Fujiimoto et al., 2007

Materials and Methods

2.1 Biomaterial

The porous collagen sponges were provided by Davol (Cranston, RI, USA). Collagen scaffolds were cut and shaped to obtain patches of the dimensions 0.8x0.8x0.3 cm^3 and were conditioned in MEMα for 16 h before the *in vitro* and *in vivo* experiments. This pre-treatment allows hydration and swelling of the scaffold and is necessary to avoid volume changes post-implantation and to enhance and favour cell adhesion. Besides its mechanical and physical properties, it is worth noting that this material has been selected because its clinical use is FDA approved.

2.2 In vitro cell seeding of the biomaterial

Vascular smooth muscle cells (SMC) were harvested from thoracic aorta of adult Wistar rats by tissue explants obtained after a 20 min collagenase digestion of minced tissue. SMC were grown for 10 days *in vitro* on plastic dishes (Falcon) coated with 1% gelatine and in the presence of 10% fetal calf serum (Gibco) in DMEM (Sigma).
Human umbilical vein endothelial cells (HUVECs) were purchased from PromoCell (Heidelberg, Germany) and cultured in DMEM with 20% FCS plus 2% Endothelial Growth Medium (Sigma). Cultures of cardiomiocytes (CMs) were obtained from neonatal heart rats. Tissue was digested with trypsin (Worthington; 50 mg/ml in Hanks's balanced salt solution) overnight at 4° C, followed by collagenase digestion (Worthington; 300U/ml in L-15 medium) for 45 min at 37° C. Cells were collected by centrifugation and then re-suspended in 68% DMEM (Life Tech), 17% M-199 (Sigma), 5% fetal bovine serum (Life Tech), 10% horse serum (Life Tech). Cardiac fibroblasts were removed by a selective pre-plating for 30 min at 37° C on Falcon dishes. CMs were then seeded on gelatine-coated Falcon dishes and grown for 10 days *in vitro*. Collagen scaffolds were pre-treated with the specific media for each type of culture. After 24 h SMCs and HUVECs were detached from the culture dishes with trypsin–EDTA, centrifuged and re-suspended in the specific culture medium; $1x10^4$ cells in 70 ml of medium were then dropped onto the collagen scaffold. Similarly for CM, $2x10^6$ cells were resuspended in 70 ml of medium containing 2 ml of Matrigel (Becton Dickinson). Seeded scaffolds were then incubated for 1 h and subsequently, 1 ml of the respective culture medium was added. In parallel, the same inoculum of SMCs, HUVECs or CMs was seeded on standard gelatine-coated Falcon dishes. After 10–15 days, the three types of cell cultures, either seeded on collagen scaffolds or on Falcon dishes, were rinsed in PBS and fixed in 2% para-formaldehyde in PBS, pH 7.2, before analysis.

2.3 In vitro cell culture of MSC

Bone marrow was obtained from transgenic rats that express Enhanced Green Fluorescent Protein (EGFP) constitutively under the β-actin promoter . All cells in the bone marrow express green fluorescent protein (GFP), and his fluorescence can be visualized . We prepared MSC from the marrow of 8-week-old rats. Both femora and tibias were removed aseptically and soft tissues were detached. Metaphysis from both ends were resected and bone marrow cells were collected by flushing the diaphysis with culture medium consisting of Modified Eagle's medium alpha (MEMα, Invitrogen) with 20% heat-inactivated fetal bovine serum (Sigma-Aldrich) and 1% penicillin-streptomycin (Sigma-Aldrich) using a 25 gauge needle and a 10 mL syringe. The released cells were isolated by centrifugation at 1500 rpm for 5 min and the supernatant was discarded. The cells were re-suspended as a single-cell suspension in culture medium, seeded onto 75 cm^2 culture dishes in culture medium, and incubated in a humidified atmosphere consisting of 95% air and 5% CO_2 at 37°C. The medium remained unchanged for the first 7-10 days. Subsequently the floating cells were removed and the

medium was changed two or three times a week. Before the culture reached confluence, 2 to 3 weeks after seeding, the cells were passaged by trypsinization (0.05% trypsin/EDTA solution) and then plated. For our experiments we used cells from passage 4 to passage 6.

2.4 Experimental animals

Eighty adult male Wistar rats (Charles River, Milan, Italy) weighing about 250-300 g and 2 adult male rNu rats (Charles River, Milan, Italy) weighing about 200 g were housed and maintained in a controlled environment. All surgical and pharmacological procedures used in this study were performed in accordance with the regulations expressed in the Guide for Care and Use of Laboratory Animals prepared by the Institute of Laboratory Animal Resources, National Research Council, published by the National Academy Press, revised 1996 (NIH Publication No. 85-23) and the Italian Health Minister Guidelines for Animal Research. The protocol was approved by the University of Padua Animal Care Committee.

2.5 Implantation of the collagen scaffold in a model of AMI

Thirty Wistar rats were divided into three experimental groups: in group 1 (n=10) cryoinjury alone was provoked; in group 2 (n=10) the scaffold was applied to the intact heart; in group 3 (n=10) the scaffold was sutured to a cryoinjured heart. The cryoinjury procedure was as follows: rats were anesthetized by tiletamine hydrochloride–zolazepam (Zoletil; Virbac, Carros, France; i.m.; 9 mg/100 g body weight) along with atropin (VaxServe, Scranton, PA; i.p.; 5 μg/100 g) and xylazin (Xilor; Bio 98, s.r.l., Bologna, Italy; s.c.; 0.4 mg/100 g) and subsequently intubated and ventilated mechanically with room air (Harvard, South Natick, MA). The heart was exposed through a left thoracotomy (third or four intercostal space) and a left ventricular acute necrotizing injury (ANI, freeze-thaw procedure) was created by three sequential exposures (60 s each, 20 s of non-freezing interval) of a liquid nitrogen-cooled cryoprobe (a stainless-steel cylinder, 8mm of diameter) (Harvard, South Natick, MA). Instauration of ANI was confirmed by wall blanching followed by hyperemia. Within 10 min after the injury, the collagen scaffold was placed on the epicardial anterolateral region corresponding to the cryoinjured area (about 12 mm^2) identified by the pale appearance with respect to the surrounding myocardium. In groups 2 and 3, the collagen cardiac patches were fixed to the epicardium with a cranially positioned 7–0 prolene suture. The chest was then closed and the animals weaned from the respirator, extubated and treated with antibiotics for 24 h (20 mg/100 g; Baytrill, Bayer, Milan). Animals were sacrificed at day 15 (n=5 per group) and 60 (n=5 per group) after surgery. An additional 10 rats were sacrificed at different intervals after ANI induction (3, 15, 30 and 60 days) for histological and immunocytochemical evaluation of the post-injury inflammatory response.

2.6 Implantation of the collagen scaffold in a model of CMI

Studying the effect of the cardiopatch in a model of CMI, a total of 26 male Wistar rats were used. We employed the same surgical procedures as the model of ventricular AMI, but after injury the thoracotomy was closed and the animals allowed to recover for 30 days. After this period the animals had a second thoracotomy to expose the heart.

Experimental groups similar to the model of AMI were used: group 1 (n=8) received the cryoinjury alone; in group 2 (n=8) the scaffold was applied to the intact heart; in group 3 (n=10) the scaffold was sutured to a cryoinjured heart. Animals were sacrificed at day 15 (n=5 per group) and 30 (n=5 per group). An additional 8 rats were sacrificed at different intervals from CNI induction (33, 45 and 60 days) for histological and immunocytochemical evaluation of post-injury inflammatory response.

2.7 Implantation of the collagen scaffold and rat CM GFP$^+$ in a model of AMI

Cardiomiocytes were obtained from the hearts of neonatal EGFP-transgenic rats using the method described in 2.2. After instauration of ANI in athymic rat rNu (n=2) the collagen scaffold was attached to the injured myocardium. 4x10^6 cells diluted in 90µl of αMEM were then injected within the patch right after the suture.

2.8 Implantation of the collagen scaffold and GFP$^+$ BM-MSCs in a model of CMI

10 Wistar male rats were used in experiments with rat GFP$^+$ BM-MSCs in a model of CMI . The day before the second operation the rats started the treatment with 10mg/Kg/day of Cyclosporine i.m. (CsA) (Sandimmun 50mg/ml injectable solution, Novartis Farma) until sacrifice. The animals were divided into the following groups: in group 1 (n=1) the animal received cryoinjury alone; in group 2 (n=1) the rat with CMI received via an intra-myocardial route the BM-MSC alone near the damaged zone; in group 3 (n=1) the patch was attached to the injured myocardium and than injected with medium alone; in group 4 (n=1) the patch was attached to the normal myocardium and the cells injected within it; in group 5 (n=4) the scaffold was implanted in the damaged hearts and subsequently injected with about 4x10^6 GFP$^+$ BM-MSCs.

BM-MSCs to be transplanted were extensively washed with αMEM and re-suspended in 90 µl of αMEM. In group 2 the cells were injected in the periphery of the damaged area at three distinct injection sites.

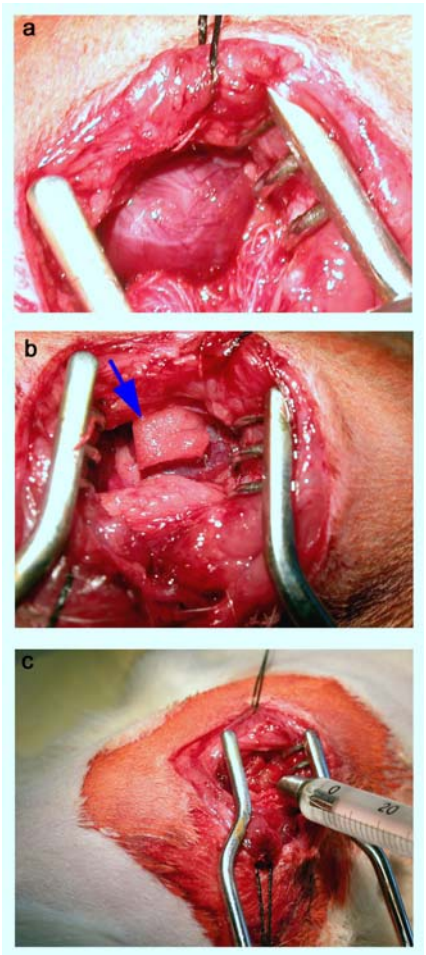

Figure 4. Events in the implantation of the collagen patch and GFP$^+$ BM-MSCs in a model of CMI. After 30 days, at the second operation, the cryoinjured area was identified by its pale appearance with respect to the surrounding myocardium (a). The collagen scaffold (blue arrowhead) was fixed on the epicardial anterolateral region corresponding to the damaged area with a 7-0 prolene suture (b). GFP$^+$ BM-MSCs resuspended in αMEM were injected into the patch (c).

2.9 Scanning electron microscopy

Critical point dried scaffolds were analyzed by scanning electron microscopy (SEM) using a Cambridge Steroscan 250 (Cambridge Instruments, Cambridge, MA). Samples were fixed in 2.5% glutaraldehyde in 50mM Na-phoshate buffer, pH 7.2 for 2 h at room temperature followed by dehydration through a series of graded ethanol solutions before critical point drying. The dehydrated scaffold was sputter coated with 9–12 Au–Pd before imaging at an accelerating voltage of 5 kV.

2.10 Flow Cytometry Analysis of GFP$^+$ BM-MSCs

Flow cytometry analysis was performed at passages 2 and 6. Rat BM-MSCs were detached by adding Trypsin-EDTA (Sigma) for 10 minutes, rinsed and resuspended in PBS at a concentration of $5x10^4$ cells per 100 µl. Cells were stained directly with 10 µl fluorescein isothiocyanate fluorochrome-labelled anti-rat CD90 and CD44, (Bioscience Pharmingen™), phycoerythrin- conjugated anti rat antibodies to the progenitor markers CD45, (Immunotech, Brussels, Belgium) MHCII (Biosience Pharmingen) and CD73 (Bioscience Pharmingen). Cytometric analysis was performed using a Coulter® EPICS® XL-MCL cytometer and data were elaborated by EXPO™ 32.

2.11 Cytospin of GFP$^+$ BM-MSCs

To monitor cytoplasmic antigens, GFP$^+$ BM-MSCs cells were collected using a Shandon Cytospin 4 centrifuge (Thermo Fisher Scientific, Inc., Waltham, MA) and than processed to immunofluorescence.

Semiquantitative evaluation of the cell expression profile in cytospins ($6–8 \times 10^4$ cells/spot) was carried out in a blinded fashion by two investigators who manually counted positive cells with respect to Hoechst-stained nuclei. There were at least 50 cells/field per count and five fields per each cytospin preparation were counted. Data were expressed as mean ± S.D.

2.12 Histology, histochemistry and morphometry

Ten-micron thick frozen sections were cut from the hearts of animals in each experimental group and stained with hematoxylin–eosin or Masson's trichrome staining. For each cardiac sample from each animal, five equatorial sections which included the collagen scaffold and/or the cryoinjury zone were reacted with antibodies against von Willebrand factor (wWf; for capillaries) and smooth muscle) SM α-actin (for arterioles and small arteries). The density of capillaries, arterioles and specifically immunoreactive interstitial cells, normalized to area (mm^2), were blindly evaluated by two independent investigators. The following zones were analyzed: the cryoinjury zone, the patches applied to injured or uninjured heart and the ''border zone'' between the cryoinjury zone and/or the intact myocardium. Leica Qwin software was used for collecting data and statistical analysis. Results of morphometric analysis were expressed as mean ± SEM. Statistical significance was evaluated by a paired Student's t test. A probability of <0.05 was considered significant.

2.13 Immunoperoxidase and immunofluorescence

Specific antibodies for cardiovascular differentiation markers were employed to determine the phenotypic profile of seeded (deriving from *in vitro* procedures) or infiltrating (*in vivo*) cells. Cryosections from the hearts of animals of different groups and the scaffold seeded with SMCs, CMs or HUVECs or cytospits of GFP$^+$ BM-MSCs cells were incubated at 37 °C with the appropriate dilution of the primary antibody in PBS+1% bovine serum albumin. The following primary monoclonal antibodies were used: anti-GFP (Molecular Probes), anti-SSEA4 (Chemicon. Milan, Italy), anti-Oct-4 (Chemicon), anti-c-kit (CD117, Dako, Dakopatts, Denmark), anti NGF-R (CD271, Pharmingen), anti-endoglin (CD105, Cymbus), anti-Thy-1 (CD90, Cymbus) anti-pan-cytokeratin (Sigma), anti-β1-integrin (Chemicon) anti-

Sca-1 (Cedarlane, Hornby, Ontario, Canada), anti-MDR1 (Chemicon), anti-vimentin (Dako), anti-VE-cadherin (Santa Cruz), anti-CD31 (Chemicon), anti-von Willebrand factor (vWf; Dako), anti-Flk-1 (Santa Cruz), anti-SM α-actin (Sigma), anti-SM-1 (SM-type myosin heavy chain isoform-1; Abcam), anti-sarcomeric tropomyosin (scTM; Sigma), anti-sarcomeric myosin (scMyosin; MF-20; Iowa Hybridoma Bank), anti-cardiac troponin T (cTnT; Abcam), anti-connexin 43 (Sigma), anti-nestin (Rat 401, Hybridoma Bank), GFAP (clone GA5; Chemicon). To study the spatio-temporal development of cryoinjury lesions in the heart and biocompatibility in the peritoneum, the following primary antibodies were used: anti-granulocytes (MCA149; Serotec, Oxford, UK), ED2 anti-macrophages (CD163; Serotec), anti-pan T lymphocytes (Cymbus), anti-CD45 (MRC OX-1; Chemicon), anti-dendritic cells (OX-62), anti-NK cells (CD161, Abcam), anti-fibronectin (fetal isoform; IST-9, Abcam). The secondary antibodies were Cy3- (Chemicon) or HRP-conjugated (Dako) goat Fab' to mouse IgG, and swine anti-rabbit IgG (Dako). Immunofluorescence observations were carried out using a Zeiss Axioplan epifluorescence microscope (Zeiss, Oberkochen, Germany), and images were acquired with a Leica DC300F digital videocamera (Leica, Wetzlar, Germany). For immunoperoxidase experiments binding of secondary antibodies was revealed by 3-amino-9- ethylcarbazole (AEC, Sigma) as substrate. Optical images were acquired by a Leica DMR microscope connected to a Leica DC300 videocamera. Controls were performed using non-immune mouse IgG instead of the primary antibodies, or by applying the secondary antibodies alone.

2.14 Western blotting

SDS-electrophoresis and Western blotting were carried out in a Biorad minigel apparatus using crude tissue extracts prepared by boiling for 3 min collagen cardiac patches carefully isolated from intact or cryoinjured hearts under a dissecting microscope. After electrophoresis, the separated polypeptides were transferred overnight to nitrocellulose paper (Schleicher & Schuell, Dassel, Germany) at 220mA at 4 °C; the paper was then dipped in 5% milk. The primary and secondary antibodies were diluted in 20mM Tris–HCl, 140mM NaCl containing 0.01% Triton X-100 and 3% bovine serum albumin. The following antibodies were used: anti-cTnT (Abcam), anti-SM α-actin (Sigma), anti-desmin (Chemicon) and anti-CD31 (Chemicon). HRP-conjugated rabbit IgG against mouse IgG (Dako) was used as secondary antibody. The Pierce chemiluminescence kit (Rockford, IL) was applied to reveal bound antibodies. Controls were performed using non-immune mouse IgG instead of the primary monoclonal antibody.

Table 6. Primary antibodies utilised for experimental analysis.

Antibody	Recognized antigen	Reference
Anti-β1	B1-Integrin: membrane protein, fibronectin coreceptor. Used as merker of mesenchymal stem cells.	Chemicon®
Anti SM α-actin	SM α-actin: isoform α of actin, expressed in vascular and visceral smooth muscle cells.	Sigma®
Anti- SM-1	SM-1: heavy chain (type 1) of smooth muscle myosin.	Chemicon®
Anti- SM-2	SM-2: heavy chain (type 2) of smooth muscle myosin.	Sigma®
Anti-CD161	CD161:expressed on Natural Killer cells.	Abcam®
Anti-CD45 rat	CD45: expressed on all the rat leucocytes.	Serotec®
Anti-c-Kit	c-kit or CD117: stem cell factor (SCF) receprtor.	Dako®

Anti-Collagen I	Collagen I: protein structured in fibrils in the extracellular matrix.	Sigma®
Anti-Collagen III	Collagen III: protein structured in fibrils in the extracellular matrix.	Chemicon®
Anti-Connexin 43	Connexin 43: gap junction protein found in the heart and brain that is known to bind tubulin.	Sigma®
Anti-cTnT	cardiac troponin T: expressed on cardiomyocytes.	Abcam®
Anti-Desmin	Desmin: subunit of intermediate filaments in skeletal muscle tissue, smooth muscle tissue, and cardiac muscle tissue	Chemicon®
Anti-Endoglin	Endoglin or CD105: tumour growth factor β1 (TGFβ1) receptor.	Cymbus®
Anti-Flk-1	Flk-1: vascular endothelial growth factor (VEGF) receptor.	Santa Cruz®
Anti-GFAP	GFAP (Glial Fibrillary Acidic Protein): typical of astrocytes and glial cells.	Chemicon®
Anti-GFP	GFP: green fluorescent protein.	Mol. Probes®
Anti-Granulocytes	The antibody recognizes antigens expressed on rat granulocytes.	Serotec®
Anti-MDR1	MDR1 (Multi Drug Resistence-1).	Chemicon®
Anti-MHC II	Major histocompatibility complex class II: found on a few specialized cell types, including macrophages, dendritic cells and B cells, all of which are professional antigen-presenting cells (APCs), it plays an important role in the immune response.	Pharmingen®
Anti-Nestin	Nestin: intermediate filament produced during central nervous system development and present in other embryonic tissues.	Chemicon®
Anti-NGFr	NGFr: Nerve growth factor receptpor.	Pharmingen®
Anti-Oct-4	Octamer-4: it is a homeodomain transcription factor of the POU family. It is used as a marker for undifferentiated cells.	Chemicon®
Anti-pan-Ck	Epitope localized in cytokeratines of type II 1, 5, 6 and 8: it is characteristic of epithelial cells	Sigma®
Anti-pan-T lymphocyte	Recognizes an antigen expressed on rat T lymphocytes.	Chemicon®
Anti-PECAM	PECAM or CD31: endothelial marker.	Chemicon®
Anti-sarcomeric Tropomyosin	The antibody recognizes an epitope on skeletal and cardiac tropomyosin.	Sigma®
Anti-Sca-1	Sca-1 (Stem cell antigen- 1): surface antigen of hematopoietic stem cells.	Cederlane®
Anti-SSEA4	Stage Specific Embryonic Antigen-4: it is commonly used as a cell surface marker to identify the pluripotent embryonic stem (ES) cells.	Chemicon®
Anti-Thy1	Thy1 or CD90: it can be used as a marker for a variety of stem cells and for the axonal processes of mature neurons.	Cymbus®
Anti-VE-caderin	VE caderin: adhesion molecule localized to endothelial cells.	Santa Cruz®
Anti-Vimentin	Vimentin: protein of intermediate filaments. High specificity for cells of mesenchymal origin.	Dako®
Anti-vWf	von Willebrand factor or factor VIII: factor released from endothelial cells and involved in coagulation.	Dako®
ED2	CD163: membrane protein expressed on the macrophages.	Serotec®
Ist-9	Fetal Fibronectin: extracellular matrix protein.	Abcam®
MF-20	Specific to Sarcomeric Myosin.	Hybridoma Bank®
OX-62	Integrin E2α: expressed on dendritic cells.	Serotec®

Results

3.1 Characterization of the collagen scaffold before transplantation

Before evaluating the suitability of collagen scaffold for supporting vascular and non-vascular cell growth *in vivo*, we examined the scaffold morphology and the *in vitro* capability of supporting cardiovascular cell differentiation.

3.1.1 Scaffold morphology

At the optical and SEM analyses (Figure 5) the collagen scaffold appears like a sponge and demonstrates the presence of highly interconnected channels and a porous appearance. At high resolution it is possible also to observe its microfibrillar structure.

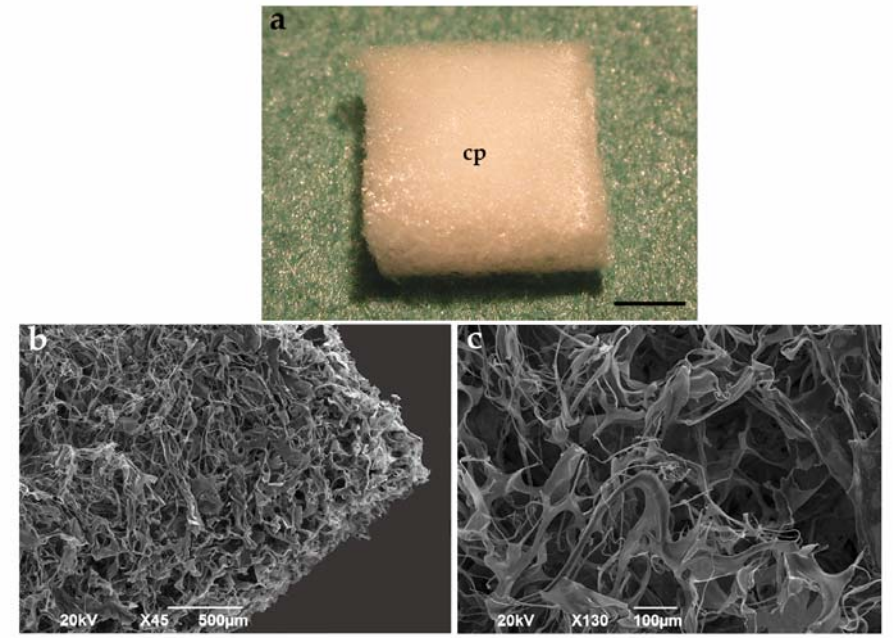

Figure 5. Optical (A) and SEM (B-C) images of the collagen scaffold. Cp = cardiopatch. Bar in a: 20 mm.

3.1.2 Ability to support cell seeding *in vitro*

The ability of the scaffold to support growth and differentiation of CM, SMC and EC *in vitro* is shown in Figure 6. The collagen sponge could be seeded with all cell types that easily engrafted to the biomaterial as shown by hematoxylin–eosin staining (Figure 6d). All cell types connected very tightly with the collagen fiber and retained a round morphology within the biomaterial (panels f, h and j) in contrast to the corresponding cells grown on plastics which displayed spread features (panels e, g and i). Differentiation markers such as cTnT, scTM, scMyosin for CM, SM α-actin, SM-1, SM-2 for SMC and vWf, CD3, VE-cadherin for EC are well expressed in cells grown both on plastic and on collagen sponges (see Table 7). As a general rule, rat SMC and HUVEC showed a similar differentiation pattern, independent of the substrate. Conversely, marked differences were found with rat CM: seeding of these cells on the collagen scaffolds markedly increased the expression of CM markers such as cTnT, sarcomeric tropomyosin and myosin. Nestin expression was also improved in CM cultivated on scaffolds. Moreover CMs seeded on the collagen scaffold could survive usually 1 week longer than those seeded on plastic.

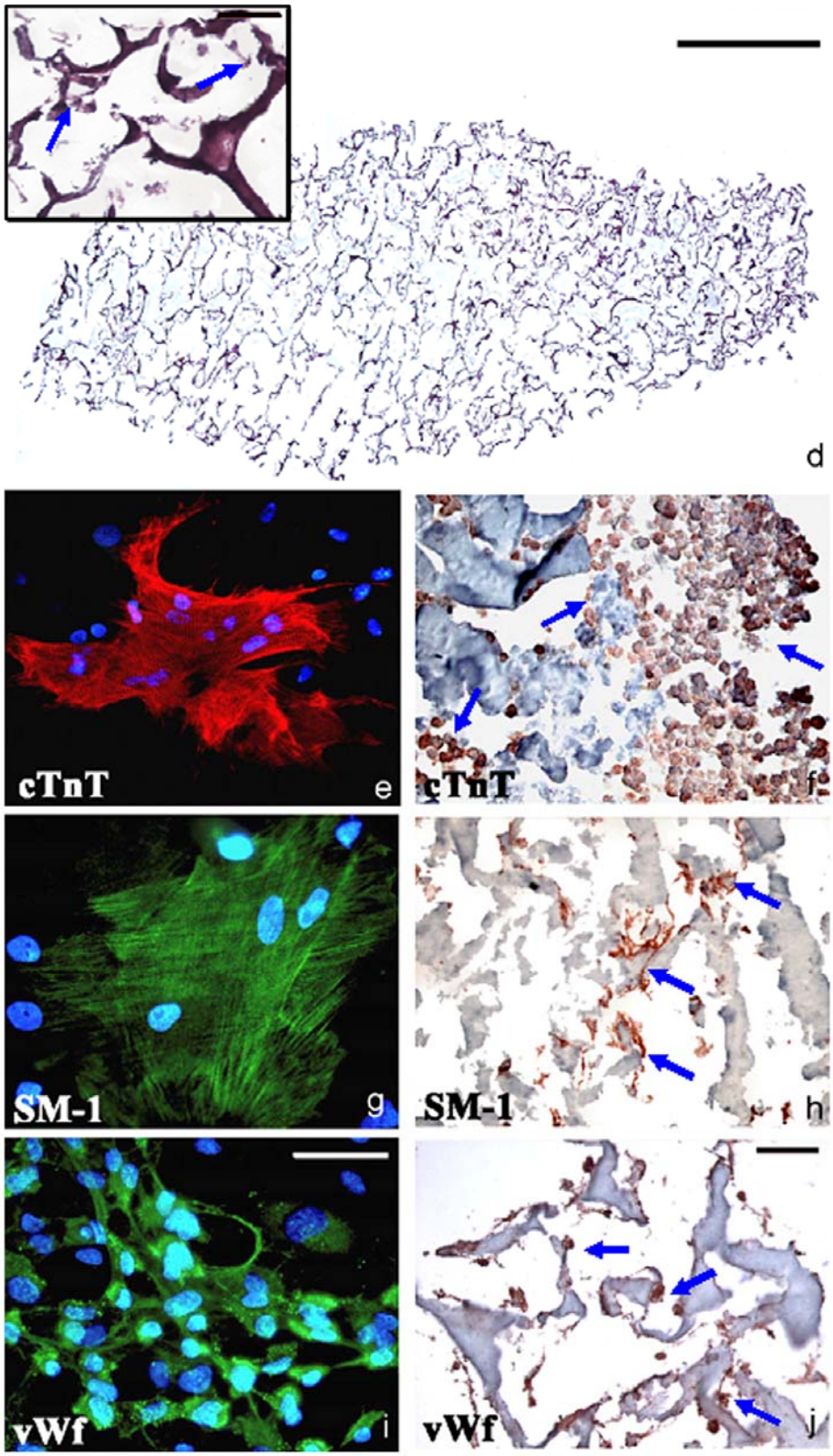

Figura 6. Effects of in vitro cardiovascular cell seeding on this biomaterial (d, f, h and j) in comparison with standard plastic substrate (e, g and i). Differentiation patterns achieved by neonatal CM, aortic SMC and HUVEC on the two substrates after 15 days in vitro are shown in panels e-f, g-h and i-j respectively. A low magnification image of the hematoxylin–eosin staining of the biomaterial seeded with HUVEC is shown in panel d. Cells in the sponge are identified by blue arrowheads (inset in panel d). Cells grown on plastics were analyzed by immunofluorescence whereas those grown on the biomaterial were analyzed by immunoperoxidase staining. Brown arrowheads in panels f, h and j indicate examples of the different morphologies. Bars: d, 1mm (inset 50 mm); e–j, 50 mm.

Table 7. *In vitro* expression of cardiovascular differentiation markers in rat SMC and CM, and HUVEC seeded on plastics or collagen scaffold.

Antigen	**Type of substrate**	
	Plastics	**Scaffold**
1. Rat SMC		
SM a-actin	+++	+++
SM-1	++	++
SM-2	+/-	+/-
Vimentin	+++	+++
2. Rat CM		
cTnT	+	++
scTM	+	++
scMyosin	+	++
Nestin	+	++
3. HUVEC		
vWf	+++	+++
CD31	+++	+++
VE-cadherin	+++	+++
Vimentin	+++	+++

Legend: SM a-actin, smooth muscle type a-actin; SM-1 and -2, type-1 and -2 SM myosin isoforms; cTnT, cardiac troponin T; scTM, sarcomeric-type tropomyosin; scMyosin, sarcomeric-type myosin; vWf, von Willebrand factor.
Number of cells positive for the respective antibody: +++, >90%; ++, 40–90%; +, 5–40%; +/-, <5%; -, no immunoreaction. Rat SMC/HUVEC and rat CM were studied after 15 and 10 days in culture, respectively.

3.2. Implantation of the collagen scaffold in a model of Acute Myocardial Infarction (AMI)

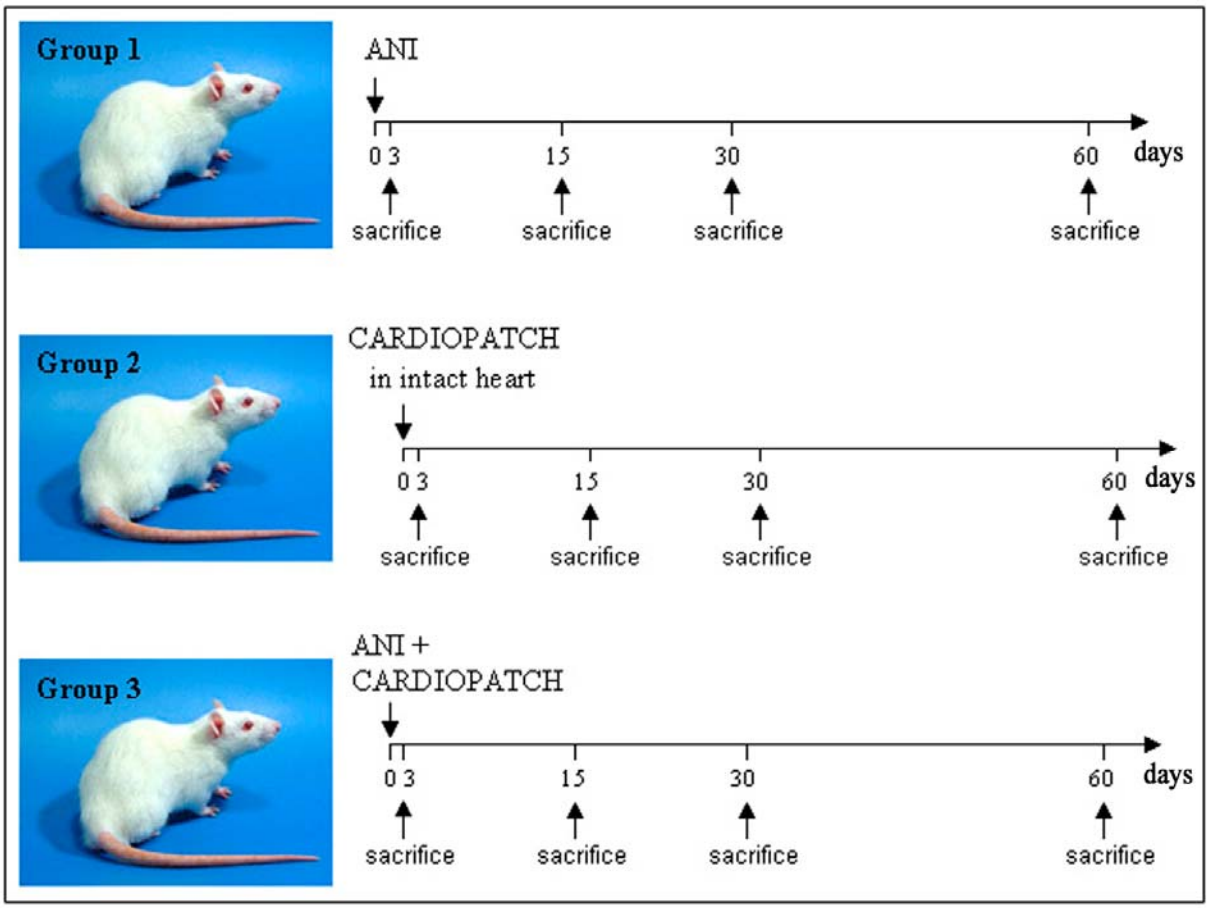

Figure 7. The Wistar rats were divided into three experimental groups: in group 1 the cryoinjury alone was provoked; in group 2 the scaffold was applied to the intact heart; in group 3 the scaffold was sutured to a cryoinjured heart. ANI = acute necrotizing injury.

3.2.1 Gross appearance, Haematoxylin-eosin and Masson's Trichrome staining

The effects of the collagen cardiac patches on both healthy (groups 2) and cryoinjured (group 3) rat hearts were studied and compared to animals that underwent a heart cryoinjury only (group 1). At explantation, all animals revealed no thoracic adhesions. By gross observation, the cardiac patch was firmly attached to the epicardial surface independently from the previous cryoinjury (Figure 8a–c). Sixty days after cardiac patch implantation, 40% of the original scaffold volume was still evident with Masson's staining (Figure 8d).

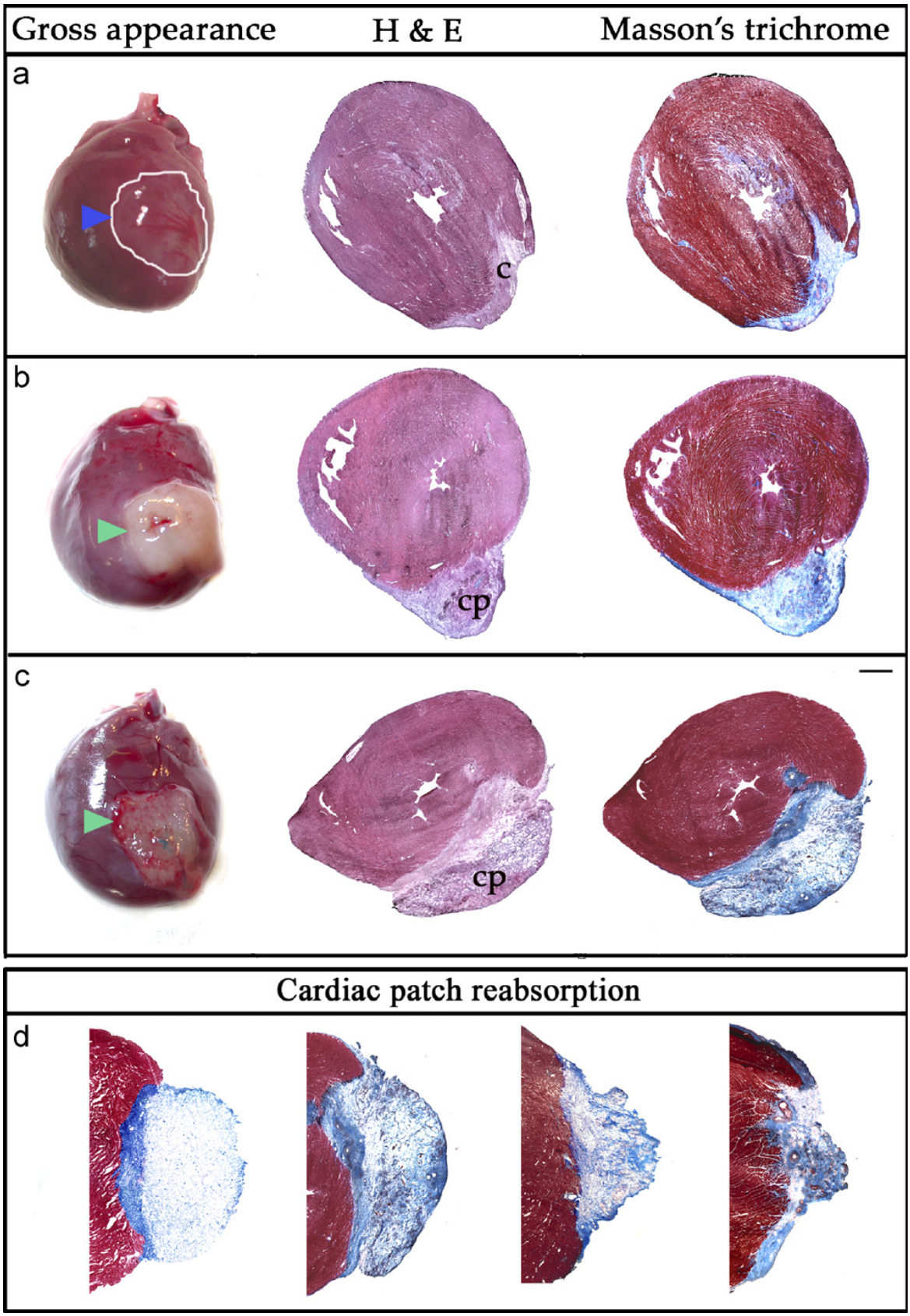

Figure 8. Gross appearance, hematoxylin–eosin, and Masson's trichrome staining of cryoinjured heart (a), intact heart with collagen cardiac patch (b), cryoinjured heart with collagen cardiac patch (c) and time-related absorption of collagen cardiac patch on the cryoinjured heart (d). All specimens shown in panels (a–c) were taken 15 days post-injury. Green arrowhead indicates the collagen cardiac patch. Blue arrowhead in (a) indicates the localization of cryoinjury. c, cryoinjury; cp, collagen cardiac patch. Biomaterial absorption was evaluated at days 3, 15, 30 and 60 post-injury (panel d; from left to right). Bar = 1 mm.

3.2.2 Identification of analysis zones

To study the spatio-temporal pattern of blood vessel formation and interstitial cell growth/activation in the cardiac patch and the influence of intact or cryoinjured cardiac tissue on the cardiac patch cell accumulation, we identified four zones (as schematically reported in Figure 9). Zones 1 and 3 correspond to the cryoinjured area in hearts without or with the implanted cardiac patch, respectively. Zones 2 and 4 correspond to the cardiac patch applied to intact or cryoinjured hearts, respectively. In this way we may determine whether (1) cryoinjury healing is influenced by the presence of the cardiac patch, and (2) the cryoinjury itself is able to drive the pattern of cardiac patch cell growth and organization.

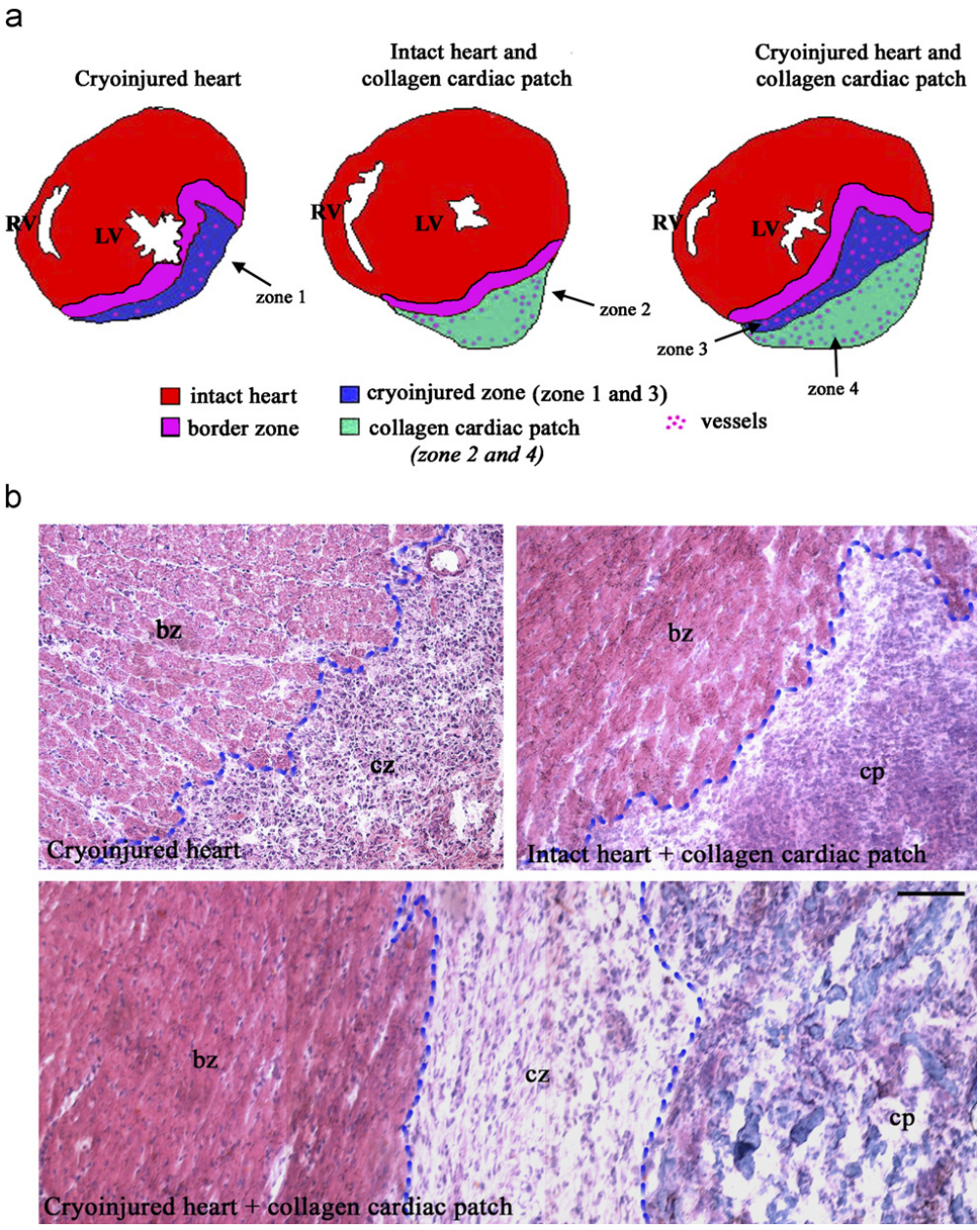

Figure 9. In (a): schematic representation of the tissues examined for the cryoinjured heart, intact heart with collagen cardiac patch and cryoinjured heart with collagen cardiac patch. Four zones are identified: the border and the cryoinjured zone (zone 1) in the cryoinjured heart; the border zone and the collagen cardiac patch (zone 2) in the intact heart with the collagen cardiac patch; the border and cryoinjured zone (zone 3) and the collagen cardiac patch (zone 4) in the cryoinjured heart with the collagen cardiac patch. In (b): hematoxylin–eosin staining of the different zones taken from cardiac samples 15 days from implantation. bz, border zone; cp, collagen cardiac patch; cz, cryoinjury zone. Bar = 50 μm.

Histological analysis of cryoinjured hearts, with or without application of the cardiac patch (Figure 9b), also revealed the presence of a border zone which is intermediate between the intact heart and the cryoinjury/cardiac patch (Figure 9b) in which CM showed minor morphological changes (mostly degenerative).

3.2.3 Inflammatory cells

Cryoinjured tissues (zones 1 and 3) always displayed (from day 3 to day 60 post-injury) a great number of inflammatory cells typical of a wound-healing process, i.e. CD45+ cells. The initial presence of granulocytes was followed by macrophages (Figure 10) and accompanied by a transient wave of T lymphocytes. No dendritic cells or foreign body giant cells were seen and only trace amounts of $CD161^{+}$ (NK cells) were detected. Inflammatory cells in the cardiac patches (zones 2 and 4) showed a similar spatiotemporal behavior, except for granulocytes which peaked at day 15 instead of day 3 as observed with the cryoinjured zones.

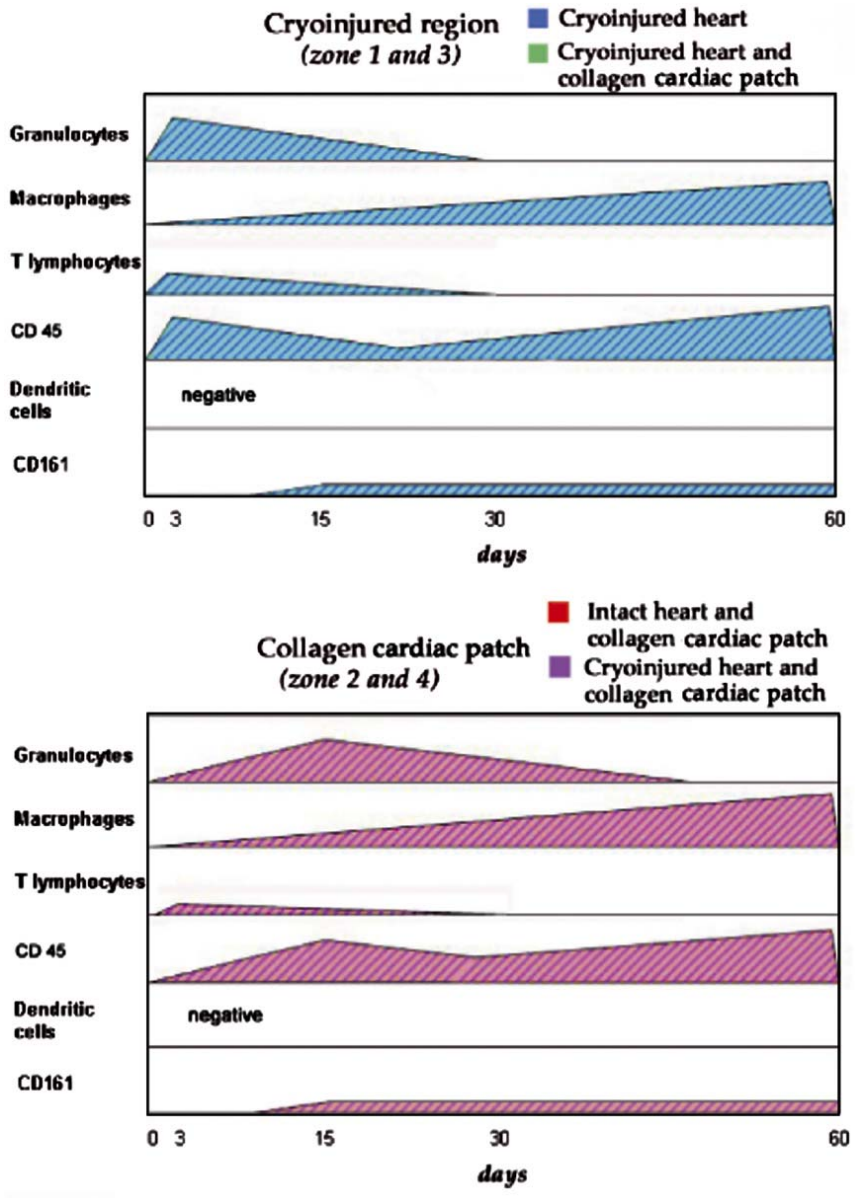

Figure 10. Cartoon showing the time-dependent cellular changes in some parameters characterizing the cryoinjury region and the collagen cardiac patch from days 0 to 60. The base of each polygon indicates the duration of each event whereas its height represents the peak of the specific event.

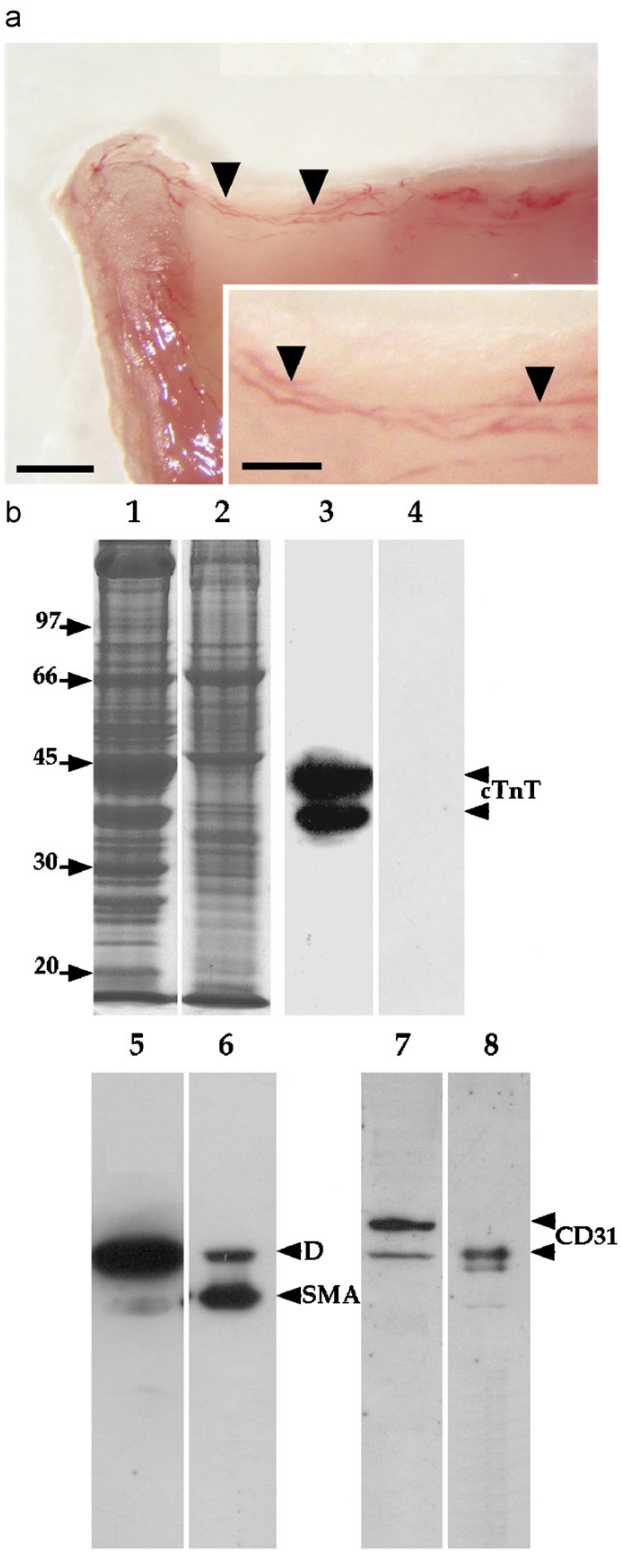

Figure 11. Gross appearance (a), electrophoresis and Western blotting (b) of crude extracts from a collagen cardiac patch taken from the intact heart 15 days after transplantation in comparison with uninjured myocardium. In (a): note the presence of new blood vessels (arrowheads), particularly evident in the inset. (lane 1). In (b): extracts from uninjured heart (lanes 1, 3, 5, 7) and collagen cardiac patch (lanes 2, 4, 6, 8) examined in electrophoresis (lane 1,2) and in Western blotting (lanes 3–8). Antibodies to cTnT (lanes 3, 4), desmin (D; lanes 5, 6), SM α-actin (SMA; lanes 5, 6), and CD31 (lanes 7, 8). Note that cTnT is not present in the collagen cardiac patch extract.

3.2.4 Blood vessels

Besides the time-dependent accumulation of inflammatory cells, the cryoinjured zones and the cardiac patches contained cells organized in blood vessels of different sizes (Figure 12) and interstitial cells with a peculiar phenotypic profile (Figure 14). In particular, cardiac patches carefully detached from the epicardial surface of either intact (Figure 11a) or cryoinjured hearts appeared to be richly vascularized. This was confirmed by Western blotting of the cardiac patches isolated from intact hearts 15 days after implantation using specific differentiation markers for cardiac (cTnT) and sarcomeric and non-sarcomeric muscle (desmin) as well as for smooth muscle (SM α-actin) and EC (CD31) (Figure 11b). It turned out that, , all other markers, except cTnT, were expressed in the cardiac patches implanted on intact hearts. A similar result was obtained from cardiac patches applied to cryoinjured hearts (data not shown).

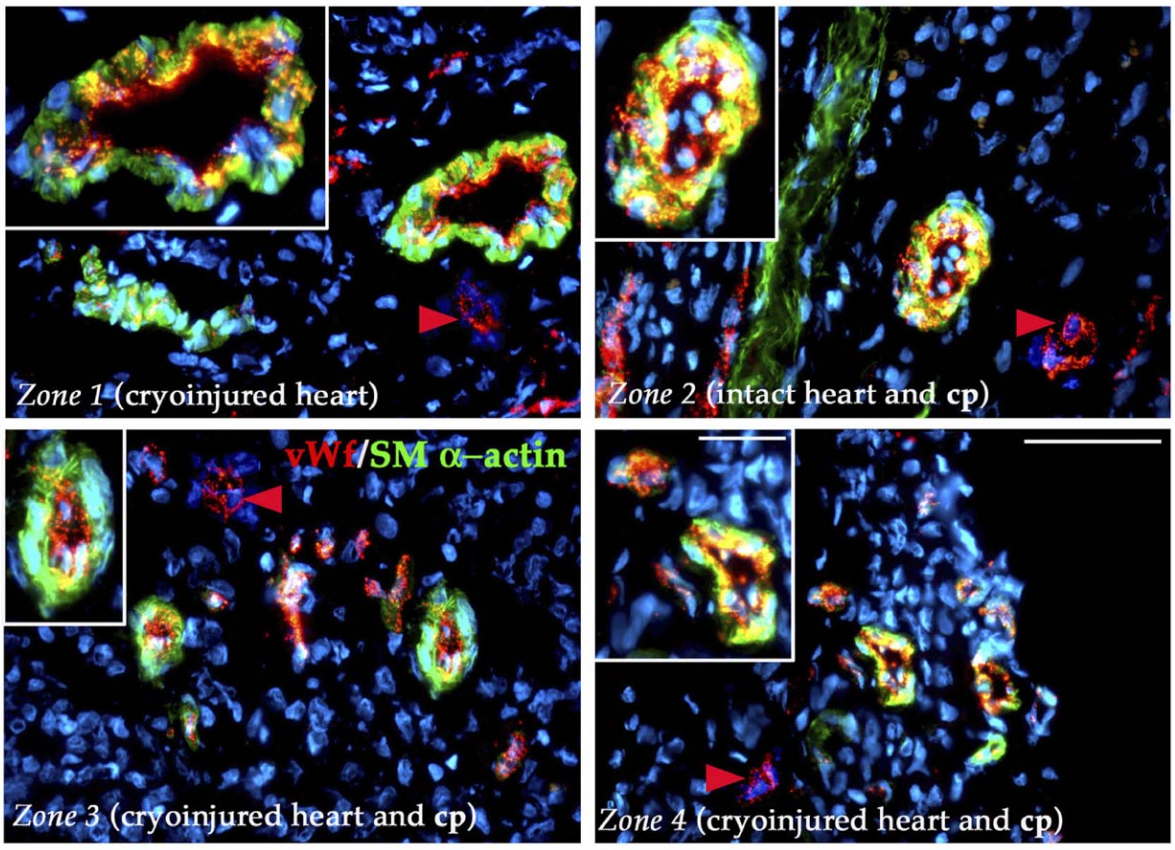

Figure 12. Panels shown a typical aspect of arterioles (identified by the double color green+red) and capillaries (in red; some of them are indicated by red arrowheads) 15 days from implantation and used for the blood vessel counting reported in Figure 13. Bars: 80 and 30 mm (insets).

Density and phenotypic profile (Figure 13) of blood vessels in the cryoinjured zones and cardiac patches were studied at day 15 (Figure 13a) and day 60 (Figure 13b) after scaffold implantation on intact and cryoinjured hearts. Two types of vessels with a clearly defined lumen encircled by a complete wall were taken into account: capillaries (50 μm or less in diameter; identified by vWf expression alone) and arterioles (450 μm in diameter; identified by expression of vWf in the cells facing the lumen and SM α-actin in the outer cell layer; (see Figure 12). At day 15 and 60 post-implantation, and as a general feature, density of capillaries was higher than that of arterioles. The presence of the cardiac patch was able to induce the formation of new vessels inasmuch as the density was 19.84 ± 10.69 (arterioles/mm^2) and

52.25 ± 22.38 (capillaries/mm^2) in zone 1, and 101.85 ± 24.68 (arterioles/mm^2) and 213.63 ± 22.90 (capillaries/mm^2) in zone 3. In addition, when the cardiac patch was applied on the cryoinjured zone, the density of newly formed vessels within the collagen patch was increased (zone 2 vs. zone 4) from 87.30 ± 30.62 (arterioles/mm^2) and 138.23 ± 64.06 (capillaries/mm^2) to 202.38 ± 31.19 (arterioles/mm^2) and 240.74 ± 66.72 (capillaries/mm^2) (see Figure 13). The border zone in both the intact heart with the cardiac patch and cryoinjured heart with cardiac patch was generally characterized by an overwhelming presence of capillaries. Comparison of vascular density in the border zone from intact heart with cardiac patch and zone 2 gave: 18.52±3.74 (arterioles/mm^2) and 391.53±99.36 (capillaries/mm^2) vs. 87.30±30.62 (arterioles/mm^2) and 138.24±64.06 (capillaries/mm^2). Similarly, these values were 21.16±7.49 (arterioles/mm^2) and 398.81±106.62 (capillaries/mm^2) in the border zone of cryoinjured heart with cardiac patch vs. 202.38±31.19 (arterioles/mm^2) and 240.74±66.72 (capillaries/mm^2) in zone 4. At day 60 post-implantation, the pattern was substantially maintained for neovascularization in zones 1 and 3, whereas zones 2 and 4 attained a similar relative proportion of arterioles vs. capillaries. More adherent to the pattern displayed at day 15, appeared to be the comparison between border zones and zone 2 or 4 (Figure 13).

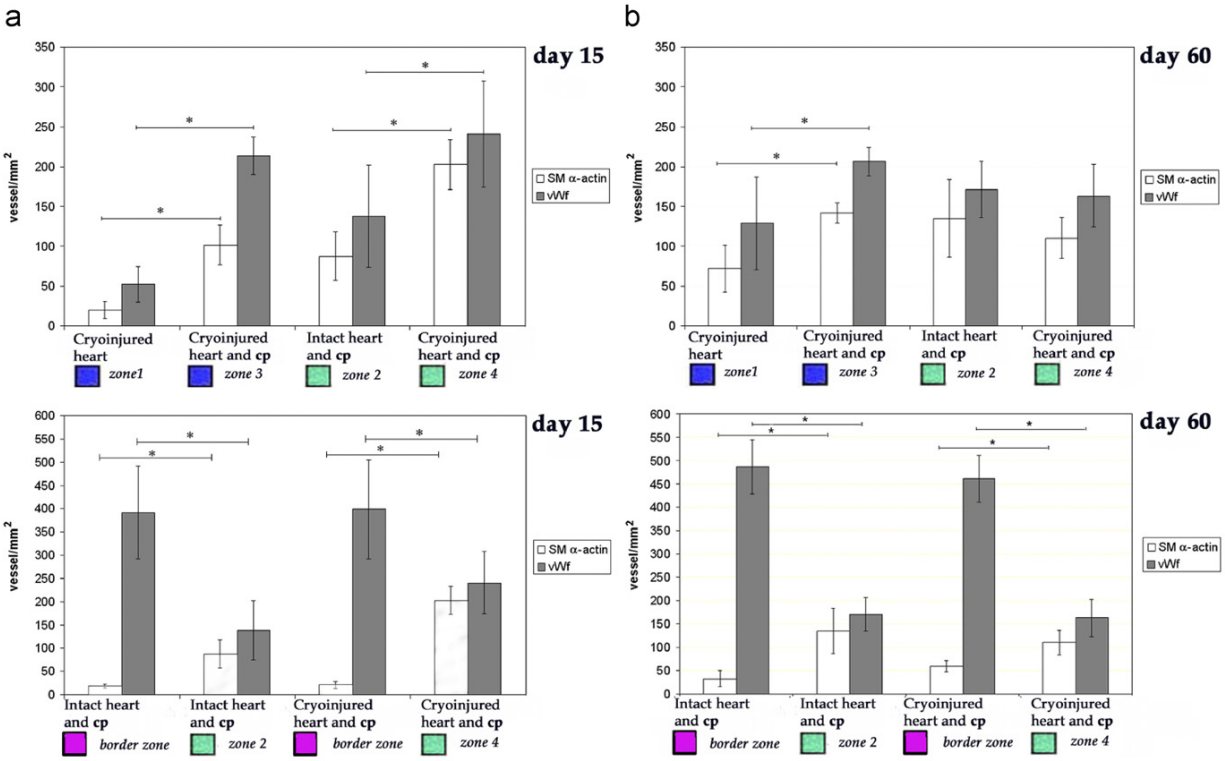

Figure 13. Bar graphs (a,b) showing the vessel density of capillaries (about 10 μm in diameter) and arterioles (about 50 μm or more in diameter) identified by vWf and SM α-actin immunoreactivity, respectively, in the zones described in Figure 9. Samples were analyzed 15 or 60 days after injury. *p<0.05.

3.2.5 Interstitial cells and markers of cardiogenic stem cells

Interstitial, non-inflammatory cells that accumulated in the cryoinjured zone and in the cardiac patch were studied for their expression of differentiation markers recently suggested to be indicators of cardiac or neural stem cells. The results of these experiments are shown in Fig. 14 and summarized in Table 8. Myofibroblasts, identified by expression of SM α-actin,

were quite numerous in the cryoinjury zone without the collagen scaffold (zone 1) whereas they were less present in the cryoinjured zone with the collagen scaffold (zone 3). vWf^{+} cells were detected in the cardiac patch independently from the presence or absence of a cryoinjury. As to markers of neural stem cells, nestin and GFAP-positive interstitial cells were rarely expressed in zone 1 or 3 (Figure 14) but accumulated to a greater extent in the cardiac patch, with or without the accompanying cryoinjury, especially around newly forming vessels (Figure 14). By contrast, Sca-1 and MDR1 markers of cardiogenic stem cells were seldom seen in zones 1/3 or zone 2/4.

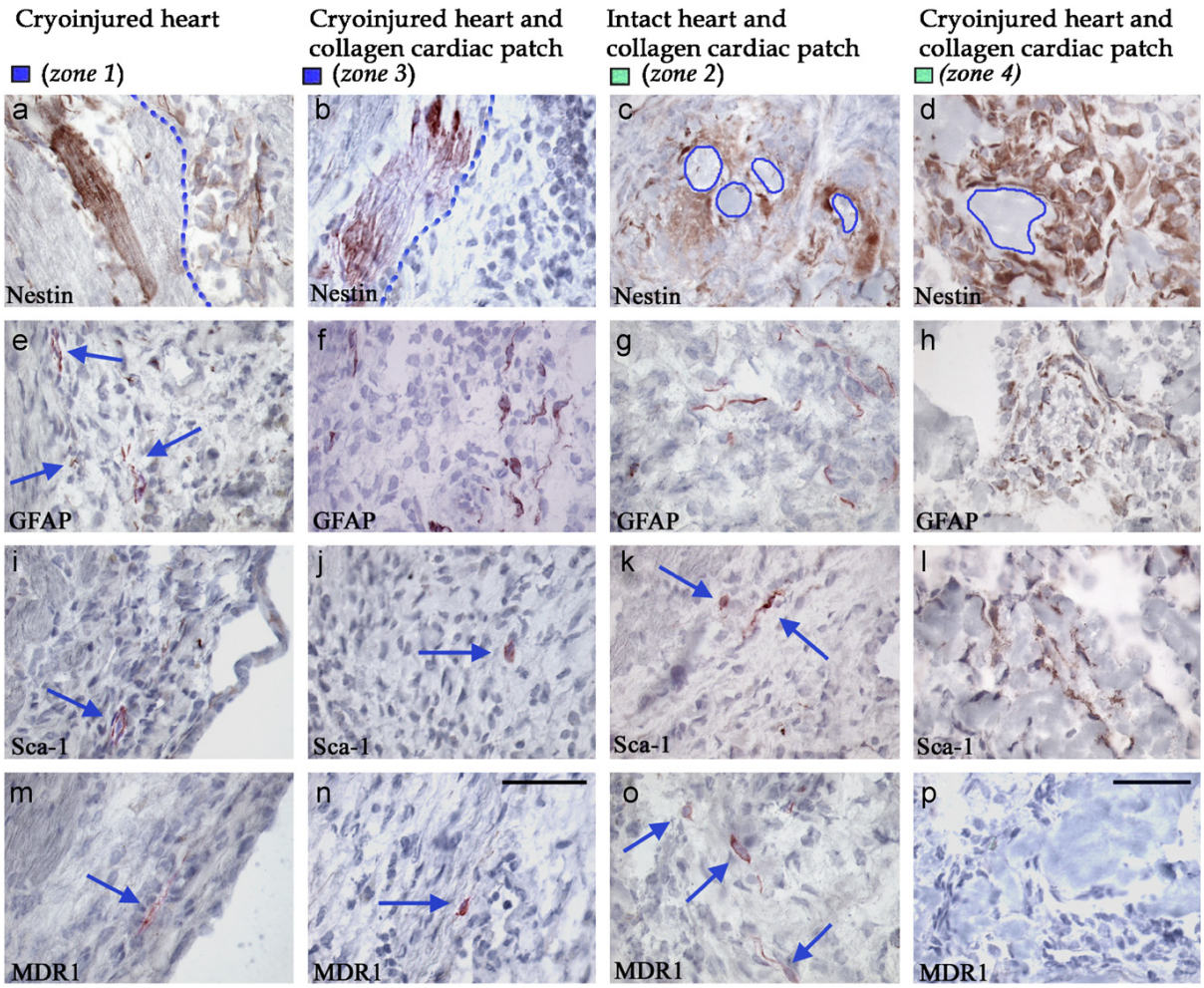

Figure 14. Immunocytochemical profile of cardiac interstitial cells in cryoinjured heart, zone1 (panels a, e, i, m); and cryoinjured heart with collagen cardiac patch, zone 3 (panels b, f, j, n) and collagen cardiac patches sutured to intact heart (zone 2; panels c, g, k, o) and cryoinjured heart (zone 4; panels d, h, l, p) examined for neural and cardiac stem cell antigen expression. Note the expression of nestin in some CM from the border zone (bz) facing the cryoinjury zones 1 and 3 (cz). Only a few cells, identified by blue arrows, are labeled with anti-GFAP (e, f), anti-Sca-1 (I, j) and anti-MDR1 (m, n) antibodies in cryoinjury zones 1 and 3. In the collagen cardiac patch, nestin expression is quite abundant especially around forming vessels (drown blue loops; c, d). Conversely, cells in collagen cardiac patch very rarely express GFAP (g, h) Sca-1 (k, l) or MDR1 (o, p). Bar, 50 mm.

Table 8. Phenotypic profile of non-inflammatory interstitial cells at day 15 after cryoinjury/cardiopatch implantation vs. intact heart.

.

Antigen	Intact heart	Cryoinjury zones		Cardiopatches	
		- cardiopatch (zone 1)	+ cardiopatch (zone 3)	- cryoinjury (zone 2)	+ cryoinjury (zone 4)
cTnT	-	-	-	-	-
Desmin	-	-	-	-	-
Sm α-actin	-	++	+/-	-	-
vWf	-	+/-	-	+	+
Vimentin	+++	+++	+++	+++	+++
Nestin	+	+	+	+	++
GFAP	-	+/-	+	+	++
Sca-1	-	+/-	+/-	+/-	
MDR1	-	+/-	+/-	+/-	-

Legend: cTnT, cardiac troponin T;SM α−actin, smooth muscle type α−actin; vWf, von Willebrand factor; GFAP, glial fibrillary acidic protein; Sca-1, stem cell antigen-1; MDR1, multiple drug resistance protein.
Number of cells positive for the respective antibody: +++, >90%; ++, 40-90%; +, 5-40%; +/-, < 5%; -, no immunoreactivity.

3.3 Implantation of the collagen scaffold and rat cardiomyocytes GFP$^+$ in a model of AMI

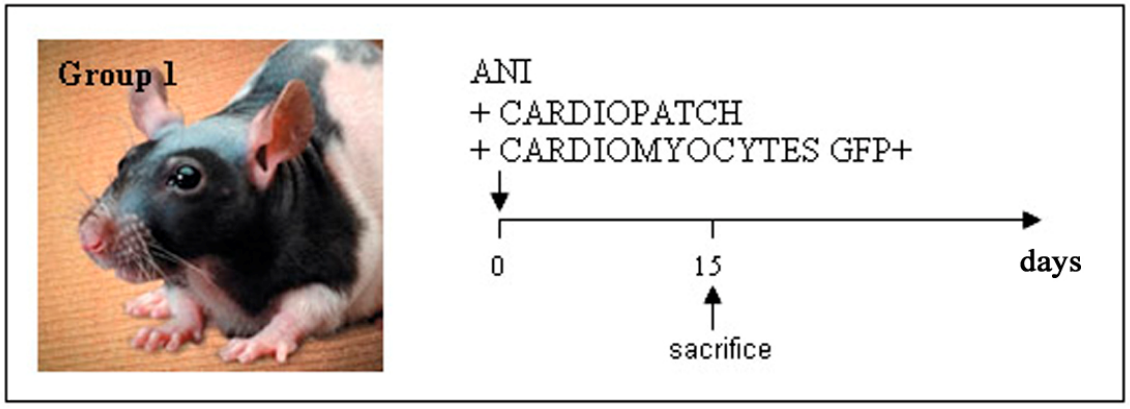

Figure 15. After ANI (acute necrotizing injury) on the left ventricular wall of rNu rats, a collagen patch was attached to the damaged area and then injected with fetal GFP$^+$ cardiomyocytes. The animals were sacrificed after 15 days.

3.3.1 Haematoxylin-eosin and Masson's Trichrome staining

By gross appearance, the cardiac patch was firmly attached to the epicardial surface independently from previous cryoinjury. Haematoxylin-eosin (Figure 16) and Masson's trichrome (Figure 17) revealed that the patch was richly populated. The patch was well fused with the host myocardium (Figure 16a) and the border between the patch and the cryoinjury zone was not well defined.

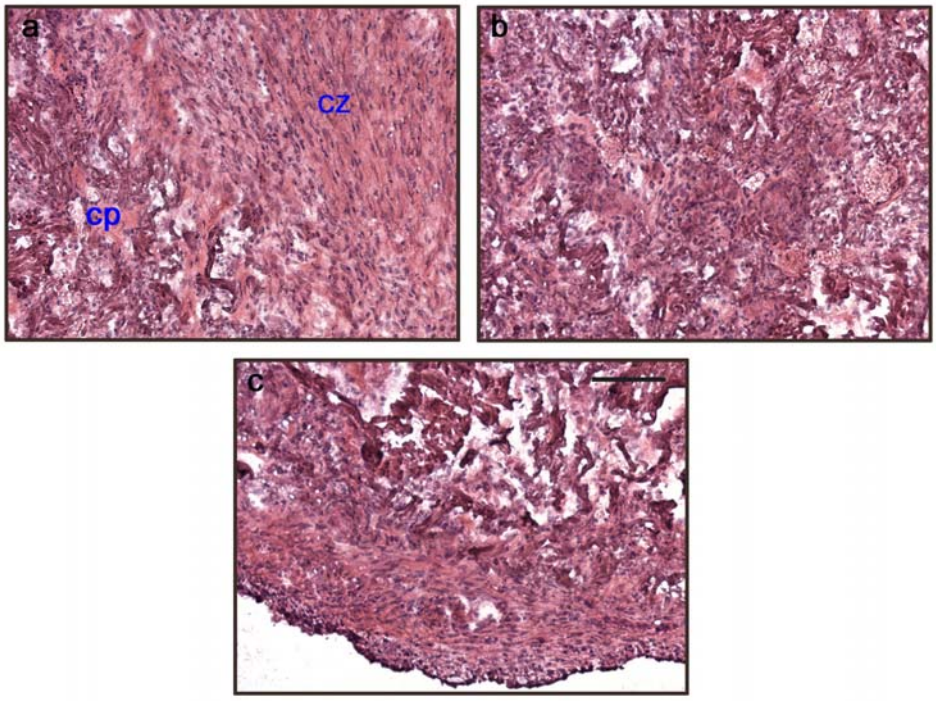

Figure 16. Haematoxylin-eosin staining of the border between cryoinjury and patch (a), inner patch (b) and outer patch (c). Bar = 10μm.

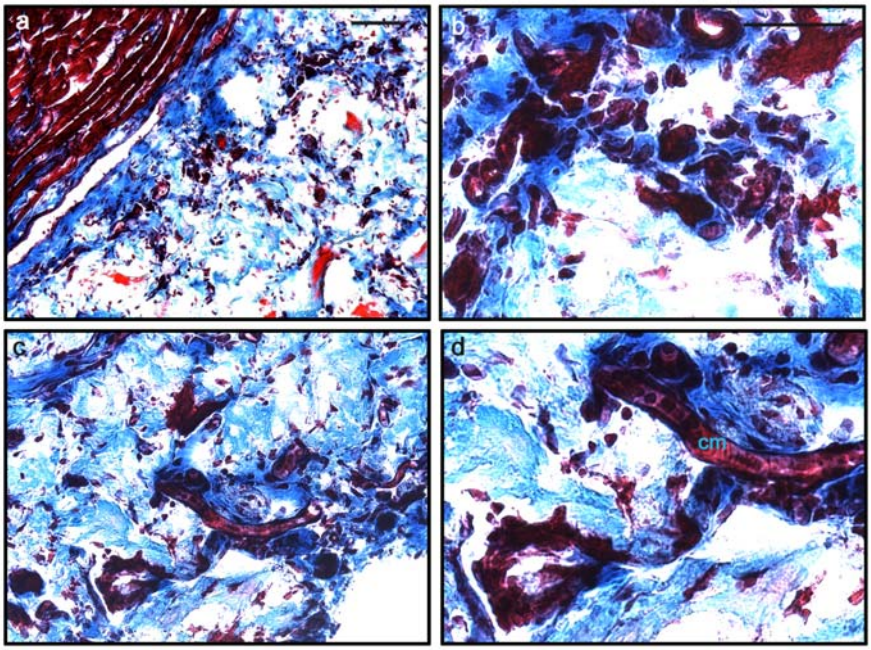

Figure 17. Masson's trichrome staining of rat heart sections that received cryoinjury, collagen patch and GFP^+ cardiomyocytes at 15 day of time. The cryoinjured zone (a and b) and collagen patch (c and d) contain several cells. It is possible to distinguish some cardiomyocytes (bands, arrows). Blue = collagen; red/purple = living cells; cm = cardiomyocytes. Bar = 10 μm.

3.3.2 Survival of the injected GFP$^+$ cardiomyocytes

After 15 days numerous vessels stained for von Willebrand factor (capillaries) or also for SM α-actin (arterioles) were present in the patch and in the damaged area (data not shown). Transplanted CMs positive for GFP were detectable both in the patch (Figure 18 c and d) and in the cryoinjury zone (Figure 18 a and b). This suggests that cardiomyocytes can move from the patch to the lesion. These cells maintained staining for Troponin T and were able to form connections with other GFP$^+$ CMs (staining for connexin 43). No connections with cells of the host myocardium were found.

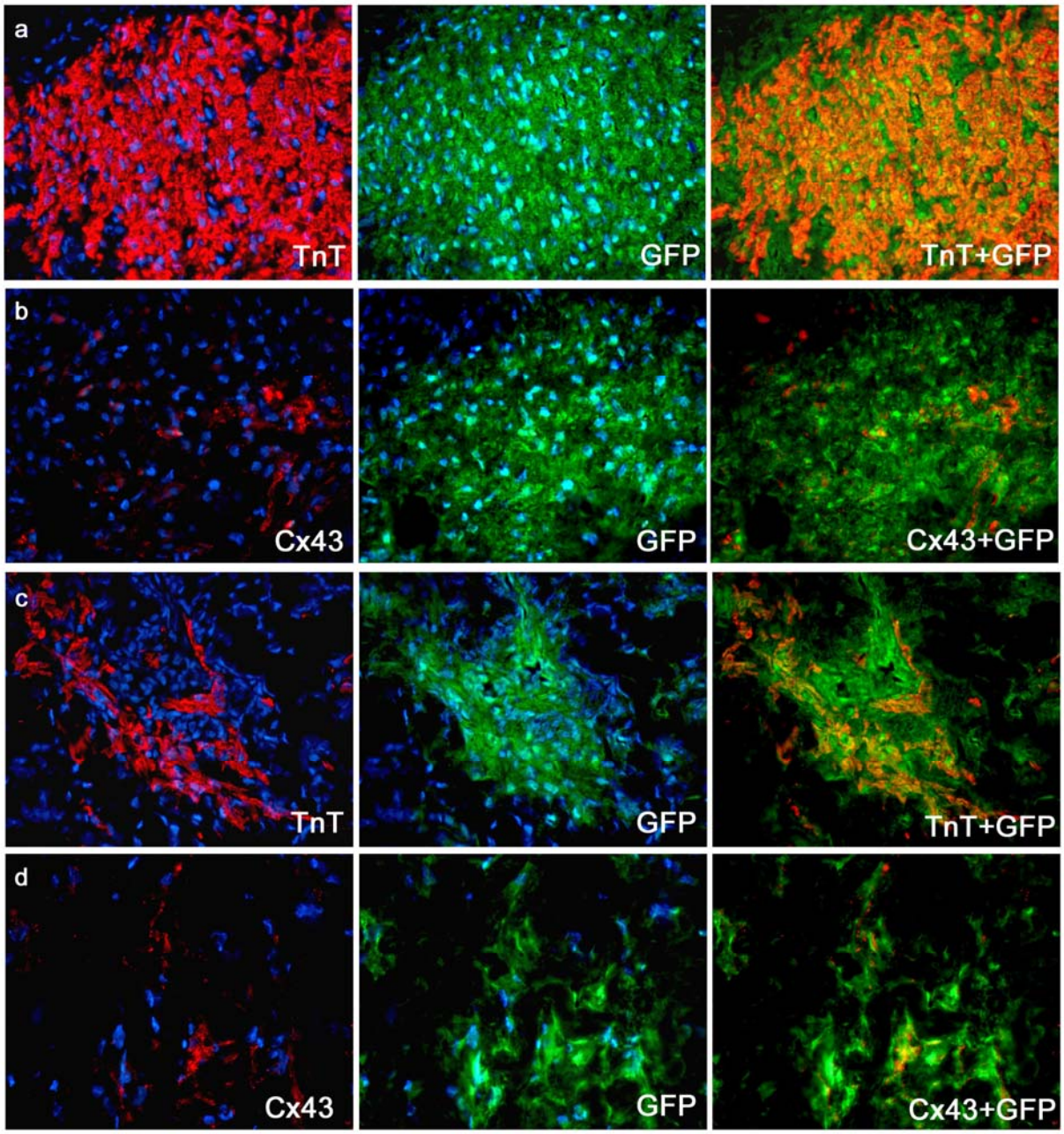

Figure 18. Immunofluorescence of GFP$^+$ CMs 15 days after being transplanted to a patch *in vivo*. The GFP$^+$ cells (green) are still detectable in the patch (c-d) and are able to migrate in the cryoinjury zone (a-b). They express TnT and connexin43 (red). Blue = Hoechst nuclear staining. Bar = 50μm

3.4 Implantation of the collagen scaffold in a model of Chronic Myocardial Infarction (CMI)

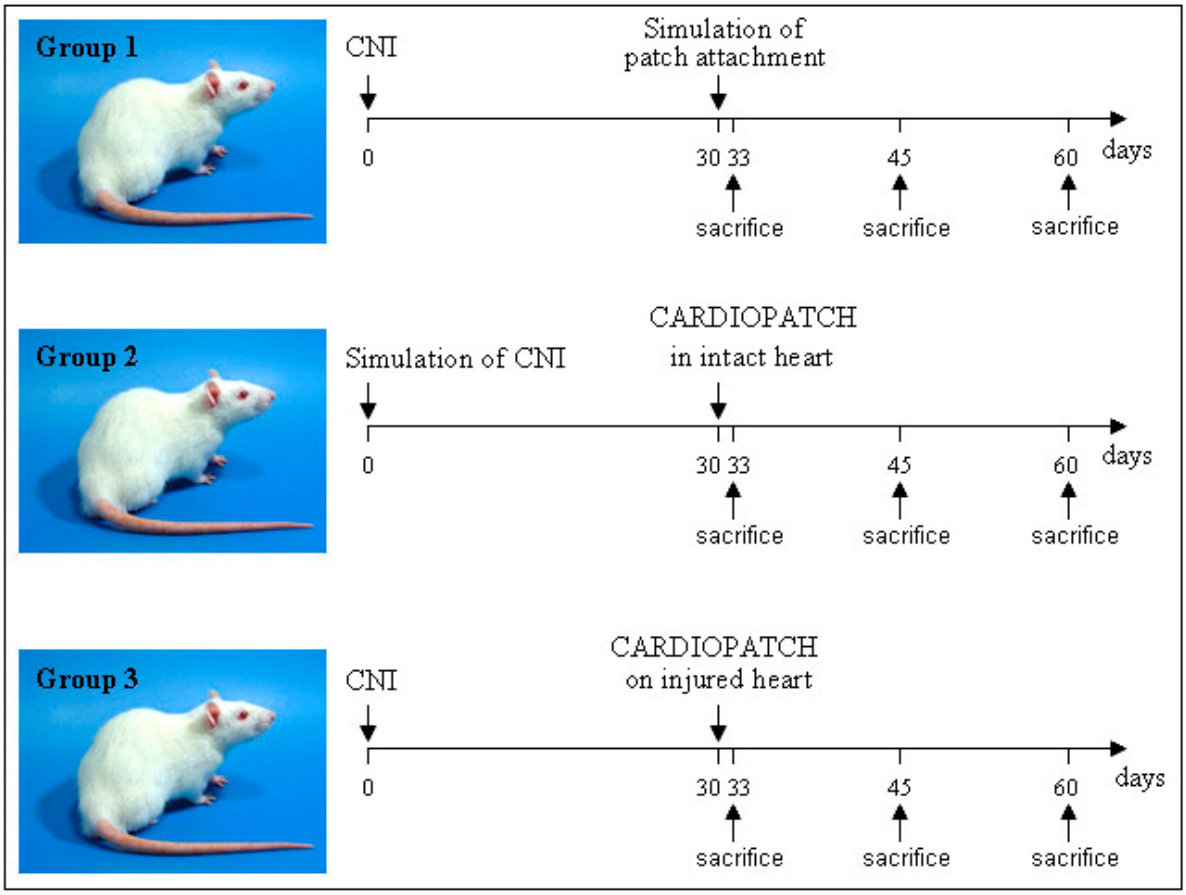

Figure 19. After cryoinjury the thoracotomy was closed and the animals recovered for 30 days. After this period they had a second thoracotomy to expose the heart. At this time the animals were divided into 3 experimental groups: in group 1 a simulation of patch attachment was performed; in group 2 the scaffold was applied to the intact heart; in group 3 the scaffold was sutured to a cryoinjured heart. CNI = chronic necrotizing injury.

3.4.1 Gross appearance, Haematoxylin-eosin and Masson's Trichrome staining

The effects of application of the collagen cardiac patches on the rat heart were studied on animals of groups 2 and 3 and compared to animals that underwent cryoinjury only (group 1). At explantation, all animals revealed no thoracic adhesions. By gross observation, the cardiac patch was firmly attached to the epicardial surface independently of previous cryoinjury (Figure 20 a–c). Unlike the model of acute myocardial infarction, the cardiopatch in this model is not able to completely cover the damaged area (Figure 20 c). The material is progressively absorbed over time: it was estimated about a 10% reduction of the original volume for every week after implantation (data not shown).

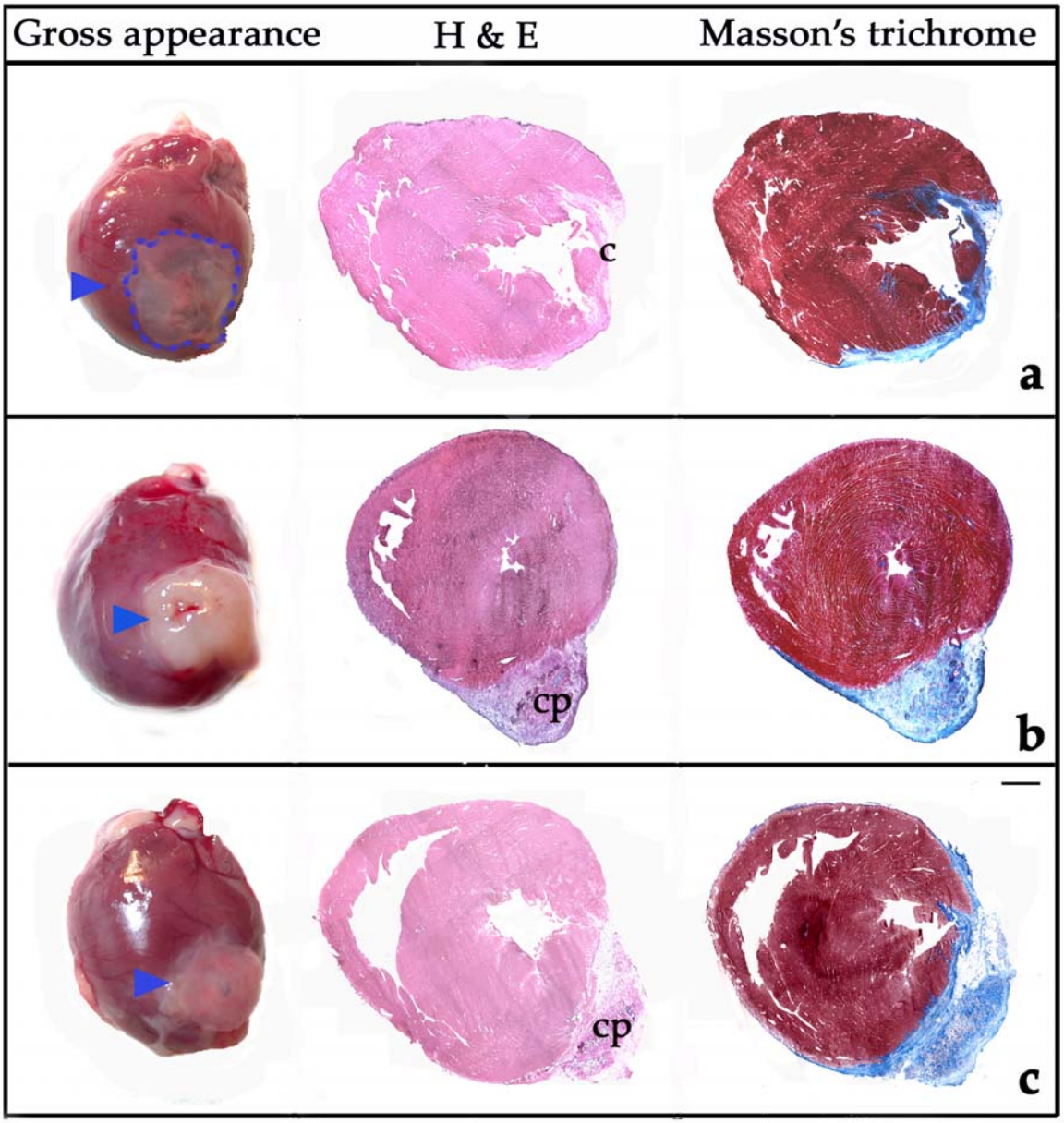

Figure 20. Gross appearance, haematoxylin–eosin, and Masson's trichrome staining of heart with CNI (a), intact heart with collagen cardiac patch (b), heart with CNI and collagen cardiac patch (c). All specimens shown in panels (a–c) were taken 45 days post-injury (a: 45 days of CNI, b: 30 days without lesion and 15 days with cardiopatch, c: 30 days of CNI and 15 days with cardiopatch). The blue line in (a) that include a paler region, indicates the localisation of CNI; blue arrowheads in (b) and (c) indicates the collagen cardiac patch. Bar = 1 mm.

3.4.2 Identification of analysis zones

As in the acute model, the spatio-temporal pattern of blood vessel formation and interstitial cell growth/activation in the cardiac patch and the influence of intact or cryoinjured cardiac tissue on the cardiac patch cell accumulation was studied in four different zones (as schematically reported in Figure 21). Zones 1 and 3 correspond to the cryoinjured area in hearts without or with the implanted cardiac patch, respectively. Zones 2 and 4 correspond to the cardiac patch applied to intact or cryoinjured hearts, respectively.

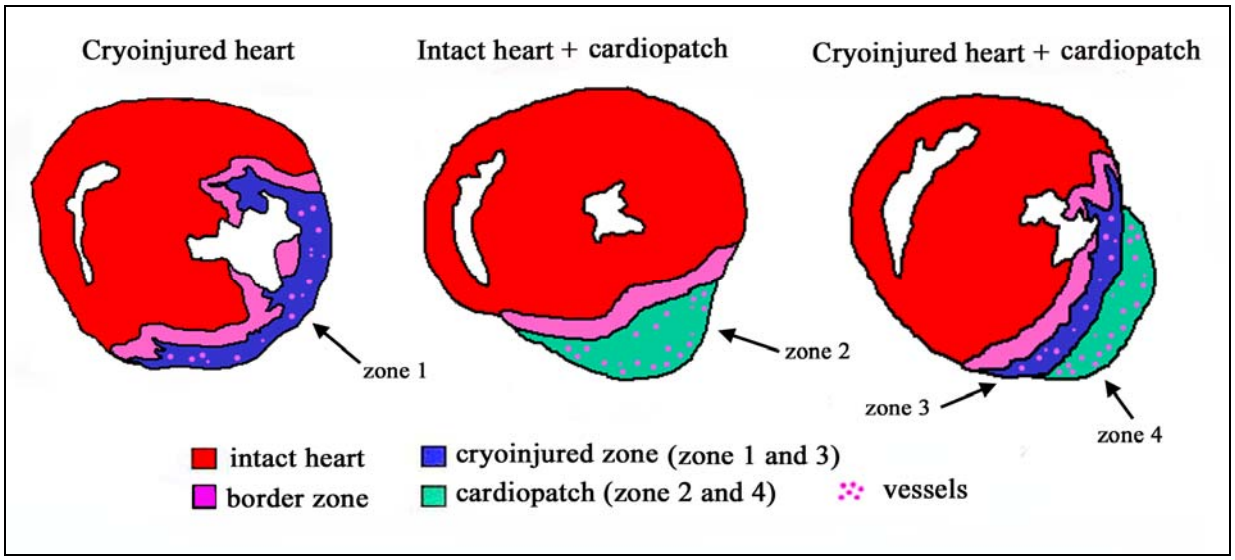

Figure 21. Schematic representation of the tissues examined to evaluate the blood vessel and heart interstitial cell pattern. Four zones are identified: the border and cryoinjured zone (zone 1) in the cryoinjured heart; the border zone and collagen cardiac patch (zone 2) in the intact heart with patch; the border and cryoinjured zone (zone 3) and the collagen cardiac patch (zone 4) in the cryoinjured heart with patch.

3.4.3 Inflammatory cells

The damaged tissue (zones 1 and 3) analyzed at different time points (from day 0 to 60) showed a large number of $CD45^+$ cells. These cells are characteristic of an inflammatory response following the damage induced by CNI. In particular, granulocytes were abundant at the beginning, with a peak by the first week after injury and 15 days after application of the cardiopatch. Decrease in the number of granulocytes were accompanied by the contemporaneous increase in macrophages (Figure 22). In addition T lymphocytes and dendritic cells were absent or present only in traces.

The inflammatory cells in the cardiopatch (zone 2 and 4) showed a similar behaviour: granulocytes peaked at 15 days after application of the cardiopatch and macrophages were the most abundant cells. The results are summarized in Figure 23.

In sham-operated animals, the hearts did not show an inflammatory response.

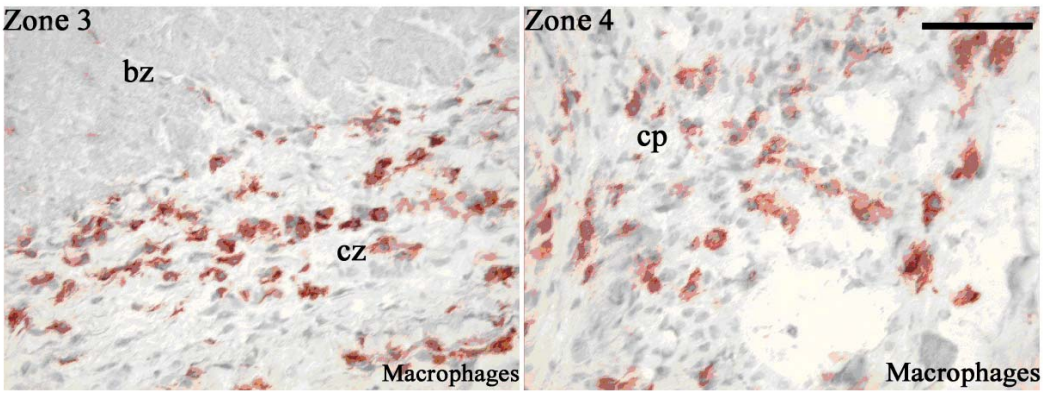

Figure 22. Presence of macrophages revealed by immunoperoxidase. Cells are positive for the macrophage-specific marker CD163 in the zone with CNI (zone 3) and in the cardiopatch (zone 4) (brown staining) in a rat heart with CNI 15 days after the cardiopatch application. Bz = border zone; cz = cryoinjured zone; cp = cardiopatch. Bars= 20µm.

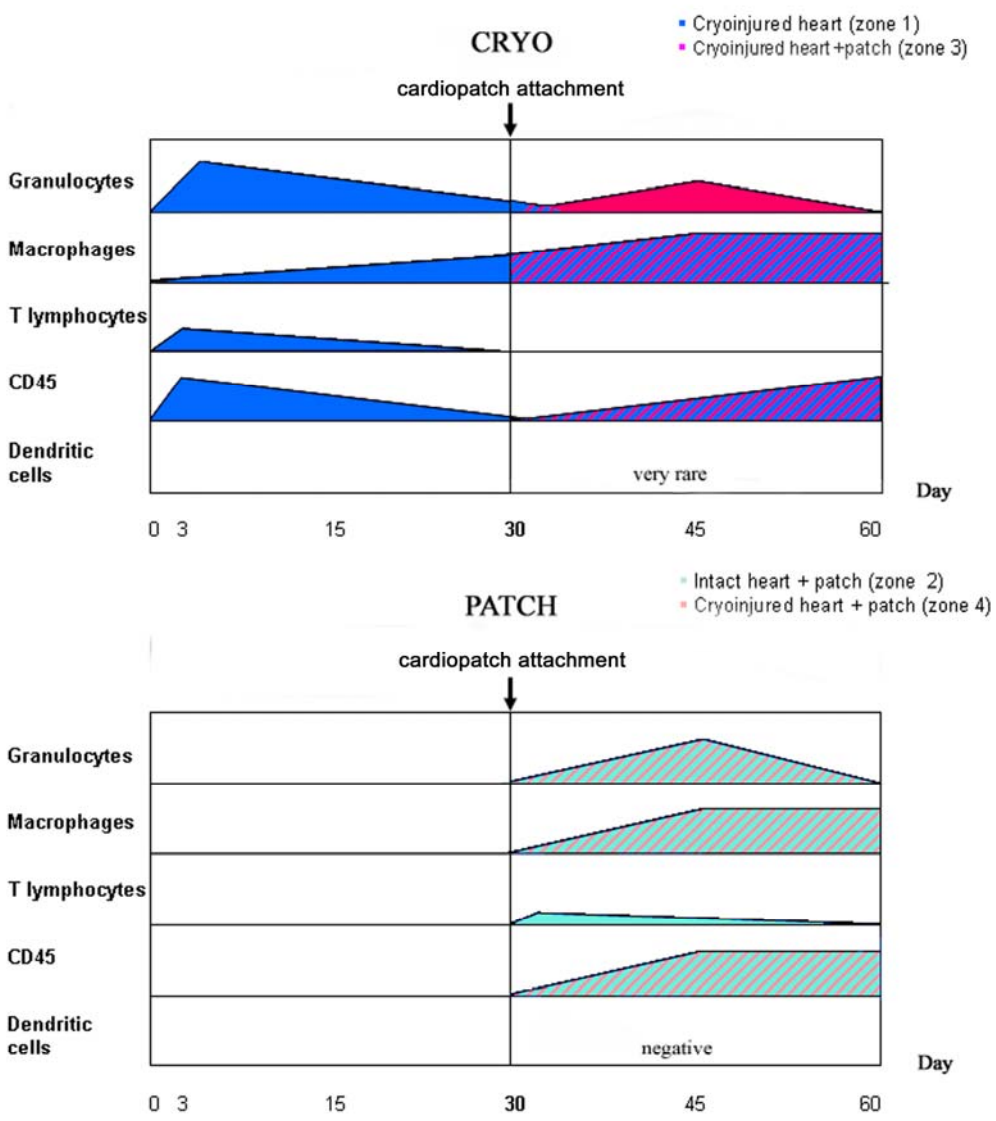

Figure 23. Cartoon showing time-dependent changes in cell population within the cryoinjury region and the collagen cardiac patch from days 0 to 60. The base of each polygon indicates the duration of each event whereas its height represents the peak of the specific event.

3.4.4 Blood vessels

Besides inflammatory cells, the cryoinjured zones and the cardiac patches contained blood vessels of different sizes (Figure 24) and interstitial cells with a peculiar phenotypic profile (Table 9).

The density and phenotypic profile of the blood vessels were examined in zones 1-4 at 15 and 30 days after the implantation of the scaffold. Capillaries were identified by expression of vWf, while arterioles were visualized by simultaneous expression of vWf and SM α-actin (Figure 24). Moreover, the grade of maturation of these vessels was studied using markers of vascular smooth muscle differentiation, such as SM1 (Smooth muscular Myosin heavy chain type 1) and SM2 (Smooth muscular Myosin heavy chain type 2). The two isoforms are both expressed in adults, and expression of isoform 1 alone is characteristic of the fetal stage (*Makoto and al., 1989*). As shown in Figure 25, both isoforms were present in the analyzed samples.

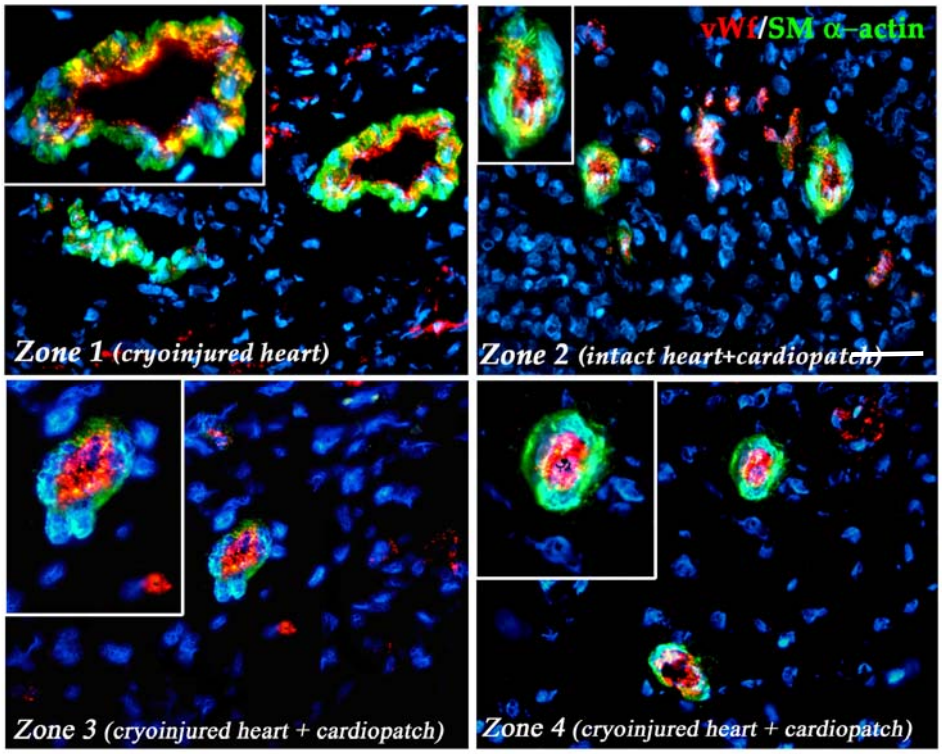

Figure 24. Immunofluorescence for vWf (red) and SM α-actin (green) 15 days after implantation. Arterioles are identified by double staining (green + red), while capillaries are stained only in red. Blue = Hoechst nuclear staining. Bars= 80 μm.

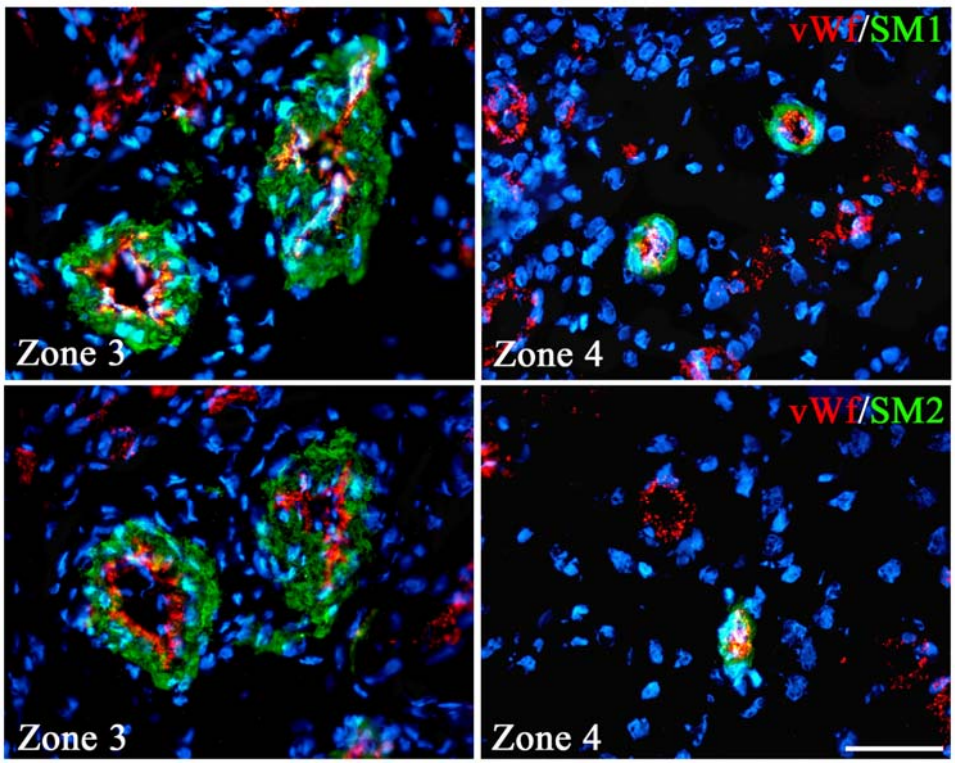

Figure 25. Immunofluorescence for SM1 and SM2 (green) and vWf (red) in zone 3 (cryonjured heart) and 4 (cardiopatch) in heart with CNI at 15 days after implant. Blue = Hoechst nuclear staining; Bar=80 μm

As a general feature, at days 15 and 30 post-implantation, the density of capillaries was higher than that of arterioles. At 15 days the scaffold was able to stimulate the formation of new vessels in the damaged area (Figure 10a): the density in zone 1 was 22.48±5.06 (arterioles/mm^2) and 57.03±15,42 (capillaries/mm^2), while in the zone 3 it was 60.52±16.07 (arterioles/mm^2) and 111.11±33.62 (capillaries/mm^2). The difference between the two zone was significant ($p<0.05$): in zone 3 the number of arterioles and capillaries was 2.7 and 1.9 time higher respectively.
Unlike the acute model, in the chronic model the vessel count showed that there was a non-significant decrease when the scaffold was applied in the lesion zone, compared with application to an intact heart. In zone 2 the density was 74.07±12.03 (arterioles/mm^2) and 113.75±22,34 (capillaries/mm^2), while in zone 4 it was 52.91±14.87 (arterioles/mm^2) and 86.31±22.59 (capillaries/mm^2).

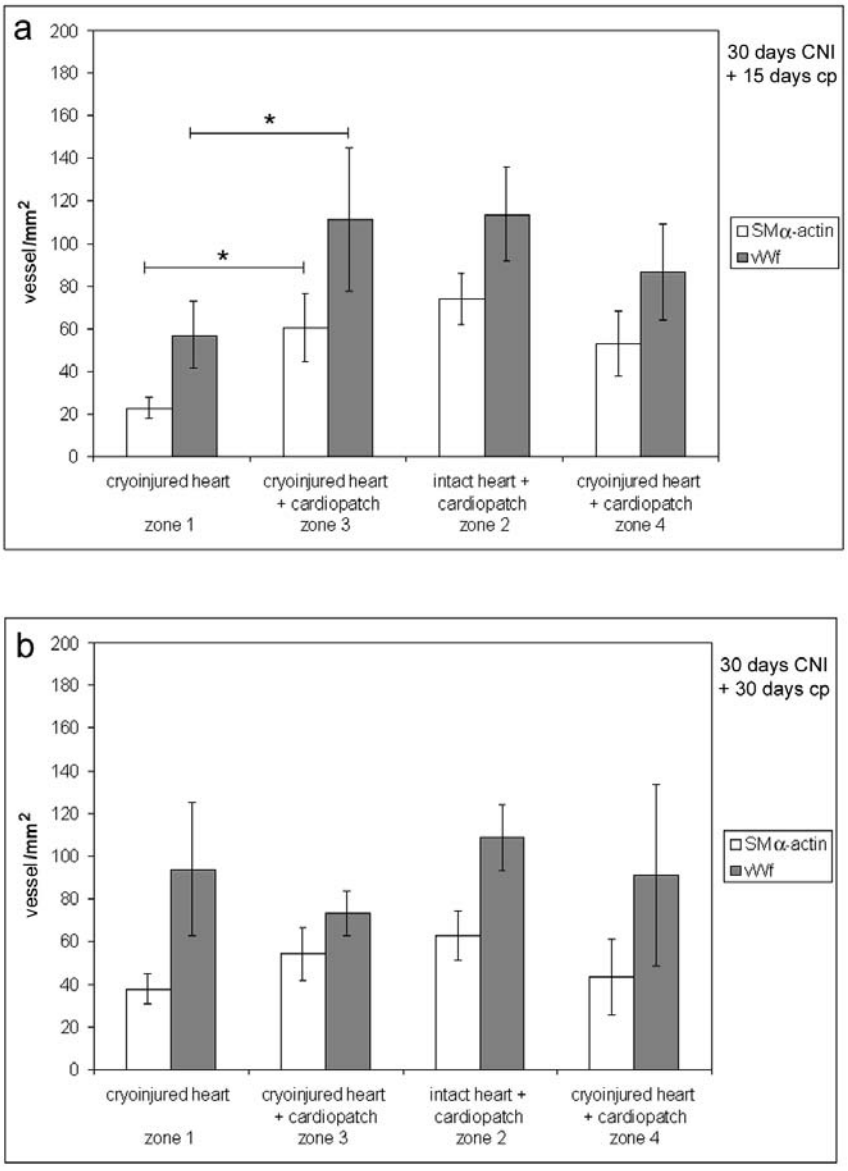

Figure 26. Bar graphs (a,b) showing the vessel density of capillaries and arterioles identified by vWf and SM α-actin immunoreactivity, respectively, in the zones described in Figure 21. Samples were studied after 15 or 30 days post-implantation. *$p<0.05$.

At 30 days the number of arterioles in zone 3 was higher than in zone 1, while the capillaries appeared to be fewer, probably because the cardiopatch was no longer able to stimulate meaningful angiogenesis in the damaged area. Comparing zones 2 and 4, the cardiopatch applied on an intact heart had more vessel than one applied on a zone of CNI. The growth of vessels in this area stopped or decreased over time.
In reference to the time point of 15 days and comparing acute and chronic models, the cardiopatch was able to stimulate vessel formation in the area of lesion in both models, although in the acute model the augmentation was certainly more significant. After 15 days in the CNI model, the cardiopatch contained fewer total vessels than the ANI model at the same time point, but the ratio capillaries/arterioles was comparable.

3.4.5 Interstitial cells and markers of cardiogenic stem cells

Interstitial cells in the lesion area and in the cardiopatch, which do not belong to the group of inflammatory cells nor to blood vessels, were analyzed for the expression of markers of cardiomyocytes, myofibroblasts, macrophages and markers recently discovered to be indicators of "haematopoietic" or "neuronal" cardiogenic stem cells (Table 9).

Table 9. Phenotypic pattern of interstitial cells. The presence of several antigens was compared between zones 1-4, in reference to the intact heart. Legend: Number of positive cells: +++: > 90%, ++: 40-90%, +: 5-40%, +/-: < 5%, - : negative.

Antigen	Intact heart	Cryoinjured heart			Intact heart + cardiopatch			Cryoinjured heart + cardiopatch					
		30	45	60	30+3	30+15	30+30	30+3		30+15		30+30	
		cryo zone 1	cryo zone 1	cryo zone 1	c.patch zone 2	c.patch zone 2	c.patch zone 2	cryo zone 3	c.patch zone 4	cryo zone 3	c.patch zone 4	cryo zone 3	c.patch zone 4
cTnT	++	-	-	-	-	-	-	-	-	-	-	-	-
SM α-actin	-	++	++	+	-	-	-	-	-	+/-	-	+/-	-
vWf	-	-	-	-	+/-	-	-	-	-	-	-	-	-
Vimentin	++	+++	+++	++	++	+++	+++	++	-	+++	+++	+++	+++
Collagen I	-	+	++	+	-	-	-	+	+/-	+	++	++	++
Collagen III	-	+++	+++	++	-	-	-	+	+/-	+++	+++	++	++
Fetal Fibronectin	-	+	+	+/-	+	-	-	+++	+++	+	+++	-	-
Nestin	+/-	+/-	-	+/-	-	+	+	+	-	+	+/-	+/-	-
GFAP	-	+/-	+/-	+/-	+/-	+/-	-	+/-	-	+/-	-	-	+/-
Sca-1	-	+/-	-	+/-	+/-	+/-	-	+	-	-	-	-	+/-
MDR1	-	+/-	+/-	+/-	-	+/-	+/-	-	-	-	-	-	-

The cardiomyocytes characterized by expression of cardiac Troponin T are absent in the CNI zone both in the presence and in the absence of the cardiopatch; cardiomyocytes were not present in the scaffold.
Myofibroblasts, identified by SM α-actin and vimentin, decreased significantly ($p<0.05$) in the lesion area following application of the cardiopatch. In zone 1 the number of fibroblasts present at (30+15) days after lesion was 274.07±34.07/mm^2, while in zone 3 at 15 days post-implantation there were 43.80±15.32 fibroblasts/mm^2 ($p<0.05$). Also in hearts with 30+30 days of CNI or 30 days of CNI and 30 days of cardiopatch we noticed a significant decrease ($p<0.05$) in the number of fibroblast: the density in zone 1 was 84.65±31.80 cells/mm^2 and in zone 3 was 2.65±2.79 cells/mm^2. In the cardiopatch (zones 1 and 4) myofibroblasts were absent.
Positivity to collagen I, III and fetal fibronectin in zones 1 and 3 was analyzed as an index of the repair process, characterized by deposition of extracellular matrix proteins by myofibroblasts/fibroblasts. At 30 days post cryoinjury there is a fibrotic area. In intact hearts with cardiopatch only a few cells expressed collagen I and III: probably the application of the cardiopatch itself generated mild damage with resulting attraction of fibroblasts specialized in deposition of extracellular matrix proteins.

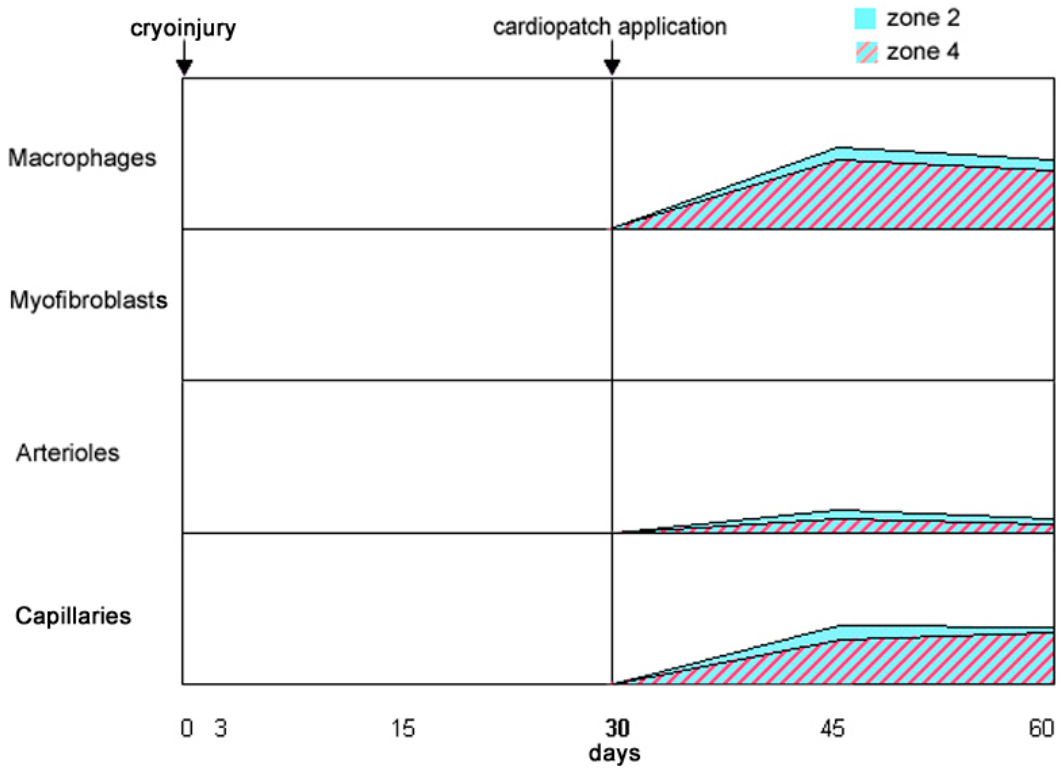

Figure 27. Cartoon showing the time dependent changes in macrophage, myofibroblast, arteriole and capillary in zone 2 (cardiopatch on intact heart) and zone 4 (cardiopatch on heart with CNI) . The increase of number of macrophages is related to the increase in the number of vessels. The base of each polygon indicates the duration of each event whereas its height represents the peak of the specific event.

At 15 days, analysis of macrophages, identified by expression of CD163, showed in the different experimental groups (1, 2 and 3) that the density in zone 3 (806.38±73.09 cells/mm^2) was greater then in zone 1 (very rare) and in zone 4(595,75±103.69 cells/mm^2). In zone 2 (631.91±83.97 cells/mm^2) macrophage density was comparable to zone 4 (595,75±103.69 cells/mm^2). ($p<0.05$). At 30 days after cardiopatch application to the zone with CNI, the

macrophage density was about the same amount in zone 3 and 4 (614.89±91.02 and 595.74±83.09 cells/mm^2, respectively).
With regard to markers of cardiogenic stem cells of "neuronal" origin, nestin positive cells were found in zone 2 in intact hearts with cardiopatch and in zone 3 of hearts with CNI and cardiopatch, while they were rare in zone 4. GFAP positive cells were rare in zones 1 and 2 and almost absent in zones 3 and 4. The markers for cardiogenic stem cells of the reported "haematopoietic" type *(Anversa and al., 2006)*, such as Sca-1 and MDR, were rare in zones 1 and 2 and almost completely absent in zone 3 and 4. C-kit$^+$ cells were absent as well.

3.5 Implantation of the collagen scaffold and GFP$^+$ BM-MSCs in a model of Chronic Myocardial Infarction

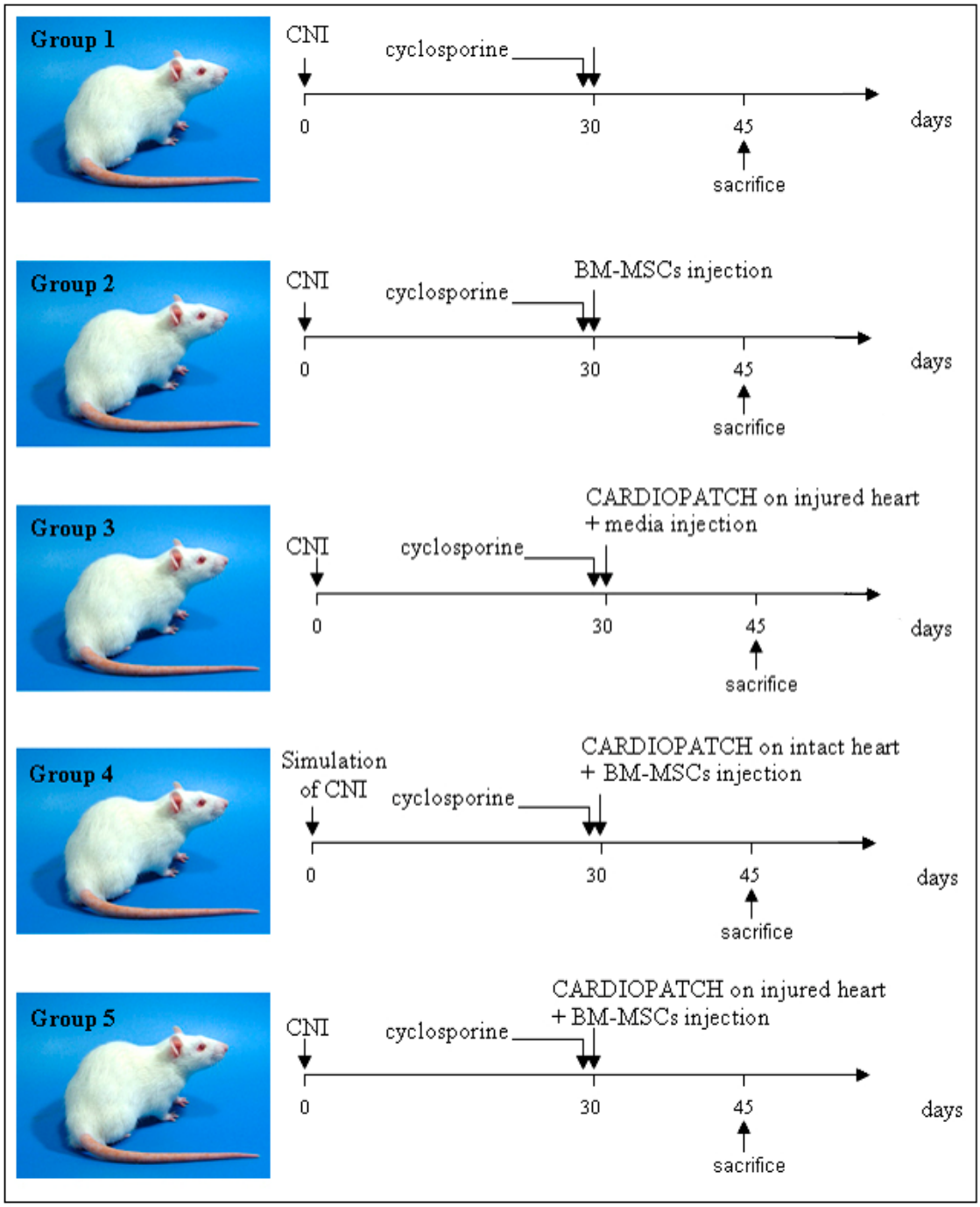

Figure 28 (page 49). Rats used in experiments with rat GFP$^+$ BM-MSCs in a model of CMI. The day before the second operation the rats began treatment with Cyclosporine and continued until sacrifice. The animals were divided into the following groups: in group 1 the animals received cryoinjury alone; in group 2 rats with CMI received via an intra-myocardial route BM-MSCs alone near the damaged zone; in group 3 the patch was attached to the injured myocardium and then injected with medium alone; in group 4 the patch was attached to normal myocardium and the cells injected within it; in group 5 the scaffold was implanted in damaged hearts and subsequently injected with approximately 4x10^6 GFP$^+$ BM-MSCs.

3.5.1 Characterization of rat GFP$^+$ BM-MSCs before transplantation

Rat GFP$^+$ BM-MSCs used for cell transplantation were studied by flow cytometry and cytocentrifugation assays (Figure 29 and Table 10). By flow cytometry these cells expressed for mesenchymal CD44, CD73 and CD90, but were negative for the haematopoietic marker CD45. In the cytocentrifugation assay (Table 6), the BM-MSCs were positive for mesenchymal markers CD29, CD271 and CD105, the stem cell markers SSEA4 and Oct-4 and, to a lesser extent, some cell lineage-specific markers such as Flk-1 and vWf (ECs), SM22/SM α–actin (SMCs). No immunoreactivity was found for CD117 (haematopoietic stem cells) and the pan-cytokeratin antigen (epithelial cells). Vimentin, highly specific for cells of mesenchymal origin, was strongly expressed.

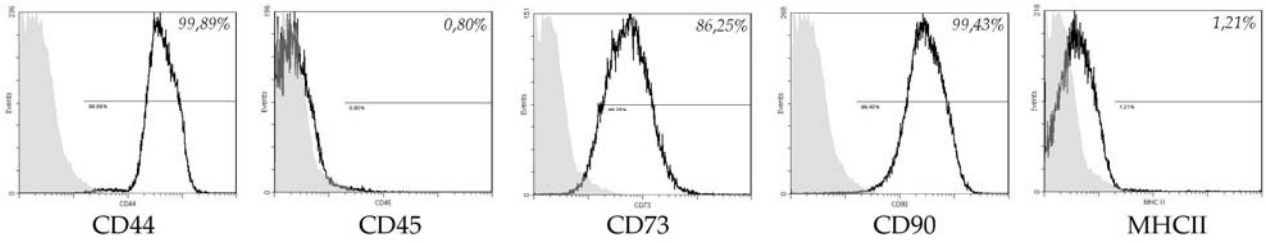

Figure 29. Flow cytometry phenotype of rat GFP$^+$ BM-MSCs. The cells express the MSC markers CD44, CD73 and CD90.

Table 10. Immunophenotyping of rat GFP$^+$ BM-MSCs as determined by cytospin analysis (before transplantation).

Antigen	BM-MSCs
SSEA4	+/- (8%)
Oct-4	+/- (4%)
vWf	+ (14%)
Flk-1	+/- (7%)
CD117	-
CD29 (β1-integrin)	++++ (98%)
CD105 (endoglin)	+++ (70%)
CD271 (NGF-R)	++ (35%)
SM α–actin	+ (15%)
SM22	+ (17%)
Vimentin	++++ (90%)
Pan-cytokeratin	-

Legend: - no positive cells;+/- < 10%; + 10-30%;++ 30-60%;+++ 60-90%;++++ > 90%.

3.5.2 Gross appearance and Haematoxylin-eosin

To investigate a more complex therapeutic use of this biomaterial, rat GFP^+ BM-MSCs were injected into a cardiac patch applied to myocardium after 30 days of CNI. The effects of the collagen cardiac patches and the stem cells on the rat heart were studied at 15 days post-implant.

At explantation, all animals revealed no thoracic adhesions. By gross observation, the cardiac patch was firmly attached to the epicardial surface independently from the previous cryoinjury, but was not able to completely cover the damaged area (Figure 30).

By haematoxylin-eosin staining, the cardiac patch appeared well-fused with the host myocardium and richly populated.

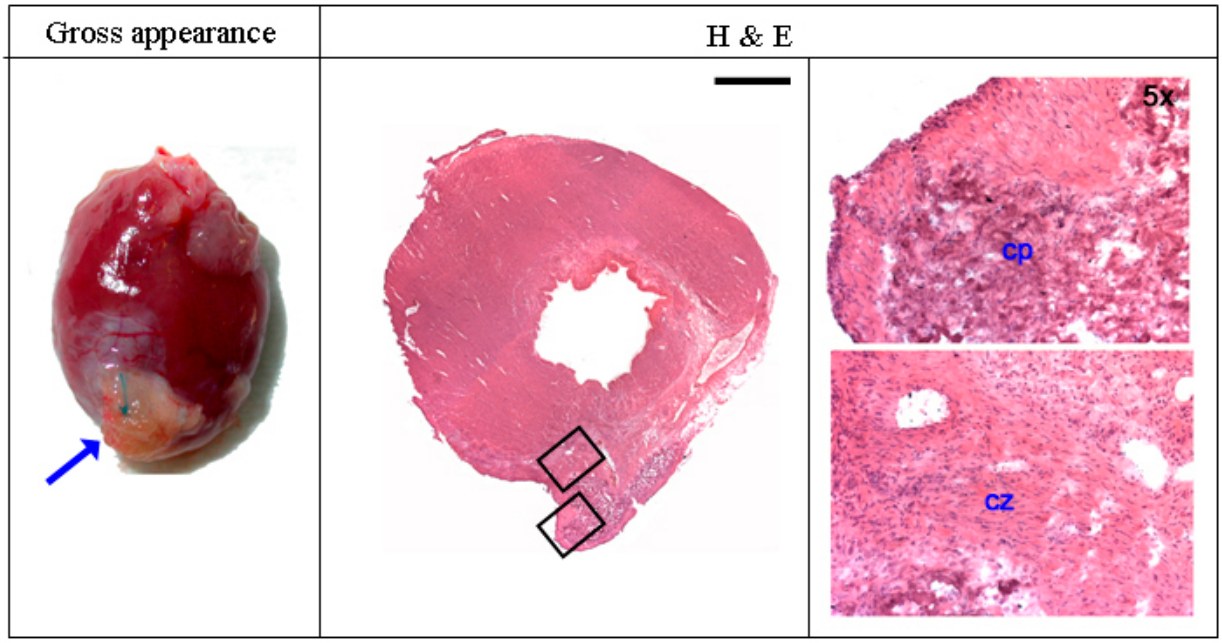

Figure 30. Gross appearance, haematoxylin–eosin staining and magnifications (5x) of heart with collagen cardiac patch and injection of BM-MSCs (30 days of CNI and 15 days after application of cardiopatch and injection of BM-MSCs). Blue arrowhead indicates the collagen cardiac patch. Cp=cardiopatch; cz=cryoinjured zone. Bar = 1 mm.

3.5.3 Identification of transplanted cells

After 15 days post-injection numerous GFP^+ cells were found in the myocardium of animals of group 2, or in the cardiac patch and fibrotic myocardium of animals in groups 4 and 5.

The cryoinjured zones and the cardiac patches of groups 2-5 contained cells organized into blood vessels of different sizes. Capillaries stained for CD31 and arterioles stained for SM α-actin were present in both the patch and in the damaged area (data not shown).

GFP^+ BM-MSCs transplanted into groups 2 or 4 (control groups) were detectable in the cryoinjured zone (Figure 31 a and b) or in the patch (Figure 31 c and d) respectively. Most of the cells were dispersed into the interstice, but several were part of new vessels. Vessel GFP^+ cells also expressed CD31 (capillaries) or SM α-actin (arterioles).

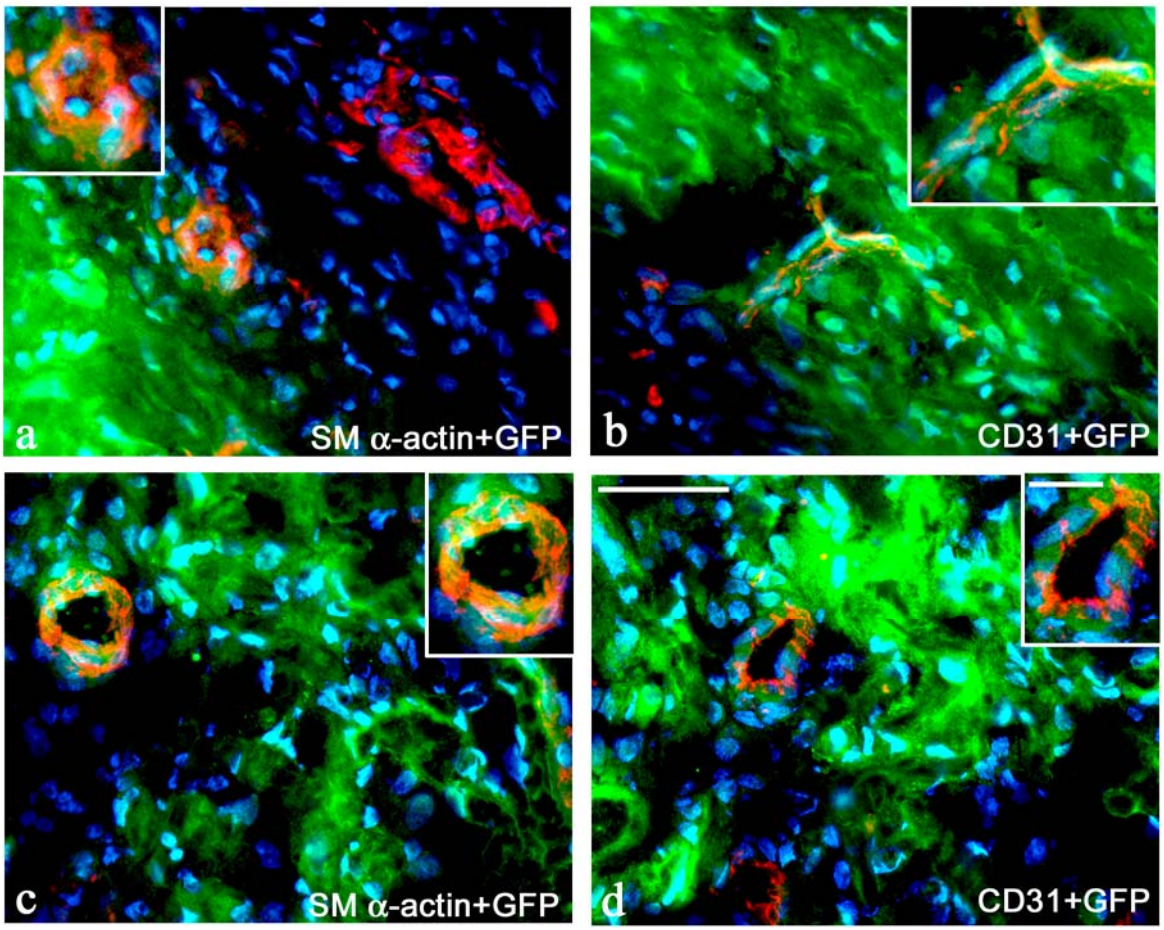

Figure 31. Immunofluorescence on sections of rat hearts of group 2 (a-b; animals with CMI that received the BM-MSCs alone near the damaged zone) and group 4 (c-d; animals where the patch was attached to the normal myocardium and the cells injected within it). In the panel arterioles are identified by staining for SM α-actin (red, a and c), while capillaries are identified by staining for CD31 (red, b and d); GFP^+ cells are identified by the colour green. The colour orange in the vessels results from a merging of green and red and indicates cells that are GFP^+/SM α-$actin^+$ or $GFP^+/CD31^+$. Blue = Hoechst nuclear staining. Bars: 80 and 30 mm (insets).

GFP^+ BM-MSCs also survived well after 15 days post-transplant in group 5 (scaffold implanted in damaged hearts and subsequently injected with stem cells). GFP^+ cells were found dispersed in the scaffold and in the cryoinjured zone. This suggests that the cells can move from the patch to the lesion.

Staining for CD31 and SM α-actin suggested that several new vessels originated both in the cardiac patch and in the cryoinjured zone. Some of these (Figure 33) derived from BM-MSCs, as GFP^+/SM α-$actin^+$ and $GFP^+/CD31^+$ cells were detected. However, the contribute of GFP^+ cells to neoangiogenesis in the cryoinjured zone is very limited. As general indication, the number of capillaries was higher than that of arterioles.

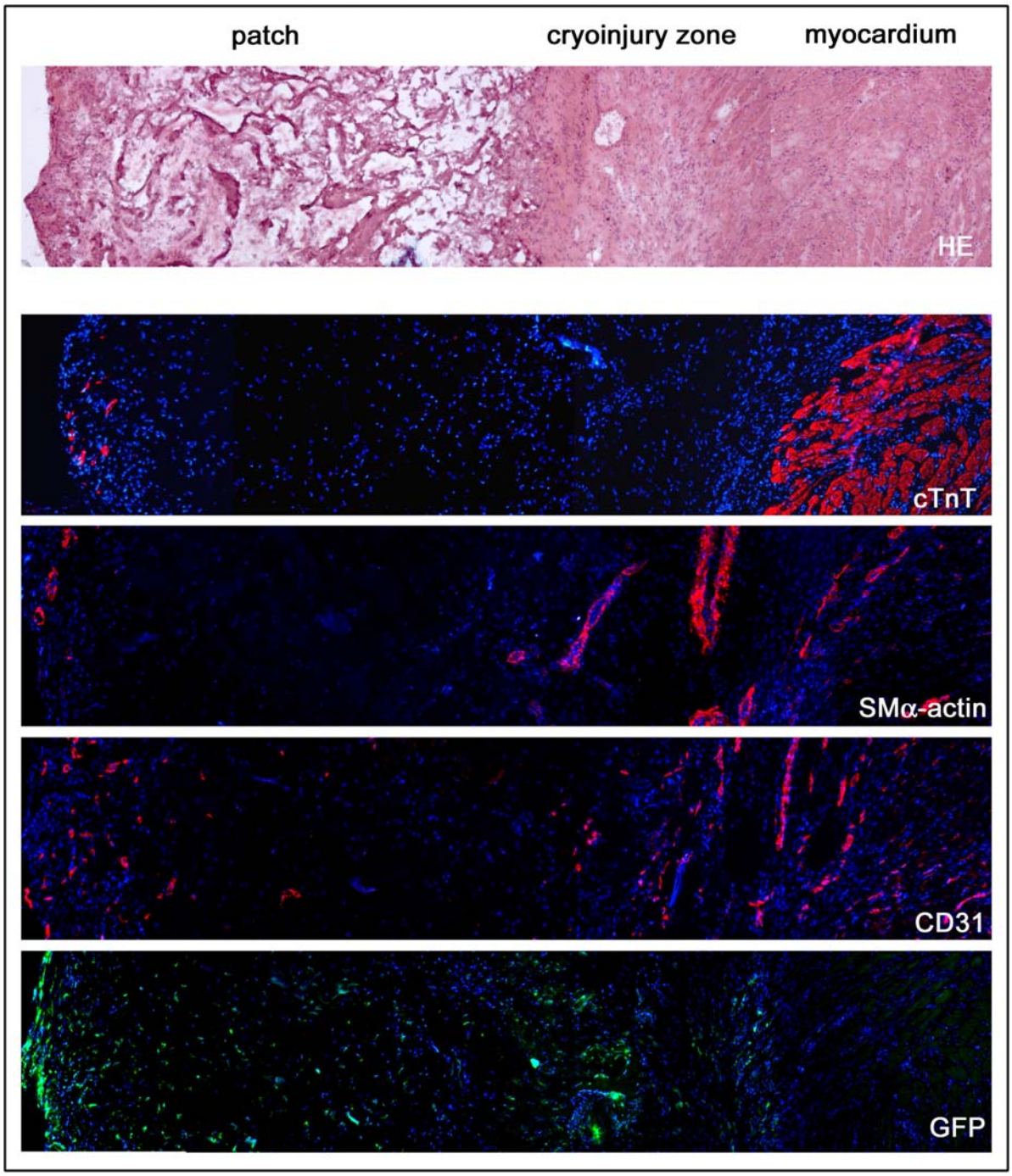

Figure 32. From top to bottom: haematoxylin-eosin staining and immunofluorescence for cTnT, SM α-actin, CD31 and GFP performed on serial sections of hearts of rats from group 5 (patch implanted in hearts with CNI and subsequently injected with GFP^+ BM-MSCs). Patch area, cryoinjured zone and intact heart are shown in that order from left to right. Blue = Hoechst nuclear staining.

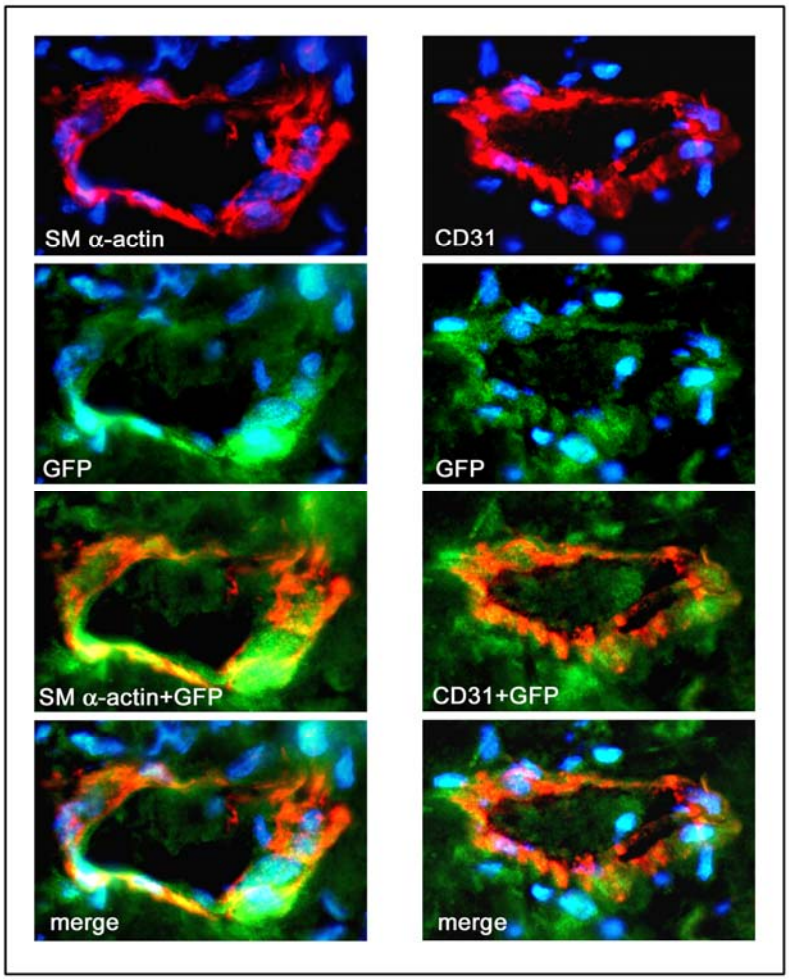

Figure 33. The panel shows immunofluorescence of a vessel detected in the patch of group 5 animals at 15 days post-transplant. The vessel contains SMCs, stained for SM α-actin (red, left column) and ECs, stained for CD31 (red, right column). These cells are also GFP^+ (green). The GFP is coexpressed with SM α-$actin^+$ (orange from merger, left column) or $CD31^+$ cells (orange from merger, right column). Blue = Hoechst nuclear staining.

The BM-MSCs were also able to differentiate into cardiomyocytes. Cells positive both for TnT and GFP were found in the outer zone of patches in group 5 (Figure 34). No cardiomyocytes expressing GFP were found in the cryoinjured zone or intact heart.

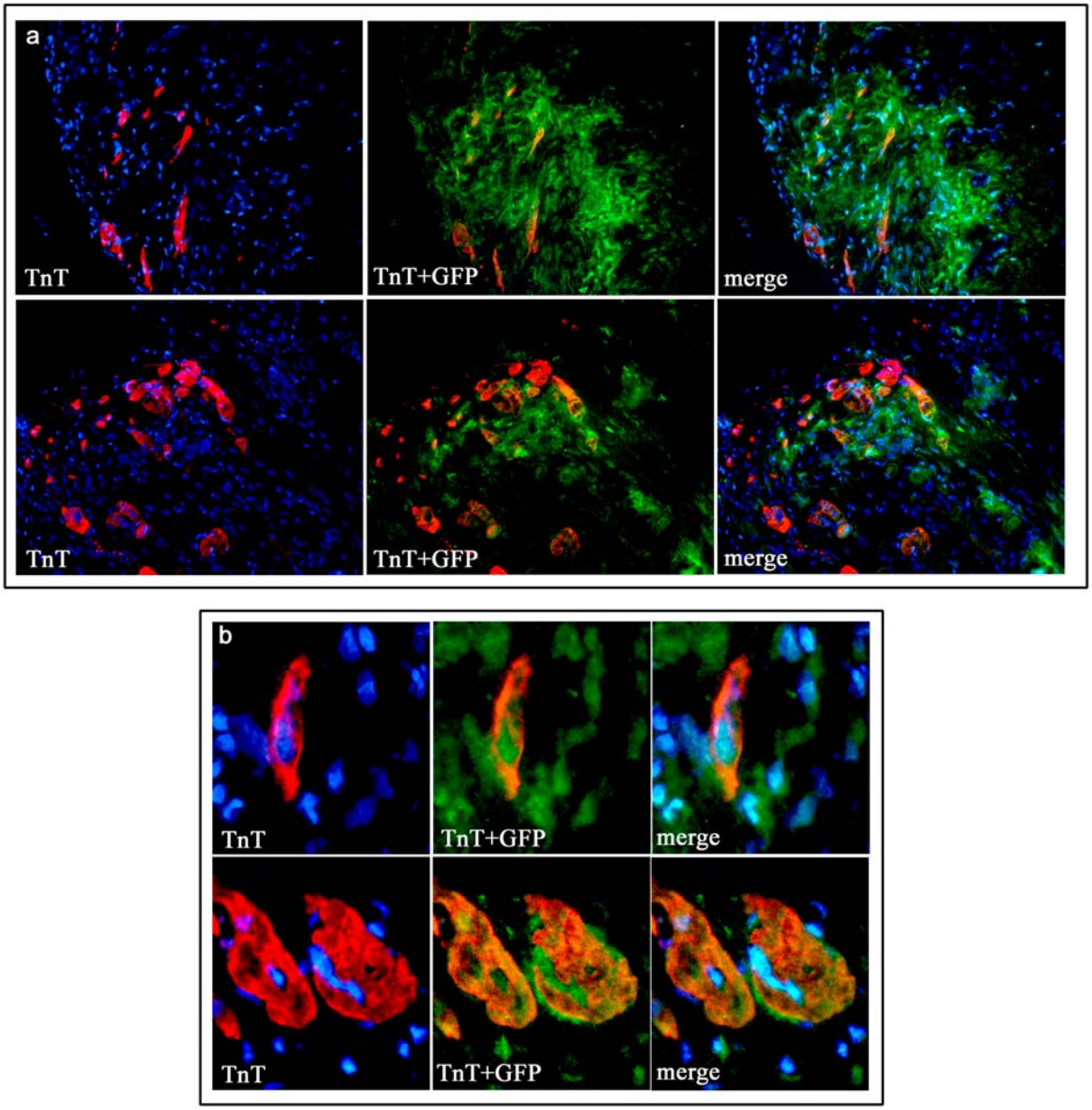

Figure 34. Immunofluorescence of GFP^+ BM-MSCs detected in the patches of group 5 animals at 15 days post-transplant. These cells are able to differentiate into cardiomyocytes expressing TnT (red). Green = GFP staining. Orange = GFP^+/TnT^+ cells. Blue = Hoechst nuclear staining.

3.5.4 Inflammatory cells

Generally, the inflammatory cells showed the same time dependent changes in number seen in the model of CNI with cardiac patch.

$CD45^+$ cells were present in the cardiopatch and/or in the zone of CNI 15 days post transplant in animals that received BM-MSCs (group 2, 4 and 5). In particular, macrophages were very abundant, especially in the late stages.

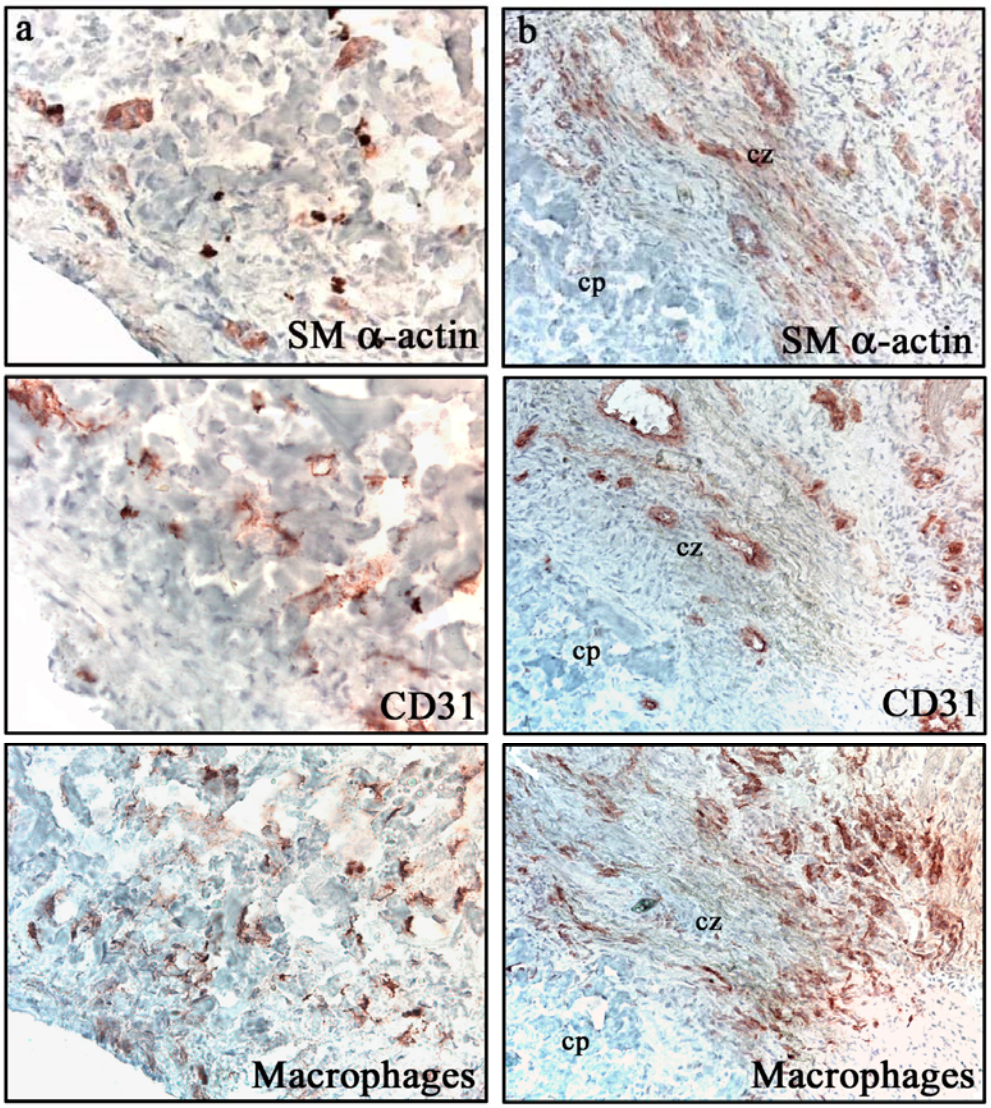

Figure 35. Immunocytochemestry of cells in the collagen cardiac patch (column a) or cryoinjured zone (column b) examined for SM α-actin, CD31 and CD168 expression in group 5 animal 15 days after transplant. The expression for machrophages is quite abundant, Bar, 50 mm.

Discussion

After myocardial infarction, extensive tissue damage leads to the development of congestive heart failure in many survivors. Heart transplantation has remained the only viable treatment for end-stage congestive heart failure, but unfortunately lack of available donor hearts has remained an insurmountable problem. In the search for alternative therapies, myocardial repair via cell therapy has generated a great deal of enthusiasm. However, traditional cell therapy has limitations associated with cell retention, survival and differentiation. In addition, preclinical and clinical studies based on such treatments have generated mixed results. For this reason, hybrid therapies that incorporate tissue engineering are being developed as potentially new therapeutic approaches for repair of myocardial tissue.

The microfibrillar type I collagen-made scaffold is currently used as a topical procoagulant drug for wound healing. This specific biomaterial, in association with Matrigel, was previously used *(Radisic et al., 2003)* as a scaffold for cell seeding of CM *in vitro*, but thorough investigation *in vivo* of its ability to attract new blood vessels and non-vascular cells was lacking. Data from the present study suggest that this collagen scaffold could not only allow for the growth and differentiation of cardiovascular cells *in vitro* but also, when implanted into an intact or cryoinjured rat heart *in vivo (cardiopatch)*, it could induce a marked neovascularization characterized by formation of capillaries and arterioles, and support the growth and differentiation of stem cells. Therefore, this biomaterial may have many interesting applications to tissue engineering after cardiac injury. *(Zimmerman et al., 2006)*.

Three different approaches to evaluating the *in vivo* effectiveness of the scaffold were utilized. The collagen patch alone was implanted in a model of acute necrotizing injury (ANI) or in a model of chronic necrotizing injury (CNI) on rat myocardium. In another experiment, the scaffold implanted in a model of CNI was injected with BM-MSCs labelled with GFP.

The **biocompatibility** features of the collagen scaffold are comparable to other biomaterials used for studies of cardiac tissue regeneration *(Eschenhagen et al., 2005; Gerecht-Nir et al., 2006)*. In fact when implanted in rat peritoneum this biomaterial induces a marked neovascularization response of essentially capillary type which is accompanied by the presence of a marked monocyte-macrophage infiltrate both within the patch and at the tissue-implant interface. The presence of foreign body giant cells at the periphery of the implant, however, indicated that this biomaterial is able to induce and sustain a two-wave

inflammatory response. It could be hypothesized that initially there was a recruitment of phagocytic neutrophils followed by accumulation of activated macrophages which participated transiently in the proliferation and remodelling phases that culminated in the cellular organization of the implant and hence in completion of the wound healing process *(Singer et al., 1999)*. The presence of macrophages and foreign body giant cells at day 30 post-implantation indicated that cell debris and stimulatory signals were persistently generated in high amounts at the interface with the serosal surface of the peritoneum. These signals were likely to be responsible for the second wave of innate immune response. T cells were not found around the implant, thus indicating that a xenogeneic adaptive immune response was not elicited, despite species differences between donor (the collagen scaffold is derived from pig) and host (rat). Though we are aware that the privileged site for assaying biocompatibility is subcutaneous implantation of the biomaterial *(Jansen et al., 2004)*, we purposefully selected peritoneal implantation for this test because it is highly susceptible to inflammation and would be expected to produce the maximal immune response if incompatibility existed between the biomaterial and the host *(Nachtsheim et al., 2006)*.

Another aspect of biocompatibility of the collagen scaffold is dystrophic calcification *(Morsi et al., 2004)*. Restoration of altered cardiac function with this biomaterial could be hampered if an unexpected severe calcification occurred with exogenous transplanted or endogenous mobilized stem cells *(Yoon et al., 2004)*. Not only is type I collagen a well recognized enhancer of osteogenic differentiation of these cells *(Kihara et al., 2006)*, but it can be induced to calcify when a calcification factor contained in the serum is added to a devitalized biomaterial *(Price et al., 2006)*. Collagen scaffold did not induce the formation of von Kossa+ cells when implanted in the peritoneum, except for a very rare EC of infiltrating neovessels. Though cell mineralization in the implant is a rare event, the immunoreactivity of forming vessels for osteopontin and osteocalcin (but not for osteonectin) does not exclude a limited "osteogenic" differentiation in this environment.

As to another basic property of this biomaterial, its time-dependent absorption, our *in vivo* results shown in Figure 8d demonstrate that it was reduced markedly in size after 30 days of implantation and was perfectly integrated with the intact or cryoinjured epicardial surface of the rat heart. The chemical and biophysical nature of the scaffold allowed good adhesion and differentiation of cardiovascular cells *in vitro* (see Figure 6), thus suggesting it was appropriate for *in vivo* tests of its ability to attract and support neovascularization and bone marrow-derived mesenchymal stem cells.

The spatiotemporal cellular sequence of the **inflammatory response** showed some features shared with the peritoneal implant but also some differences in the cardiopatch implanted on intact or cryoinjured heart (zone 2 and 4, respectively) in the acute model (Figure 10). At day 30 post-implantation, macrophages, and to a lesser extent CD161+ cells (NK cells), were abundantly present in the *cardiopatch* along with a minor infiltration of neutrophils *(van Amerongen et al., 2006)*, whereas T cells were absent. Notably, foreign body giant cells were not detected.

The inflammatory cells in the cardiopatch (zones 2 and 4) showed a similar behaviour in the model of CNI: granulocytes peaked at 15 days after application of the scaffold and the macrophages were the most abundant cells up to day 30 (Figure 23).

This was in keeping with the absence of adhesions and the progressive absorption of the *cardiopatch* with the duration of implant. These differences were in concordance with data from van Amerongen et al. (2006) who also found that the host response to the scaffold depends on the site of implantation.

Cryoinjured zones 1 and 3 in the model of ANI displayed an inflammatory response which was quite similar to that with the *cardiopatch* itself except for an earlier neutrophil infiltration which rapidly subsides as happens in a "classical" wound healing process *(Singer et al., 1999)*.

In the model of CNI, the damaged tissue (zones 1 and 3) showed a large number of $CD45^+$ cells (leucocytes). These cells are characteristic of the inflammatory response following the damage induced by CNI. In particular, granulocytes were abundant at the beginning, with a peak by the first week after lesion and 15 days after application of the cardiopatch. Subsequent decrease in the number of granulocytes was accompanied by the simultaneous increase in macrophages, which are the most abundant cells up to day 60 (Figure 23). In addition, T lymphocytes and dendritic cells were absent or present only in traces.

The results obtained with the *cardiopatch* applied to intact or cryoinjured heart in the acute model suggested that scaffold implantation evoked a two-way response: factors released from the cryoinjury zone induced **neovascularization** in the implant, and degradation products from the implant increased the reactive neovascularization inherent to wound healing of ANI *(Vracko et al., 1991)*.

Interesting aspects of reciprocal influence have been highlighted by the comparative evaluation of neovessel distribution in the different zones (see Figures 13 and 26).

First, in the model of ANI, blood vessel development in cardiopatches vs. border zones suggested that, in the latter, the manner by which neovascularization was activated is via angiogenesis and not arteriogenesis. This behaviour may be a consequence of hypoxic stress caused by placement of the cardiopatch on the epicardial surface which induced local tissue degeneration and, hence, death of a thin rim of underlying myocardial cells. This in turn could spark a limited local inflammatory response with the characteristics of reactive neovascularization (prevalence of capillaries). The "border zone" that ensued with the application of cryoinjury was likely to be significantly influenced by granulation tissue formation and organization (not tested for vessel density).

Second, in cardiopatches the newly formed vessels were quite stable and did not undergo an apoptotic dismantling process, up to 60 days after implantation. Third, the presence of a cryoinjury zone adjacent to the cardiopatch enhanced the development of capillaries and arterioles compared to application of the cardiopatch to an intact heart. This effect was attributable to growth factors released from the organizing granulation tissue *(Ertl et al., 2005)*. On the other hand, it is plausible that the granulation tissue received a further angiogenic/arteriogenic stimulus from the contact with the cardiopatch and stimulating factors, such as VEGF and bFGF released from macrophages accumulated in this tissue during 30-60 days after implantation; *(Losordo et al., 2004; Heil et al., 2004; Ertl et al., 2005)*) in such a way as to increase its vascular content.

When applied into the chronic model, the cardiopatch was able to attract neovascularization, with formation of capillaries and arterioles. The scaffold promoted neovascularization in the damaged zone, but this zone was no longer able to induce neovascularization in the cardiopatch, such as occurred in the ANI model. The mutual influence between cardiopatch and zone with CNI was lacking, probably due to a reduction of angiogenic/arteriogenic growth factors released from the granulation tissue. After 30 days post-lesion, granulation tissue undergoes a process of maturation and transforms into fibrous tissue (*Cleutiens et al., 1999*). 15 days after application of the cardiopatch in hearts with CNI, the increase in blood vessels was significant in zone 3, but it lightly decreased at 30 days. The efficacy of the biomaterial for long-term use is thus debatable. In this condition it may be necessary to use angiogenic growth factors (such as VEGF) in order to improve neovascularisation.

In the neovascularization response, both at the cryoinjury and in the cardiopatch, capillary production (neoangiogenesis) generally predominates but the arteriole formation seen represented a novel and important finding in the use of biomaterials for tissue engineering. In fact, other studies reporting on collagen I patching of cardiac lesions failed to demonstrate the

presence of non-capillary blood vessels *(van Amerongen et al., 2006)* or were not described in detail *(Kofidis et al., 2005)*. Formation of larger vessels and not solely capillaries can guarantee an adequate perfusion and hence improve survival and function of CM or phenotypically converted stem/precursor cells *(Davani et al., 2005)*.

Adult heart vessels are normally quiescent, but they expand when provoked by stress or pathologic conditions such as myocardial infarction. The blood vessels in the cardiopatch may originate by three different mechanisms. They may grow by angiogenesis from pre-existing ones, i.e. from the damaged myocardium next to the biomaterial. That happens normally for capillaries, while arterioles may form by muscularization of capillaries (arteriogenesis): the muscular component may derive from myofibroblasts recruited to the damaged zone, from circulating precursors of SMCs and pericytes, or from ECs that trans-differentiate *(Luttun et Carmeliet, 2003)*. Altough, in the model of ANI there was no evidence of myofibroblast, so we can assume a derivation from one of the other sources.

The vessels may also form by vasculogenesis, in a process that involves the recruitment of endothelial, smooth muscle and macrophage precursor cells recruited from the bone marrow *(Luttun et Carmeliet, 2003)*.

In addition, the arterioles may derive from collateral enlargement of pre-existing arteriolar anastomosis *(Schaper et al., 2006)*.

Based on the current results, it is difficult to say if blood vessels originated by angiogenesis-arteriogensis or vasculogenesis or if a connection between the vasculature in the region of injury and in the cardiopatch was present.

It seems reasonable to hypothesize that the marked vascularization within cardiopatches was directly linked to the major cellular phenotype present in the extra-vascular tissue: the **monocyte-macrophage**. Resident/circulating precursors of macrophages have been proposed to be precursors of two cell phenotypes that may accumulate in the cardiopatch, namely, myofibroblasts *(Jabs et al., 2005)* and EC *(Rehman et al., 2003; Ito et al., 2003)*. In addition, macrophages are potent producers of promitogenic and pro-angiogenic/pro-arteriogenic factors *(Losordo et al., 2004; Heil et al., 2004; Rehman et al., 2003)*. Moreover in the skeletal muscle it has also been shown that circulating myeloid cells, in response to inflammatory cues, migrated to regenerating skeletal muscle and took part in myofiber formation. *(Camargo et al., 2003)*. Finally, macrophages also have the ability to integrate into contractile heart tissue and undergo cardiac differentiation when cocultured with cardiac explants. It is possible that longer in vivo experiments would be necessary in order to observe cardiomyocyte

differention within the patches. *(Eisemberg et al., 2004)*. In both our models, however, there was no evidence for SM actin$^+$ myofibroblasts in zones 2 and 4, though we cannot rule out that more immature forms of this cell lineage (e.g., protomyofibroblasts) were present *(Tomasek et al., 2002)*. Thus, it seemed that the major commitment of the unabated recruitment of macrophages in the cardiopatch may have been participating in capillary and arteriole formation.

As the number of macrophages was comparable in zones 2 and 4 in hearts at 15 days after transplant in the model of CNI, the cardiopatch was able to function as an attractor if applied to either intact or cryoinjured heart. Moreover, counting of macrophages and blood vessels showed that both peaked at 15 days after application of the scaffold, consistent with the hypothesis that macrophages were involved in the neo-formation of blood vessels in the cardiopatch (Figure 27).

Though regulation of such a cellular response could be a problem in applying this procedure to cardiac tissue engineering, the use of macrophages or circulating precursors that exhibit a mesenchymal cell differentiation *(Kuwana et al., 2003)* opens new perspectives in the field, possibly via a two-step approach that entails the use of collagen scaffold followed by the CM or stem/precursor cells of endogenous or exogenous origin.

Our collagen scaffold could support growth and differentiation of cardiomyocytes *in vitro* but it was not able to recruit the **cardiogenic stem cells** described by Anversa and coworkers *(2006) in vivo*. Among the infiltrating extra-vascular cells present in the *cardiopatch* (or in the cryoinjury zones 1 and 3; see Figure 14 and table 26) only very few were Sca-1$^+$or MDR1$^+$. Cells expressing the markers nestin and GFAP appear to be more numerous *(El-Helou et al., 2005; Tomita et al., 2005)*, compatible with the phenotype of neural crest-derived cells described by Tomita et al. *(2005)* in the mouse heart. GFAP and nestin were also expressed by rare CM in the border zones and to a lesser extent by CM in the intact heart (*El-Helou et al., 2005)*. In this context expression of nestin has been ascribed to the emergence of a de-differentiated CM phenotype (*El-Helou et al., 2005).*

In the acute model, nestin$^+$ cells found around forming vessels in *cardiopatches* of zones 2 and 4 (Figure 14) are likely to be related to recruiting immature EC *(Mokry et al., 2004)* or pericytes/SMC *(Tomita et al., 2005; Howson et al. 2005)*. In the chronic model, nestin$^+$ cells were present only in zone 2 (table 26).

The GFAP$^+$ cells may be precursors of myofibroblasts: in the stellate cells of the liver this protein seems to be a marker related with the acquisition of contractile properties in a subpopulation more closely associated with precocious stages of fibrosis *(Morini et al., 2005)*. Collectively, these data suggest that these newly designed cardiopatches were able to be colonized by vascular cells, macrophages and progenitor cells expressing nestin. However, the creation of a complete cardiovascular functional unit was lacking.

As these results were encouraging, but not sufficient with regard to a more complex therapeutic use of this biomaterial, it became essential to test an additional manipulation of the cardiopatch.

The patch applied in a model of CMI was therefore injected with **BM-MSCs**, a phenotypically well-characterized cell population that is extensively used as therapy for myocardial infraction both in animal models (see Table 4 for ref.) and in human trials *(Strauer et al., 2002; Tateishi-Yuyama et al., 2002; Tse et al., 2003; Chen SL et al., 2004; Wollert et al., 2004; Chen S et al., 2006; Mohyeddin-Bonab et al., 2007)*.

In particular, MSCs appear useful for transplant due to their low immunogenicity and ability to home to the site of myocardial injury *(Saito et al., 2002; Bittira et al., 2003; Pittenger et Martin, 2004)*. However, the BM-MSCs injected into the patch constitutively expressed EGFP, a green fluorescent marker easy to track after transplantation, but capable of inducing an immune response. In fact, some studies have shown that GFP-derived peptides, processed and presented by MHC on the cell surface, lead to an immunitary response induced by T lymphocytes. *(Stripecke et al., 1999)*. For this reason all animals receiving GFP$^+$ BM-MSCs were treated with cyclosporine to avoid rejection. In the immunosuppressed animals, inflammatory cells showed the same time-dependent changes in number that were seen in the model of CNI with the cardiac patch alone. CD45$^+$ cells were present in the cardiopatch and/or in the zone of CNI 15 days post-transplant in animals that received BM-MSCs (groups 2, 4 and 5). In particular, macrophages were very abundant, especially in the late stages.

It seems possible that BM-MSCs injected directly into an adult heart may differentiate in cardiomyocytes, endothelial cells and smooth muscle cells *(Gojo et al., 2003)*. This fact was confirmed in our study, and also seen when the cells were injected into the patch and not into the damaged myocardium directly.

After 15 days post-injection numerous GFP$^+$ cells were found in the myocardium of animals in group 2 (rats with CMI that received GFP$^+$ BM-MSCs alone near the damaged zone), and in both the cardiac patch and fibrotic myocardium of animals in groups 4 (patch attached to

normal myocardium and the cells injected within it) and 5 (scaffold implanted in damaged hearts and subsequently injected with GFP^+ BM-MSCs). This suggests that the cells injected into the patch were able to move from the patch to the myocardium.

Some of the transplanted GFP^+ BM-MSCs were positive for endothelial (CD31) and smooth muscle (SM α-actin) cell markers and were found in capillaries and arterioles, respectively. In particular, in group 5, most of the BM-MSCs were dispersed into the interstice and several participated in vessel formation both in the cardiopatch and in the cryoinjured zone. However, the contribution of GFP^+ cells to neoangiogenesis in the cryoinjured zone was very limited.

Recently Simpson et al. *(2007)* revealed that hMSCs, embedded into a rat tail type I collagen matrix and transplanted into infarcted rat myocardium, were able to improve heart function, but they did not express SM α-actin. We did not determine if the BM-MSCs transplanted in the cardiopatch significantly increased vessel density in the myocardium, however these cells expressed SM α-actin, which plays an important role in vessel maturation.

We can not also exclude that BM-MSCs may also induce a therapeutic angiogenesis, as shown in previous studies *(Murohara et al., 2000; Tateishi-Yuyama et al., 2002; Tse et al., 2003)*. The angiogenic potential of MSCs is mediated at least in part by production of a variety of angiogenic factors, such as vascular endothelial growth factor (VEGF), hepatocyte growth factor (HGF), adrenomedullin (AM) and insulin-like growth factor-1 (IGF-1) *(Nagaya et al., 2005)*. Taking these findings together, BM-MSCs may contribute to neovascularization in the myocardium not only through their ability to generate capillaries and arterioles but also through growth factor–mediated paracrine regulation.

Two weeks after transplantation some of the engrafted MSCs were stained positive for cardiac troponin T. No presence of cTnT positive cells was revealed in the injured myocardium of animals in group 5.

In previous models, use of the collagen scaffold only in cardiac repair was not sufficient to mobilize locally resident cardiogenic stem cells. The use of BM-MSCs was able to avoid the lacking of cells with the phenotypic profile of cardiomyocytes, even if the percentage of conversion to this kind of cell was not large enough to ensure adequate functional recovery.

Regardless, it has been demonstrated that BM-MSCs exert their role in cardiac regeneration not only by differentiating into specific cell types such as cardiomyocytes and vascular endothelial cells but also through paracrine effects via secretion of a variety of angiogenic, antiapoptotic, and mitogenic factors *(Kinnaird et al. 2004; Nagaya et al., 2005; Gnecchi et al., 2005)*.

These studies suggested that BM-MSCs have a cardioprotective effect also acting in a

paracrine manner, demonstrating the importance of secreted factors in cardiac repair. Additional studies are necessary to optimize the constructs for myocardial repair. Further manipulations should include, for example, introduction on the engineered collagen scaffold of factors, such as IGF-I *(Davis et al., 2006)*, that can activate locally resident cardiogenic stem cells, or the transplantation of progenitors commited to the cardiomyogenic lineage *(Guo et al., 2006)*.

Bibliography

Aicher A, Zeiher AM, Dimmeler S. Mobilizing endothelial progenitor cells. *Hypertension.* 2005 Mar; 45(3): 321-5.

Anversa P, Leri A, Kajstura J. Cardiac regeneration. J Am Coll Cardiol 2006; 47:1769-76.

Asahara T, Murohara T, Sullivan A, Silver M, van der Zee R, Li T, Witzenbichler B, Schatteman G, Isner JM. Isolation of putative progenitor endothelial cells for angiogenesis. *Science.* 1997 Feb 14; 275(5302): 964-7.

Atala A. Experimental and clinical experience with tissue engineering techniques for urethral recostruction. Urol Clin North Am. 2002; 29(2):485-92, ix.

Behfar A, Zingman LV, Hodgson DM, Rauzier JM, Kane GC and Terzic A. Stem cell differentiation requires a paracrine pathway in the heart. *FASEB J* 2002; 16 , pp. 1558-1566.

Beltrami AP, **Barlucchi L**, **Torella D**, **Baker M**, **Limana F**, **Chimenti S**, **Kasahara H**, **Rota M**, **Musso E**, **Urbanek K**, **Leri A**, **Kajstura J**, **Nadal-Ginard B**, **Anversa P**. Adult cardiac stem cells are multipotent and support myocardial regeneration. *Cell.* 2003 Sep 19;114(6):763-76.

Beltrami CA, Finato N, Rocco M, Feruglio GA, Puricelli C, Cigola E, Quaini F, Sonnenblick EH, Olivetti G, Anversa P. Structural basis of end-stage failure in ischemic cardiomyopathy in humans. *Circulation* 1994; 89, pp. 151–163.

Birla RK, Borschel GH, Dennis RG, Brown DL. Myocardial engineering in vivo: formation and characterization of contractile, vascularized three-dimensional cardiac tissue. *Tissue Eng*. 2005 May-Jun; 11 (5-6): 803-13.

Bittira B, **Shum-Tim D**, **Al-Khaldi A**, **Chiu RC**. Mobilization and homing of bone marrow stromal cells in myocardial infarction. *Eur J Cardiothorac Surg*. 2003 Sep; 24(3): 393-8.

Boheler KR and Schwartz K. Gene expression in cardiac hypertrophy. *Trends Cardiovasc Med* 1992; 2, pp. 176–182.

Bradley A, Evans M, Kaufman MH and Robertson E. Formation of germ-line chimaeras from embryo-derived teratocarcinoma cell lines. *Nature*, 1984.309, pp.255-256.

Brilla CG, Janicki JS, Weber KT. Impaired diastolic function and coronary reserve in genetic hypertension. Role of interstitial fibrosis and medial thickening of myocardial coronary arteries. 1991 Circ. Res. 69, 107-115.

Cai CL, Liang X, Shi Y, Chu PH, Pfaff SL, Chen J, Evans S. Isl1 identifies a cardiac progenitor population that proliferates prior to differentiation and contributes a majority of cells to the heart. *Dev Cell.* 2003 Dec;5(6):877-89.

Camargo FD, Green R, Capetanaki Y, Jackson KA, Goodell MA. Single hematopoietic stem cells generate skeletal muscle through myeloid intermediates. *Nature Medicine.* 2003 Dec; 9 (12): 1520-7.

Chang Y, Lai PH, Wei HJ, Lin WW, Chen CH, Hwang SM, Chen SC, Sung HW. Tissue regeneration observed in a basic fibroblast growth factor-loaded porous acellular bovine pericardium populated with mesenchymal stem cells. *J Thorac Cardiovasc Surg*. 2007 Jul;134(1):65-73, 73.e1-4.

Chen S, Liu Z, Tian N, Zhang J, Yei F, Duan B, Zhu Z, Lin S, Kwan TW. Intracoronary transplantation of autologous bone marrow mesenchymal stem cells for ischemic cardiomyopathy due to isolated chronic occluded left anterior descending artery. *J Invasive Cardiol*. 2006; 18: 552-556.

Chen SL, Fang WW, Ye F, Liu YH, Qian J, Shan SJ, Zhang JJ, Chunhua RZ, Liao LM, Lin S, Sun JP. Effect on left ventricular function of intracoronary transplantation of autologous bone marrow mesenchymal stem cell in patients with acute myocardial infarction. *Am J Cardiol.* 2004; 94: 92-95.

Cleutjens JPM, Blankesteijn WM, Daemen MJAP, Smits JFM. The infarcted myocardium: simply dead tissue, or a lively target for therapeutic interventions. Cardiovascular Research. 1999; 44:232-241.

Cleutjens PM, Verluyten M, Smits JFM and Daemen MJAP. Collagen remodeling after myocardial infarction in the rat heart. *Am J Pathol* 1995; 147, pp. 325–338.

Davani S, Deschaseaux F, Chalmers F, Tiberghien P, Kantelip JP. Can stem cells mend a broken heart? *Cardiovasc Res*. 2005; 65: 305-16.

Davis ME, Hsieh PC, Takahashi T, Song Q, Zhang S, Kamm RD, Grodzinsky AJ, Anversa P, Lee RT. Local myocardial insulin-like growth factor 1 (IGF-1) delivery with biotinylated peptide nanofibers improves cell therapy for myocardial infarction. *Proc Natl Acad Sci U S A.* 2006; 103: 8155-60.

Dawn B, Stein AB, Urbanek K, Rota M, Whang B, Rastaldo R, Torella D, Tang XL, Rezazadeh A, Kajstura J, Leri A, Hunt G, Varma J, Prabhu SD, Anversa P, Bolli R. Cardiac stem cells delivered intravascularly traverse the vessel barrier, regenerate infarcted myocardium, and improve cardiac function. *Proc Natl Acad Sci U S A.* 2005 Mar 8; 102(10): 3766-71.

Deindl E, Zaruba MM, Brunner S, Huber B, Mehl U, Assmann G, Hoefer IE, Mueller-Hoecker J, Franz WM. G-CSF administration after myocardial infarction in mice attenuates late ischemic cardiomyopathy by enhanced arteriogenesis. *FASEB J*. 2006 May;20(7):956-8.

Deten A, **Volz HC**, **Clamors S**, **Leiblein S**, **Briest W**, **Marx G**, **Zimmer HG**. *et al*. Hematopoietic stem cells do not repair the infarcted mouse heart. *Cardiovasc. Res.* 2005; 65, 52−63.

Digirolamo CM, Stokes D, Colter D, Phinney DG, Class R, Prokop DJ. Propagation and senescence of human marrow stromal cells in culture: a simple colony-forming assay identifies samples with the greatest potential to propagate and differentiate. *Brith J Haemat*. 1999; 107: 275-281.

Eisemberg LM, Burns L, Eisenberg CA. Hematopoietic cells from bone marrow have the potential to differentiate into cardiomyocytes in vitro. *Anat Rec A Discov Mol Cell Evol Biol*. 2003 Sep; 274 (1): 870-82.

El-Helou V, Dupuis J, Proulx C, Drapeau J, Clement R, Gosselin H, Villeneuve L, Manganas L, Calderone A. Resident nestin+ neural-like cells and fibers are detected in normal and damaged rat myocardium. *Hypertension*. 2005; 46: 1219-25.

Ertl G, Frantz S. Healing after myocardial infarction. *Cardiovasc Res*. 2005;66:22-32.

Eschenhagen T, Didie M, Heubach J, Ravens U, Zimmermann WH. Cardiac tissue engineereng. Transpl Immunol.2002; 9(2-4):315-21.

Eschenhagen T, Zimmermann WH. Engineering myocardial tissue. *Circ Res.* 2005; 97: 1220-31.

Frid MG, Brunetti JA, Burke DL, Carpenter TC, Davie NJ, Reeves JT, Roedersheimer MT, van Rooijen N, Stenmark KR. Hypoxia-induced pulmonary vascular remodelling requires recruitament of circulating mesenchymal precursors of a monocyte/macrophage lineage. Am j Pathol. 2006; 168(2):659-69.

Fridenstein A. Stromal bone marrow cells and the hematopoietic microenvironment. *Arkh. Patol.* 1982; 44: 3-11.

Fuchs JR, Nasseri BA, Vacanti JP, Fauza DO. Postnatal myocardial augmentation with skeletal myoblast-based fetal tissue engineering. *Surgery*. 2006 Jul;140(1):100-7.

Fujimoto KL, Tobita K, Merryman WD, Guan J, Momoi N, Stolz DB, Sacks MS, Keller BB, Wagner WR. An elastic, biodegradable cardiac patch induces contractile smooth muscle and improves cardiac remodeling and function in subacute myocardial infarction. *J Am Coll Cardiol.* 2007 Jun 12;49(23):2292-300.

Gerecht-Nir S, Radisic M, Park H, Cannizzaro C, Boublik J, Langer R, Vunjak-Novakovic G. Biophysical regulation during cardiac development and application to tissue engineering. *Int J Dev Bio*. 2006; 50: 233-43.

Giulla MM, Paliotti R, Ferrero S, Braidotti P, Esposito A, Gianelli U, Busca G, Cioffi U, Bulfamante G, Magrini F. Left ventricular remodeling after experimental myocardial cryoinjury in rats. J Surg Res. 2004; 116(1):91-7.

Gnecchi M, He H, Liang OD, Melo LG, Morello F, Mu H, Noiseux N, Zhang L, Pratt RE, Ingwall JS, Dzau VJ. Paracrine action accounts for marked protection of ischemic heart by Akt-modified mesenchymal stem cells. *Nat Med* 2005; 11: 367-368.

Gojo S, Gojo N, Takeda Y, Mori T, Abe H, Kyo S, Hata J, Umezawa A. In vivo cardiovasculogenesis by direct injection of isolated adult mesenchymal stem cells. *Exp Cell Research*. 2003; 288: 51-59.

Gronthos S, Simmons P. The biology and application of human bone marrow stromal cells precursors. *J. Hematother.* 1996; 5: 15-23.

Guo XM, Zhao YS, Chang HX, Wang CY, E LL, Zhang XA, Duan CM, Dong LZ, Jiang H, Li J, Song Y, Yang XJ. Creation of engineered cardiac tissue in vitro from mouse embryonic stem cells. *Circulation.* 2006; 113: 2229-37.

Harada M, Qin Y, Takano H, Minamino T, Zou Y, Toko H, Ohtsuka M, Matsuura K, Sano M, Nishi J, Iwanaga K, Akazawa H, Kunieda T, Zhu W, Hasegawa H, Kunisada K, Nagai T, Nakaya H, Yamauchi-Takihara K, Komuro I. G-CSF prevents cardiac remodeling after myocardial infarction by activating the Jak-Stat pathway in cardiomyocytes. *Nat Med.* 2005 Mar;11(3):305-11.

Hasegawa H, Takano H, Iwanaga K, Ohtsuka M, Qin Y, Niitsuma Y, Ueda K, Toyoda T, Tadokoro H, Komuro I. Cardioprotective effects of granulocyte colony-stimulating factor in swine with chronic myocardial ischemia. *J Am Coll Cardiol.* 2006 Feb 21;47(4):842-9.

Haynesworth S, Baber MA, Caplan AI. Cell surface antigens on human marrow-derived mesenchymal cells are detected by monoclonal antibodies. *Bone*. 1992; 13: 69-80.

Heil M, Eitenmuller I, Schmitz-Rixen T, Schaper W. Arteriogenesis versus angiogenesis: similarities and differences. J. Cell. Mol. Med. 2006, 10(1):45-55.

Heil M, Schaper W. Influence of mechanical, cellular, and molecular factors on collateral artery growth (arteriogenesis). *Circ Res.* 2004;95:449-58.

Hilenski LL, Terracio L, Borg TK. Myofibrillar and cytoskeletal assembly in neonatal rat cardiomyocytes cultured on laminin and collagen. *Cell Tissue Res* 1991;264:577-87.

Howson KM, Aplin AC, Gelati M, Alessandri G, Parati EA, Nicosia RF. The postnatal rat aorta contains pericyte progenitor cells that form spheroidal colonies in suspension culture. *Am J Physiol Cell Physiol*. 2005; 289: C1396-40.

Ince H, Petzsch M, Kleine HD, Schmidt H, Rehders T, Korber T, Schumichen C, Freund M, Nienaber CA. Preservation from left ventricular remodeling by front-integrated revascularization and stem cell liberation in evolving acute myocardial infarction by use of granulocyte-colony-stimulating factor (FIRSTLINE-AMI). *Circulation*. 2005 Nov 15;112(20):3097-106.

Ito WD, Khmelevski E. Tissue macrophages: "Satellite Cells" for growing collateral vessels? A hypothesis. *Endothelium*. 2003; 10: 233-5.

Iwanaga K, Takano H, Ohtsuka M, Hasegawa H, Zou Y, Qin Y, Odaka K, Hiroshima K, Tadokoro H, Komuro I. Effects of G-CSF on cardiac remodeling after acute myocardial infarction in swine. *Biochem. Biophys. Res. Commun.* 2004; 325, 1353−1359.

Jabs A, Moncada G, Nichols C, Waller E, Wilcox J. Peripheral blood mononuclear cells acquire myofibroblast characteristics in granulation tissue. *J Vasc Res.* 2005; 42: 174-80.

Jackson BM, Gorman JH 3rd, Salgo IS, Moainie SL, Plappert T, St Jhon-Sutton M, Edmunds LH Jr, Gorman RC. Border zone geometry increases wall stress after myocardial infarction: contrast echocardiographic assessment. Am. J. Physiol. Heart. Circ. Physiol. 2003; 284(2): H475-9.

Jackson BM, Parish LM, Gorman JH 3rd, Enomoto Y, Sakamoto H, Plappert T, St John Sutton MG, Salgo I, Gorman RC. Borderzone geometry after acute myocardial infarction: a three-dimensional contrast enhanced echocardiographic study. *Ann Thorac Surg* 2005 Dec; 80(6): 2250-5.

Jansen K, van der Werff JFA, van Wachem PB, Nicolai JPA, de Leij LFMH, van Luyn MJA. A hyaluronan-based nerve guide: in vitro cytotoxicity, sunncutaneous tissue reactions, and degradation in the rat. *Biomaterials* 2004; 25: 483-9.

Jiang Y, Dudek K, Jahagirdar B, Koodie L, Marker PH, Verfaillie CM. Pluripotent nature of adult marrow derived mesenchymal stem cells. *Nature.* 2002; 418: 41-49.

Kajstura J, **Cheng W**, **Reiss K**, **Clark WA**, **Sonnenblick EH**, **Krajewski S**, **Reed JC**, **Olivetti G**, **Anversa P**. Apoptotic and necrotic myocyte cell death are independent contributing variables of infarct size in rats. *Lab Invest* 1996; 74, pp. 86–107.

Kanellakis P, Slater NJ, Du XJ, Bobik A, Curtis DJ. Granulocyte colony-stimulating factor and stem cell factor improve endogenous repair after myocardial infarction. *Cardiovasc Res*. 2006 Apr 1;70(1):117-25.

Kang HJ, Kim HS, Koo BK, Kim YJ, Lee D, Sohn DW, Oh BH, Park YB. Intracoronary infusion of the mobilized peripheral blood stem cell by G-CSF is better than mobilization alone by G-CSF for improvement of cardiac function and remodeling: 2-year follow-up results of the Myocardial Regeneration and Angiogenesis in Myocardial Infarction with G-CSF and Intra-Coronary Stem Cell Infusion (MAGIC Cell) 1 trial. *Am Heart J.* 2007 Feb;153(2):237.e1-8

Kang HJ, Kim HS, Zhang SY, Park KW, Cho HJ, Koo BK, Kim YJ, Soo Lee D, Sohn DW, Han KS, Oh BH, Lee MM, Park YB Effects of intracoronary infusion of peripheral blood stem-cells mobilised with granulocyte-colony stimulating factor on left ventricular systolic function and

restenosis after coronary stenting in myocardial infarction: the MAGIC cell randomised clinical trial. *Lancet*. 2004 363:751–756.

Kattman SJ, Huber TL, Keller GM. Multipotent flk-1+ cardiovascular progenitor cells give rise to the cardiomyocyte, endothelial, and vascular smooth muscle lineages. *Dev Cell*. 2006 Nov;11(5):723-32.

Kihara T, Hirose M, Oshima A, Ohgushi H. Exogenous type I collagen facilitates osteogenic differentiation and acts as a substrate for mineralization of rat marrow mesenchymal stem cells in vitro. *Biochem Biophys Res Commun*. 2006; 341: 1029-35.

Kinnaird T, Stabile E, Burnett MS, Lee CW, Barr S, Fuchs S, Epstein SE. Marrow-derived stromal cells express genes encoding a broad spectrum of arteriogenic cytokines and promote in vitro and in vivo arteriogenesis through paracrine mechanisms. *Circ Res.* 2004; 94: 678-685.

Kocher AA, Schuster MD, Szabolcs MJ, Takuma S, Burkhoff D, Wang J, Homma S, Edwards NM, Itescu S. Neovascularization of ischemic myocardium by human bone-marrow-derived angioblasts prevents cardiomyocyte apoptosis, reduces remodeling and improves cardiac function. *Nat Med.* 2001 Apr; 7(4): 430-6.

Kofidis T, Akhyari P, Boublik J, Theodorou P, Martin U, Ruhparwar AQ, Fisher S, Eschenhagen T, Kubis HP, Kraft T, Leyh R, Haverich A. In vitro engineering of heart muscle: artificial myocardial tissue. *J Thorac Cardiovasc Surg*. 2002;124:63-9.

Kofidis T, de Bruin JL, Hoyt G, Ho Y, Tanaka M,, Yamane T, Lebl DR, Swijnenburg R-J, Chang C-P, Quertermous T, Robbins RC. Myocardial restoration with embryonic stem cell bioartificial tissue transplantation. *J Heart Lung Transplant*. 2005; 24: 737-44.

Kofidis T, Lebl DR, Martinez EC, Hoyt G, Tanaka M, Robbins RC. Novel injectable bioartificial tissue facilitates targeted, less invasive, large-scale tissue restoration on the beating heart after myocardial injury. *Circulation* 2005b; 112(9 Suppl):I173-7.

Kofidis T, de Bruin JL, Yamane T, Balsam LB, Lebl DR and Swijnenburg RJ. Insulin-like growth factor promotes engraftment, differentiation, and functional improvement after transfer of embryonic stem cells for myocardial restoration.. *Stem Cells.* 2004; 22, pp. 1239-1245.

Kopen G, Prockop DJ, Phinney DG. Marrow stromal cells migrate throughtout forebrain and cerebellum, and they differentiate into astrocytes after injection into neonatal mouse brains. *Proc. Natl. Acad. Sci. U.S.A.* 1999; 96: 10711-10716.

Kuethe F, Figulla HR, Herzau M, Voth M, Fritzenwanger M, Opfermann T, Pachmann K, Krack A, Sayer HG, Gottschild D, Werner GS. Treatment with granulocyte colony-stimulating factor for mobilization of bone marrow cells in patients with acute myocardial infarction. *Am Heart J*. 2005 150:115 (e1–7).

Kuizinga MC, Smits JFM, Arends JW and Daemen MJAP. AT2 receptor blockade reduces cardiac interstitial cell DNA synthesis and cardiac function after rat myocardial infarction. *J Mol Cell Cardiol* 1998; 30, pp. 425–434.

Kuwana M, Okazaki Y, Kodama H, Izumi K, Yasuoka H, Ogawa Y, Kawakami Y, Ikeda Y. Human circulating CD14+ monocytes as a source of progenitors that exhibit mesenchymal cell differentiation. *J Leukoc Biol.* 2003; 74: 833-45.

Laflamme MA, Murry CE. Regenerating the heart. *Nat Biotechnol*. 2005; Jul 23(7): 845-56.

Langer R, Vacanti JP. Tissue engineering. Science. 1993 May 14; 260(5110):920-6.

Laugwitz KL, Moretti A, Lam J, Gruber P, Chen Y, Woodard S, Lin LZ, Cai CL, Lu MM, Reth M, Platoshyn O, Yuan JX, Evans S, Chien KR. Postnatal isl1+ cardioblasts enter fully differentiated cardiomyocyte lineages. *Nature.* 2005 Feb 10; 433 (7026): 647-53.

Leobon B, Garcin I, Menasche P, Vilquin JT, Audinat E, Charpak S. Myoblasts transplanted into rat infarcted myocardium are functionally isolated from their host. *Proc Natl Acad Sci U S A*. 2003 Jun 24;100 (13): 7808-11.

Leor J, Aboulafia-Etzion S, Dar A, Shapiro L, Barbash IM, Battler A, Granot Y, Cohen S. Biongineered cardiac grafts: A new approach to repair the infarcted myocardium? *Circulation* 2000; 102 (19 Suppl 3): III56-61.

Li RK, Jia ZQ, Weisel RD, Mickle DA, Choi A, Yau TM. Survival and function of bioengineered cardiac grafts. Circulation 1999; 100(19 Suppl):II63-9.

Li WG, Zaheer A, Coppey L and Oskarsson HJ. Activation of JNK in the remote non-infarcted myocardium after large myocardial infarction in rats. *Biochem Biophys Res Commun* 1998; 246**,** pp. 816–820

Linda W. van Laake, Rutger Hassink, Pieter A. Doevendans and Christine Mummery. Heart repair and stem cells. *J. Physiol.* 2006; 577;467-478.

Losordo DW, Dimmeler S. Therapeutic angiogenesis and vasculogenesis for ischemic disease. *Circulation.* 2004;109:2487-91.

Luttun A, Carmeliet P. De novo vasculogenesis in the heart. Cardiovascular Research 2003; 58: 378-389.

Ma J, Ge J, Zhang S, Sun A, Shen J, Chen L, Wang K, Zou Y. Time course of myocardial stromal cell-derived factor 1 expression and beneficial effects of intravenously administered bone marrow stem cells in rats with experimental myocardial infarction. *Basic Res Cardiol.* 2005 May;100(3): 217-23.

Makoto K, Ryozo N, Hidetsugu T, Hirohisa K, Yoshio Y, Akiyuki O, Fuminaru T. Developmentally Regulated Expression of Vascular Smooth Muscle Heavy Chain Isoforms. The Journal of Biological Chemistry 1989; 31:18272-18275.

Maltsev V A, Wobus A M, Rohwedel J, Bader M and Hescheler J. Cardiomyocytes differentiated in vitro from embryonic stem cells developmentally express cardiac-specific genes and ionic currents. *Circ Res* 1994. 75, pp. 233-244.

Martin CM, Meeson AP, Robertson SM, Hawke TJ, Richardson JA, Bates S, Goetsch SC, Gallardo TD, Garry DJ. Persistent expression of the ATP-binding cassette transporter, Abcg2, identifies cardiac SP cells in the developing and adult heart. *Dev Biol*. 2004 Jan 1; 265(1): 262-75.

Matsubayashi K, Fedak PW, Mickle DA, Weisel RD, Ozawa T, Li RK. Improved left ventricular aneurysm repair with bioengineered vascular smooth muscle grafts. *Circulation* 2003, 108 Suppl 1:II219-25.

Menasche P. Skeletal myoblast for cell therapy. *Coron Artery Dis.* 2005; Mar; 16(2): 105-10.

Menasche P. Skeletal myoblasts as a therapeutic agent. *Prog Cardiovasc Dis*. 2007 Jul-Aug; 50(1): 7-17.

Mikat EM, Hackel DB, Harrison L, Gallagher JJ, Wallace AG. Reaction of the myocardium and coronary arteries to cryosurgery. *Lab Invest.*1977; 37 (6): 632-41.

Min J Y, Yang Y, Converso K L, Liu L, Huang Q and Morgan J P. Transplantation of embryonic stem cells improves cardiac function in postinfarcted rats.. *J Appl Physiol.* 2002; 92 , pp. 288-296.

Minatoguchi S, Takemura G, Chen XH, Wang N, Uno Y, Koda M, Arai M, Misao Y, Lu C, Suzuki K, Goto K, Komada A, Takahashi T, Kosai K, Fujiwara T, Fujiwara H. Acceleration of the healing process and myocardial regeneration may be important as a mechanism of improvement of cardiac function and remodeling by postinfarction granulocyte colony-stimulating factor treatment. *Circulation.* 2004 Jun 1;109(21):2572-80.

Misao Y, Arai M, Ohno T, Ushikoshi H, Onogi H, Kobayashi H, Takemura G, Minatoguchi S, Fujiwara T, Fujiwara H. Modification of post-myocardial infarction granulocyte-colony stimulating factor therapy with myelo-suppressives. *Circ J*. 2007 Apr;71(4):580-90.

Misao Y, Takemura G, Arai M, Ohno T, Onogi H, Takahashi T, Minatoguchi S, Fujiwara T, Fujiwara H. Importance of recruitment of bone marrow-derived CXCR4+ cells in post-infarct cardiac repair mediated by G-CSF. *Cardiovasc Res.* 2006 Aug 1;71(3):455-65.

Mohyeddin-Bonab M, Mohamad-Hassani MR, Alimoghaddam K, Sanatkar M, Gasemi M, Mirkhani H, Radmehr H, Salehi M, Eslami M, Farhig-Parsa A, Emami-Razavi H, al-Mohamad MG, Solimani AA, Ghavamzadeh A, Nikbin B. Autologous in vitro expanded mesenchymal stem cell therapy for human old myocardial infarction. *Arch Iran Med*. 2007 Oct; 10 (4): 467-73.

Mokry J, Cizkova D, Filip S, Ehrmann J, Osterreicher J, Kolar Z, English D. Nestin expression by newly formed human blood vessels. *Stem Cells Dev.* 2004; 13: 658-64.

Moretti A, Caron L, Nakano A, Lam JT, Bernshausen A, Chen Y, Qyang Y, Bu L, Sasaki M, Martin-Puig S, Sun Y, Evans SM, Laugwitz KL, Chien KR. Multipotent embryonic isl1+ progenitor cells lead to cardiac, smooth muscle, and endothelial cell diversification. *Cell.* 2006 Dec 15;127(6):1151-65.

Morini S, Carotti R, Carpino G, Franchitto A, Corradini SG, Merli M, Gaudio E. GFAP expression in the liver as an early marker of the stellate cells activation. Ital. J Anat. Embryol. 2005, 110(4):193-207.

Morsi YS, Birchall IE, Rosenfeldt FL. Artificial aortic valves: an overview. *Int J Artif Organs.* 2004;27:445-51.

Mummery C, Ward-van Oostwaard D, Doevendans P, Spijker R, van den Brink S, Hassink R, van der Heyden M, Opthof T, Pera M, de la Riviere AB, Passier R, Tertoolen L. Differentiation of human embryonic stem cells to cardiomyocytes: role of coculture with visceral endoderm-like cells. *Circulation.* 2003 Jun 3;107(21):2733-40.

Murohara T, Ikeda H, Duan J, Shintani S, Sasaki K, Eguchi H, Onitsuka I, Matsui K, Imaizumi T. Transplanted cord blood-derived endothelial precursor cells augment postnatal neovascularization. *J Clin Invest*. 2000; 105:1527–1536.

Murry CE, Wiseman RW, Schwartz SM, Hauschka SD. Skeletal myoblast transplantation for repair of myocardial necrosis. J Clin Invest. 1996 Dec 1; 98 (11): 2512-23.

Nachtsheim R, Dudley B, McNeil PL, Howdieshell TR. The peritoneal cavity is a distinct compartment of angiogenic molecular mediators. *J Surg Res.* 2006 Jul; 134: 28-35.

Nagaya N, Kangawa K, Itoh T, Iwase T, Murakami S, Miyahara Y, Fujii T, Uematsu M, Ohgushi H, Yamagishi M, Tokudome T, Mori H, Miyatake K, Kitamura S. Transplantation of mesenchymal stem cells improves cardiac function in a rat model of dilated cardiomyopathy. *Circulation.* 2005 Aug 23;112(8):1128-35.

Nojiri H, Shimizu T, Funakoshi M, Yamaguchi O, Zhou H, Kawakami S, Ohta Y, Sami M, Tachibana T, Ishikawa H, Kurosawa H, Kahn RC, Otsu K, Shirasawa T. Oxidative stress causes heart failure with impaired mitochondrial respiration. *J Biol Chem*. 2006 Nov 3; 281(44):33789-801.

Norol F, Merlet P, Isnard R, Sebillon P, Bonnet N, Cailliot C, Carrion C, Ribeiro M, Charlotte F, Pradeau P, Mayol JF, Peinnequin A, Drouet M, Safsafi K, Vernant JP, Herodin F. Influence of mobilized stem cells on myocardial infarct repair in a nonhuman primate model. *Blood* 2003; 102, 4361−4368.

Oh H, Bradfute SB, Gallardo TD, Nakamura T, Gaussin V, Mishina Y, Pocius J, Michael LH, Behringer RR, Garry DJ, Entman ML, Schneider MD. Cardiac progenitor cells from adult myocardium: homing, differentiation, and fusion after infarction. *Proc Natl Acad Sci USA*. 2003 Oct 14; 100(21): 12313-8.

Orlic D, Kajstura J, Chimenti S, Limana F, Jakoniuk I, Quaini F, Nadal-Ginard B, Bodine DM, Leri A, Anversa P. Mobilized bone marrow cells repair the infarcted heart, improving function and survival, *Proc Natl Acad Sci U S A.* 98 (2001), pp. 10344–10349.

Ota T, Gilbert TW, Badylak SF, Schwartzman D, Zenati MA. Electromechanical characterization of a tissue-engineered myocardial patch derived from extracellular matrix. *J Thorac Cardiovasc Surg*. 2007 Apr;133(4):979-85.

Ozawa T, Mickle DA, Weisel RD, Koyama N, Osawa S, Li RK. Optimal biomaterial for creation of autologous cardiac grafts. *Circulation* 2002; 106(12 Suppl 1):I176-82.

Ozawa T, Mickle DA, Weisel RD, Koyana N, Wonq H, Ozawa S, Li RK. Histological changes of nonbiodegradable and biodegradable biomaterials used to repair right ventricular heart defects in rats. *J Thorac Cardiovasc Surg*.2002; 124(6):1157-64.

Ozawa T, Mickle DA, Weisel RD, Matsubayashi K, Fujii T, Fedak PW, Koyama N, Ikada Y, Li RK. Tissue-engineered grafts matured in the right ventricular outflow tract. *Cell transplant*.2004; 13(2):169-77.

Pagani FD, DerSimonian H, Zawadzka A, Wetzel K, Edge AS, Jacoby DB, Dinsmore JH, Wright S, Aretz TH, Eisen HJ, Aaronson KD. Autologous skeletal myoblasts transplanted to ischemia-damaged myocardium in humans. Histologicalanalysis of cell survival and differentiation, *J Am Coll Cardiol.* 2003; 41, pp. 879–888.

Park H, Radisic M, Lim JO, Chang BH,Vunjak-Novakovic G. A novel composite scaffold for cardiac tissue engineering. *In Vitro Cell Dev Biol Animal.* 2005; 41: 188-96.

Pittenger MF, Mackay AM, Beck SC, Jaiswal RK, Douglas R., Mosca JD, Moorman MA, Simonetti DW, Craig S, Marshak DR. Multilineage potential of adult human mesenchymal stem cells. *Science* 1999; 284: 143-147.

Pittenger MF, Martin BJ. Mesenchymal stem cells and their potential as cardiac therapeutics. *Circ Res*. Jul 2004; 95(1): 9-20.

Price PA, Chan WS, Jolson DM, Williamson MK. The elastic lamellae of devitalized arteries calcify when incubated in serum. *Arterioscler Thromb Vasc Biol.* 2006; 26: 1079- 85.

Prockop D. Marrow stromal cells as stem cells for nonhematopoietic tissues. *Science.* 1997; 276: 71-74.

Quaini F, Urbanek K, Beltrami AP, Finato N, Beltrami CA, Nadal-Ginard B, Kajstura J, Leri A, Anversa P. Chimerism of the transplanted heart. N Engl J Med. *2002 Jan 3; 346(1): 5-15.*

Radisic M, Euloth M, Yang L, Langer R, Freed LE, Vunjak-Novakovic G. High density seeding of myocyte cells for tissue engineering. *Biotech Bioeng*. 2003; 82: 403-14.

Rehman J, Li J, Orschell CM, March KL. Peripheral blood "Endothelial Progenitor Cells" are derived from monocyte/macrophages and secrete angiogenic factors. *Circulation*. 2003;107:1164-9.

Reinecke H, MacDonald GH, Hauschka SD, Murry CE. Electromechanical coupling between skeletal and cardiac muscle. Implications for infarct repair. *J Cell Biol.* 2000 May 1; 149 (3): 731-40.

Reinecke H, Poppa V, Murry CE. Skeletal muscle stem cells do not transdifferentiate into cardiomyocytes after cardiac grafting. *J Mol Cell Cardiol.* 2002 Feb; 34 (2): 241-9.

Reyes M, Dudek A, Jahagirdar B, Koodie L, Marker PH, Verfaillie CM. Origin of endothelial progenitors in human post-natal bone marrow. *J. Clin. Invest.* 2002; 109: 337–346.

Robbins, Cotran. Le basi patologiche delle malattie. 7ª edizione Elsevier. 2005.

Robinson KA, Li J, Mathison M, Redkar A, Cui J, Chronos NA, Matheny RG, Badylak SF. Extracellular matrix scaffold for cardiac repair. *Circulation* 2005; 112(9 Suppl):I135.43.

Sabbah HN, Sharov VG and Goldstein S. Programmed cell death in the progression of heart failure. *Ann Med* 1998; 30 Suppl 1 , pp. 33–38

Sakai T, Li RK, Weisel RD, Mickle DA, Kim ET, Jia ZQ, Yau TM. The fate of a tissue-engineered cardiac graft in the right ventricular outflow tract of the rat. J Thorac Cardiovasc Surg. 2001; 121(5):932-42.

Schuster MD, Kocher AA, Seki T, Martens TP, Xiang G, Homma S, Itescu S. Myocardial neovascularization by bone marrow angioblasts results in cardiomyocyte regeneration. *Am J Physiol Heart Circ Physiol.* 2004 Aug; 287(2): H525-32.

Schwartz RE, Reyes M, Koodie L, Jiang Y, Blackstad M, Lund T, Lenvik T, Johnson S, Hu WS, Verfaillie CM. Multipotent adult progenitor cells from bone marrow differenziate into functional hepatocytes-like cells. *J. Clin. Invest.* 2002; 109: 1291-1302.

Shaper W, Heil M, Eitenmüller I, Schmitz-Rixen T. Arteriogenesis versus angiogenesis: similarities and differences. *J Cell Mol Med*. 2006; 10(1):45-55.

Shimizu T, Yamato M, Isoi Y, Ajutsu T, Setomaru T, Abe K, Kikuchi A, Umezu M, Okano T. Fabrication of pulsatile cardiac tissue grafts using a novel 3-dimensional cell sheet manipulation technique and temperature-responsive cell culture surfaces. *Circ Res*. 2002; 90 (3): e40.

Simpson D, Liu H, Fan TH, Nerem R, Dudley SC Jr. A tissue engineering approach to progenitor cell delivery results in significant cell engraftment and improved myocardial remodeling. *Stem Cells*. 2007 Sep;25(9):2350-7.

Simpson DG, Terracio L, Terracio M, Price RL, Turner DC, Borg TK. Modulation of cardiac myocyte phenotype in vitro by the composition and the orientation of the extracellular matrix. *J Cell Physiol.* 1994;161: 89-105.

Singer AJ, Clark RA. Cutaneous wound healing. *N Engl J Med.* 1999; 341:738-46.

Singla DK, Lyons GE, Kamp TJ. Transplanted embryonic stem cells following mouse myocardial infarction inhibit apoptosis and cardiac remodeling. *Am J Physiol Heart Circ Physiol*. 2007 Aug; 293(2): H1308-14.

Stocum DL. Stem cells in regenerative biology and medicine. *Wound. Rep. Reg.* 2001; 9: 429-442.

Strauer BE, Brehm M, Zeus T, Kostering M, Hernandez A, Sorg RV, Kogler G, Wernet P. Repair of infarcted myocardium by autologous intracoronary mononuclear bone marrow cell transplantation in humans. *Circulation*. 2002; 106:1913–1918.

Sugano Y, **Anzai T**, **Yoshikawa T**, **Maekawa Y**, **Kohno T**, **Mahara K**, **Naito K**, **Ogawa S**. Granulocyte colony-stimulating factor attenuates early ventricular expansion after experimental myocardial infarction. *Cardiovasc. Res.* 2005; 65, 446−456.

Takano H, Qin Y, Hasegawa H, Ueda K, Niitsuma Y, Ohtsuka M, Komuro I. Effects of G-CSF on left ventricular remodeling and heart failure after acute myocardial infarction. *J Mol Med.* 2006 Mar;84(3):185-93. Epub 2006 Jan 17.

Tateishi-Yuyama E, Matsubara H, Murohara T, Ikeda U, Shintani S, Masaki H, Amano K, Kishimoto Y, Yoshimoto K, Akashi H, Shimada K, Iwasaka T, Imaizumi T. Therapeutic Angiogenesis using Cell Transplantation (TACT) Study Investigators. Therapeutic angiogenesis for patients with limb ischaemia by autologous transplantation of bone-marrow cells: a pilot study and a randomised controlled trial. *Lancet*. 2002;360:427–435.

Tomasek JJ, Gabbiani G, Hinz B, Chaponnier C, Brown RA. Myofibroblasts and mechano-regulation of connective tissue remodelling. *Nat Rev Mol Cell Biol*. 2002; 3: 349- 63.

Tomita Y, Matsumura K, Wakamatsu Y, Shibuya I, Kawaguchi H, Ieda M, Kanakubo S, Shimazaki T, Ogawa S, Osumi N, Okano H, Fukuda K. Cardiac neural crest cells contribute to the dormant multipotent stem cell in the mammalian heart. J Cell Biol 2005; 170:1135-46.

Tse HF, Kwong YL, Chan JK, Lo G, Ho CL, Lau CP. Angiogenesis in ischaemic myocardium by intramyocardial autologous bone marrow mononuclear cell implantation. *Lancet*. 2003;361:47-49.

Vacanti JP, Langer R. Tissue engineering: the design and fabrication of living replacement devices for surgical reconstruction and transplantion. Lancet 1999; 354 Suppl 1:SI32-4.

van Amerongen MJ, Harmsem MC, Petersen AH, Kors G, van Luyn MJA. The enzymatic degradation of scaffolds and their replacement by vascularizad extracellular matrix in the murine myocardium. *Biomaterials* 2006; 27:2247-57.

Volders PGA, Willems IEMG, Cleutjens JPM, Arends JW, Havenith MG, Daemen MJ. Interstitial collagen is increased in the non-infarcted human myocardium after myocardial infarction. *J Mol Cell Cardiol* 1993; 25, pp. 1317–1323.

Vracko R, Thorning D. Contractile cells in rat myocardial scar tissue. *Lab Invest.*1991; 65: 214-27.

Wei HJ, Chen SC, Chang Y, Hwang SM, Lin WW, Lai PH, Chiang HK, Hsu LF, Yang HH, Sung HW. Porous acellular bovine pericardia seeded with mesenchymal stem cells as a patch to repair

a myocardial defect in a syngeneic rat model. *Biomaterials.* 2006 Nov;27(31):5409-19. Epub 2006 Jul 17.

Westfall MV, Pasyk KA, Yule DI, Samuelson LC, Metzger JM. Ultrastructure and cell-cell coupling of cardiac myocytes differentiating in embryonic stem cell cultures. *Cell Motil Cytoskeleton*. 1997;36(1):43-54.

Wollert KC, Drexler H. Clinical applications of stem cells for the heart. *Circ Res*. 2005; 96: 151-63.

Wollert KC, Meyer GP, Lotz J, Ringes-Lichtenberg S, Lippolt P, Breidenbach C, Fichtner S, Korte T, Hornig B, Messinger D, Arseniev L, Hertenstein B, Ganser A, Drexler H. Intracoronary autologous bone-marrow cell transfer after myocardial infarction: The BOOST randomised controlled clinical trial. *Lancet.* 2004; 364:141–148.

Woodbury D, Black IB. Adult rat and human bone marrow stromal cells differentiate into neurons. *J. Neurosi. Res.* 2000; 61: 364-370.

Xu C, Police S, Rao N, Carpenter MK. Characterization and enrichment of cardiomyocytes derived from human embryonic stem cells. *Circ Res*. 2002 Sep 20;91(6):501-8.

Yang Y, Min JY, Rana JS, Ke Q, Cai J and Chen Y. VEGF enhances functional improvement of postinfarcted hearts by transplantation of ESC-differentiated cells.. *J Appl Physiol.* 2002; 93, pp. 1140-1151.

Yin AH, Miraglia S, Zanjani ED, Almeida-Porada G, Ogawa M, Leary AG, Olweus J, Kearney J, Buck DW. AC133, a novel marker for human hematopoietic stem and progenitor cells. *Blood.* 1997 Dec 15; 90(12): 5002-12.

Yoon Y-S, Park J-S, Tkebuchava T, Luedeman C, Losordo DW. Unexpected severe calcification after transplantation of bone marrow cells in acute myocardial infarction. *Circulation*. 2004;109:3154-7.

Zammaretti P, Jaconi M. Cardiac tissue engineering: regeneration of the wounded heart. *Curr Opin Biotech.* 2004;15:430-4.

Zimmermann WH, Didie M, Wasmeier GH, Nixdorff U, Hess A, Melnychenko I, Boy O, Neuhuber WL, Weyand M, Eschenhagen T. Cardiac grafting of engineered heart tissue in syngenic rats. *Circulation*. 2002; 106(12 Suppl 1):I151-7.

Zimmermann WH, Melnychenko I, Eschenhagen T. Engineered heart tissue for regeneration of diseased hearts. *Biomaterials*. 2004, 25(9):1639-47.

Zimmermann W-H, Melnychenko I, Wasmeier G, Didié Naito H, Nixdorff U, Hess A, Budinsky L, Brune K, Michaelis B, Dhein S, Shwoerer A, Ehmke H, Eschenhagen T. Engineered heart tissue grafts improve systolic and diastolic function in infarcted rat hearts. *Nature Med*. 2006;12: 452-8.

Zohlnhofer D, Kastrati A, Schomig A. Stem cell mobilization by granulocyte-colony-stimulating factor in acute myocardial infarction: lessons from the REVIVAL-2 trial. *Nat Clin Pract Cardiovasc Med.* 2007 Feb; 4 Suppl 1:S106-9.